University of Sassari

PhD Course in Life Sciences and Biotechnologies

Coordinator: Prof. Leonardo Antonio Sechi

Role of different Microorganisms in

Parkinson's Disease, Rheumatoid Arthritis and Colorectal Cancer

Supervisor:

Prof. Leonardo Antonio Sechi

PhD student:

Seyedesomaye Jasemi

Cycle XXXV (Years 2019-2022)

Foreword

This thesis is based on several manuscripts that were published during my PhD. The work of this PhD thesis has been completed during my enrolment as PhD student at the Department of Biomedical Sciences, University of Sassari, Italy, from November 2019 to January 2023 under the supervision of Professor Leonardo Antonio Sechi.

All the samples used in these studies were from subjects enrolled by the Rheumatoid Arthritis Centre, UOC Reumatologia, Dipartimento di Medicina Clinica e Sperimentale, Azienda-Ospedaliero Universitaria (AOU) di Sassari, Sassari-Italy; by the Department of Clinical and Experimental Medicine, Neurology section, University of Sassari and Centro Trasfusionale, Azienda Sanitaria Locale (ASL) Sassari- Italy and by the Imam khomini Hospital, affiliated with Tehran University of Medical Sciences, Tehran– Iran, and Taleghani Hospital, affiliated with Shahid Beheshti University of Medical Sciences, Tehran– Iran.

Abstract: In this work the role of microorganisms in three non-communicable diseases (NCDs) among others were investigated: Parkinson's disease (PD), Rheumatoid arthritis (RA) and Colorectal Cancer (CRC). Annually, 41 million deaths due to NCDs are reported that 77% are in low- and middle-income countries. The etiology of these diseases is not well understood, the genetic background and environmental risk factors play a role such as microbial pathogens infection. In this thesis, we investigated the humoral response against various bacterial and viral immunogen peptides in RA and PD patients and compared them with those in healthy controls (HCs). In addition, we evaluated whether the oral and fecal microbiomes characterization of of patients (in particular *Bacteroides fragilis*) can be suitable for CRC screening for early CRC detection.

RA. Polyclonal IgG antibodies (Abs) specific for peptides derived from *Porphyromonas gingivalis*, Pg (RgpA, Kpg); *Aggregatibacter actinomycetemcomitans*, Aa (LtxA1, LtxA2); *Mycobacterium avium* subsp. *Paratuberculosis*, MAP (MAP4027); Epstein-Barr virus, EBV (EBNA1, EBVBOLF) and human endogenous retrovirus, HERV (HERV-W env-su) were detected by indirect ELISA in serum samples from 148 consecutive RA patients and 148 sex and age-matched healthy controls (HCs). RA patients exhibit a higher prevalence of humoral immune response against all tested peptides compared to HCs with a statistically significant difference for MAP4027 (30.4% vs. 10.1%), BOLF (25.7% vs. 8.1%), RgpA (24.3% vs. 9.4%), HERV W-env (20.3% vs. 9.4%), and EBNA1 (18.9% vs. 9.4%) peptides. We also found an increased titer and prevalence of Abs against LtxA1 and LtxA2 in seropositive vs. seronegative RF ($p = 0.019$, $p = 0.018$). This study demonstrated a significantly increased humoral response against multiple pathogens in patients with RA and implies that they could be important factors in the pathogenesis of the disease. Therefore, the role of each individual pathogen in RA needs to be further investigated.

PD. In addition, in this thesis Abs response against the following peptides from Herpes Simplex virus 1, HSV-1 ($UI42_{22-36}$), human α-synuclein ($\alpha\text{-syn}_{100-114}$), *Porphyromonas gingivalis*, Pg ($RgpA_{800-812}$, $Kpg_{328-339}$), *Aggregatibacter actinomycetemcomitans*, Aa ($LtxA1_{429-445}$, $LtxA2_{64-80}$) and bacterial curli ($Curli_{133-141}$) were investigated by indirect ELISA in 51 serum samples from PD and 58 sex and age-matched HCs. Significant differences in OD (optical density) values and Abs positivity between PD patients and HCs were observed for Kpg (82.3% vs. 10.3%), followed by RgpA (60.7% vs. 24.1%), curli (51% vs. 22.4%), and UI42 (43.1% vs. 25.8%) in PD, compared to HCs sera ($p < 0.001$). Significant positive correlations between OD values obtained by ELISA were observed for UI42 and curli ($r = 0.811$, $p < 0.0001$), Kpg and RgpA ($r = 0.659$, $p < 0.0001$), followed by LtxA1 and LtxA2 ($r = 0.653$, $p < 0.0001$). The correlation between the HY scale (Hoehn and Yahr Scale) and LtxA1 ($r = 0.306$, $p= 0.028$) and HY and Kpg ($r = 0.290$, $p = 0.038$) were significantly positive. This study reports a significantly increased humoral response against curli, Pg, and HSV-1 in PD patients, implying that they could be important factors in the pathogenesis of the disease.

CRC. In the first part of the CRC study, thirty-one CRC tissue biopsies (from 31 CRC patients) and thirty-one normal colorectal tissue biopsies (from 31 HCs individual) were recruited. *Bacteroides fragilis* isolation, phenotypic and PCR identification tests were performed. Furthermore, biofilm-forming ability and expression of *bft* gene were assessed under biofilm and planktonic forms. A total of 62 *B. fragilis* strains were isolated from all colorectal tissue, of which 13 isolates (20.96%) (11 isolates from CRC and 2 from normal tissue) were positive for *bft* gene. Moreover, toxin-producing *B. fragilis* strains showed higher biofilm formation ability compared to non-toxigenic *B. fragilis* strains. Toxin expression was significantly reduced in biofilm form compared with planktonic form living bacteria. Finally, the number of toxin-producing *B. fragilis* strains and their biofilm formation ability were significantly higher in CRC patients in compared with HCs.

In the second part of study, 40 saliva and 40 fecal samples were collected from 20 CRC stage 0 and I patients and 20 HCs. 16s rRNA sequencing assays was performed to study microbiota profiles in all oral and fecal samples. Diversity of top bacterial genera in both types of specimens (fecal and saliva samples) revealed a distinction between CRC patients and HCs. In saliva samples, α- diversity index was different between HCs and CRC patients, whereas β diversity showed a densely clustered microbiome in the HCs but a more dispersed pattern in CRC cases. α and β diversity of fecal microbiota between HCs and CRC patients showed no statistically significant differences. *Bifidobacterium* was identified as a potential bacterial biomarker in CRC saliva samples, while *Fusobacterium*, *Dialister*, *Catonella*, *Tennerella*, *Eubacteriumbrachy*-group, and *Fretibacterium* were ideal to distinguish HCs from CRC patients. Moreover, an evaluation of saliva microbiota might offer a suitable screening test for the early detection of this malignancy, providing more accurate results than its fecal counterpart.

Keywords: Parkinson's disease, Rheumatoid arthritis, Colorectal cancer, Infection, Microbiota, *Bacteroides fragilis*; Toxin, Biofilm.

Table of Contents

List of Abbreviations

ACPA	Anticitrullinated Peptide Antibodies
ANOSIM	Analysis of Similarities
APCs	Antigen-Presenting Cells
AP	Adenoma Polyps
ASV	Amplicon Sequence Variant
BBE	Bacteroides Bile Esculin agar
BBA	Brucella Blood Agar
BHI	Brain Heart Infusion
B. fragilis	*Bacteroides fragilis*
BfPAI	*Bacteroides fragilis* Pathogenicity Island
BMI	Body Mass Index
CMV	Cytomegalo Virus
CRP	C-Reactive Protein
CRC	Colorectal Cancer
EBV	Epstein–Barr virus
DMARDs	Disease Modifying Antirheumatic Drugs
ESR	Erythrocyte Sedimentation Rate
ETBF	Enterotoxigenic *Bacteroides fragilis*
EDTA	Ethylene Diamine Tetraacetic Acid
ENS	Enteric Nervous System
EMT	Epithelial-Mesenchymal-Transition
LEfSe	Effect Size Method
FLS	Fibroblast-Like Synoviocytes
FIT	Fecal Immunochemical Test
FISH	Fluorescence In Situ Hybridization
GIT	Gastrointestinal tract
HCs	Healthy controls
HLA	Human Leukocyte Antigen

HP	Hyperplastic Polyp
HSV-1	Herpes Simplex virus type 1
HSP	Heat shock protein
LPS	Lipopolysaccharide
LBs	Lewy bodies
LDA	Linear Discriminant Analysis
NEBF	Non-Enterotoxigenic *Bacteroides fragilis*
NK	Natural Killer
NCDs	Non-communicable diseases
NMDS	Non-metric Multi-Dimensional Scaling (NMDS)
NSAIDs	Non-Steroidal Anti-inflammatory Drugs
OOB	Out- Of-Bag error
PAMPs	Pathogen Associated Molecular Patterns
PtpA	Protein tyrosine phosphatase A
PknG	Protein kinase G
PD	Parkinson's disease
PTPN2/22 gene	protein tyrosine phosphatase non-receptor type 2 gene
Pg	*Porphyromonas gingivalis* (Pg)
RF	Rheumatoid Factor
RF	Random Forest
(RA)	Rheumatoid Arthritis
ROS	Reactive Oxygen Species
SSA	Sessile Serrated Adenoma
TSS	Total Sum Scaling
TNF-α	Tumor Necrosis Factor alpha
α-syn	Alpha-synuclein

Chapter 1: Overview

1-1. Non-communicable diseases

Non-communicable diseases (NCDs) are diseases that are not directly transmitted from one person to another (1). NCDs include Parkinson's disease (PD), Rheumatoid arthritis (RA), Colorectal cancers (CRC), and others. 41 million deaths due to NCDs are reported globally and 77% of them are in low- and middle-income countries (2).

Although NCDs occur in elderly people, they can occur in all age groups. The etiology of these diseases is not well understood, the genetic background and environmental risk factors like infection may play a role in the etiology of NCDs. In this thesis we investigated the humoral immune response against immunogen peptides derived from bacterial amyloid curli, *Porphyromonas gingivalis*, *Aggregatibacter actinomycetemcomitans*, *Mycobacterium avium subsp. paratuberculosis*, Epstein–Barr virus, HERVs, and Herpes Simplex Virus HSV-1 in Parkinson's disease (PD) patients and Rheumatoid arthritis (RA) patients and compared the results with those obtained in healthy controls (HCs). In addition, we evaluated whether the oral and fecal microbiomes characterization of patients can be suitable for CRC screening for early CRC detection.

.

1-1-1. Rheumatoid arthritis

Rheumatoid arthritis (RA) is a chronic autoimmune disease, RA is characterized by a systemic auto-immune disease, causing joint pain, swelling, and stiffness. RA usually affects hands, feet, and wrists, leading to progressive bone and cartilage damage, resulting in deformities, joints loss of function, and reduced independence in performing daily activities (3,4). RA clinical manifestations are usually not confined to musculoskeletal system, but also involve cardiovascular system, kidneys, lungs, liver, and skin (5).

Moreover, the relative risk of death in the RA population is still significantly increased, compared to the general population, due to cancer and infections. It has been estimated that RA patients developing infectious complications may have a significant rise in death risk (up to 52%), with respect to the RA counterpart without history of infections (6).

1-1-2. Epidemiology of Rheumatoid arthritis

Worldwide prevalence ranging of RA is between 0.5–1% (7). Average point and period prevalence of RA are 51 in 10,000 and 56 in 10,000, respectively. Higher urban vs rural prevalence may be biased due to poor case findings in regions with less healthcare or differences in risk factors environment. Figure 1 shows global prevalence of RA in the word in 2022 (8).

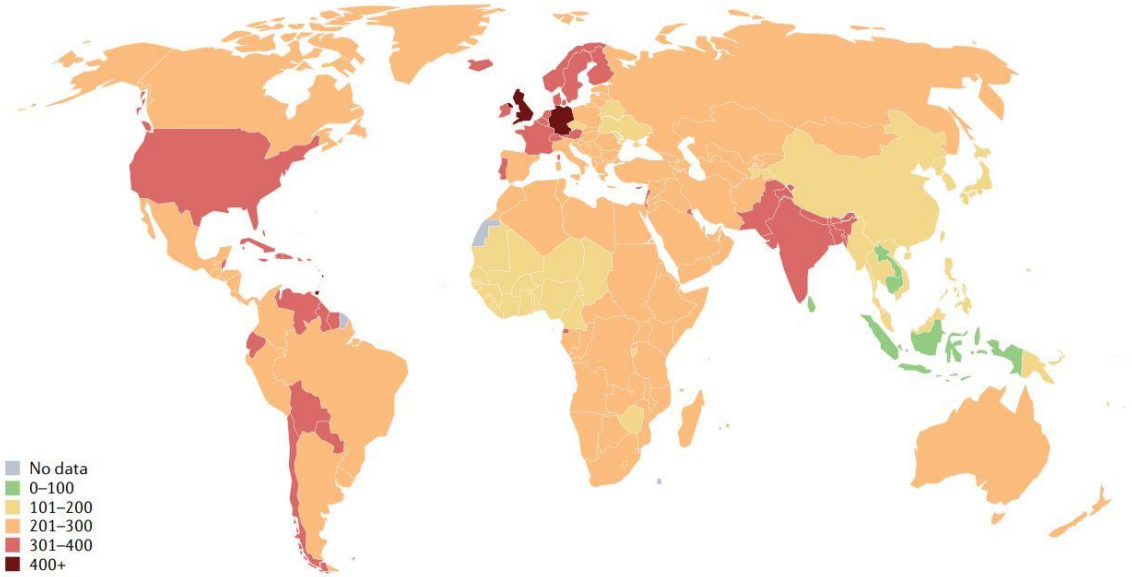

Figure 1. Global prevalence of rheumatoid arthritis.

1-1-3. Etiology of Rheumatoid arthritis

The etiology of RA is complex and cannot be described solely by genetic factors and epigenetic mechanisms (9). Many factors can contribute to the risk of developing rheumatoid arthritis (RA), including genetic factors, lifestyle infections, hormonal factors, dietary factors, oral health, and microbiota (Figure 2) (8). Genetic contribution is around 50 to 60% and therefore, genetic factors have an important impact on susceptibility to RA (7). The strongest predisposing gene variants are found in the human leukocyte antigen (HLA) genes, accounting for 30 to 50% of overall genetic susceptibility to RA (7). Environmental factors such as

smoking, infections, and microbiota have been identified as risk factors to develop RA in susceptible individuals (9).

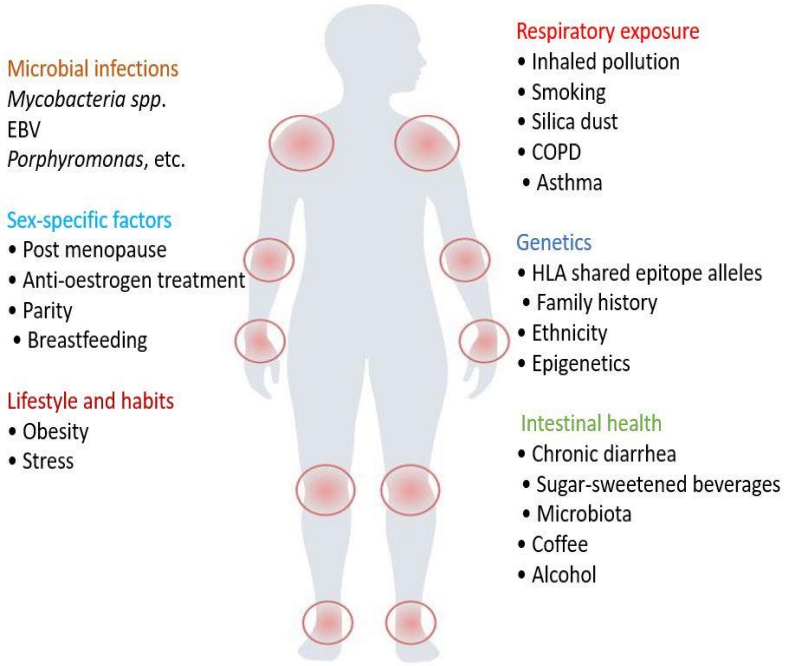

Figure 2. Risk factors associated to RA

1-1-4. Immunopathogenesis of Rheumatoid arthritis

RA is a chronic inflammatory disease characterized by synovial inflammation and bone damage, resulting from the proliferation of synovial fibroblasts, B and T lymphocytes, neutrophils, and monocytes (10,11).

Macrophages, neutrophils, mast cells, and natural killer (NK) cells are involved in the development of inflammatory response in the joint, because of innate immune response

activation. Antigen-presenting cells (APCs), such as macrophages, and effector cells, promote inflammation and mediate bone and cartilage destruction by releasing pro-inflammatory factors, such as tumor necrosis factor alpha (TNF-α), interleukin-1B (IL-1B), IL-6, IL-18, IL-23, reactive oxygen species (ROS), and matrix-degrading enzymes (10,11).

Neutrophils exacerbate inflammation and tissue destruction by releasing pro-inflammatory cytokines, ROS, granules containing destructive enzymes, and the formation of neutrophil extracellular trap (NET) (12).

In RA patients, the chronic inflammatory processes that characterize the patients' joints may be triggered by Toll-like receptors-TLRs aberrant activation. In particular, it was found that, in RA patients, TLRs activaction is increased in peripheral blood monocytes (TLR-2 and 4), synovial fibroblast (TLR-3 and 7), and in synovial fluid macrophages (TLR-2 and 4) (13,14). Moreover, microbial, and endogenous ligands were reported to be able to activate TLRs in patients' derived cells. In particular, bacterial LPS and peptidoglycan induced the expression of IL-6 and CXCL8, via TLR-2 binding, in RA synovial fibroblast. Moreover, macrophages with an increased expression of TLR-2 resulted in an aberrant response to bacterial peptidoglycan (13). Thus, upregulated expression, the presence of microbial and endogenous ligands, and increased sensitivity to TLRs signaling may confer a crucial role to TLRs in RA pathogenesis.

Despite RA being a type 1 T helper (Th1)-mediated disease, recent available evidence suggests that T helper 17 cells (Th17) are an important effector cell population in RA pathogenesis as well (15).The secretion of IL-17A cytokines, by Th17 cells, activates a number of pathways

such as Fibroblast-like synoviocytes (FLS), maturation and function of osteoclasts, activation of neutrophils, macrophages and B cells (15).

1-1-5. Role of infections in Rheumatoid arthritis pathogenesis

The role of infections in the development of autoimmune diseases has long been considered, since the infection with different pathogens can involve multiple pathways of the immune system, potentially triggering an autoimmune response (16).

To date, different molecular mechanisms have been reported to play a role in autoimmune processes, such as pathogen/host interaction, and molecular mimicry (17,18). Moreover, it has also been shown that cross-reactive Abs produced in the context of microbial infections have the potential to cause damage to host tissues (19,20). In the presence of unfavorable conditions, the host's immune response to pathogens, as well as the pathogen's direct attack against the host, may lead to self-tissue damage and release of autoantigen, resulting in the development of a self-specific immune response mounted to the host tissue (21,22). In addition, bacterial infections can lead to the proliferation, and differentiation, of B and T lymphocytes, without their antigenic specificity, resulting in direct inflammatory responses against the host, triggering the polyclonal lymphocyte activation (23). Other than that, microbial infection may trigger inflammatory pathways, by activating reactive lymphocyte cells, leading to autoimmune responses, called bystander activation (23).

The evidence of an association between microorganism's infection and RA disease dates back to the 1870s, with suspected pathogens still being added to this list (24). The use of different

laboratory methods, have allowed the detection in RA patients' joints, and serum, of several microorganisms, or their components (25), such as *Porphyromonas gingivalis* (Pg) (26), Epstein–Barr virus (EBV) and Cytomegalovirus (CMV) (27). Table 1 shows the most prevalent microbes associated with RA.

Table 1. In vivo and in vitro studies of microorganisms related to RA

Presence of microbial contents in RA patient's tissues and serum	*Mycobacteria*, *P. gingivalis*, EBV, *Mycoplasma*, *Bordetalla*, *Haemophilus*, *Acinetobacter*, *Parvovirus*, CMV, Bacterial cell wall
Presence of immune response to infection in RA patient's tissues and serum	*Mycobacteria*, *P. gingivalis*, EBV, HTLV, *Mycoplasma*, *Parvovirus B19*, *Papilloma virus*, HERV
Induction of arthritis by anfections in animal models 	*Mycobacteria*, *P. gingivalis*, *Mycoplasma*, EBV

1-1-5-1. Mycobacterial infections and Rheumatoid arthritis

Mycobacterium genus has more than 170 species, most of which are environmental organisms (28). Mycobacterial infections include tuberculosis and non-tuberculous mycobacterial infections, which cause subacute clinical symptoms with granulomatous inflammation (28). Different studies showed the link between the immune response to mycobacterial infections and autoimmune diseases, especially autoimmune arthritis (29,30). Various studies have shown the presence of mycobacterium antigens in RA patients' joints (31,32). Moreover, increased levels of Abs against *Mycobacterium* in the serum (30) and the presence of active T

cells in the synovium have been reported in RA patients (33). In a collagen-induced arthritis (CIA) mice model, mice treated with collagen plus killed Mtb developed severe arthritis, while, on the contrary, mice treated with collagen emulsion alone did not develop arthritis (34). Other studies have shown that in RA patients some mycobacterial lipids, named pathogen associated molecular patterns (PAMPs), are able to increase the immune response via TLR-2 and TLR-4 binding, resulting in the increased maturation of dendritic cells, ROS production, synthesis of pro-inflammatory RA cytokines (such as IL-1, IL-6, IL-17 and IL-23), and TNF-α secretion by neutrophils (35).

Immunization against *M. tuberculosis* has been reported to cause arthritis due to cross reaction with cartilage proteoglycans (36). In addition, some studies have shown a non-negligible prevalence of anti-CCP and anti-arginine-containing peptide (anti-CAP) positivity in the serum of patients with mycobacterial infections (37,38). Moreover, polyclonal antibodies against human lactoferrin, cross-reacted against *Mycobacterial* antigens, further support the role of such molecules in triggering molecular mimicry mechanisms in RA (39,40). In a case-control study, Bo et al. found increased levels of Abs against two main proteins of MAP, named protein tyrosine phosphatase A (PtpA) and protein kinase G (PknG), in RA patients compared to healthy controls. This finding of a previous exposure of RA patients to MAP infection suggests a potential role of MAP infection in the RA pathogenesis (30).

HSP65 increases the responses of mononuclear cells in the synovial fluid of RA patients, and the clonal expansion of T cells against mycobacterium HSP65 was detected in RA patients' blood and synovial fluid (35). Mycobacteria Heat shock protein 16 (HSP16), 70 (HSP70) and HSP65 demonstrated 18–60% identity to their human homologues (41,42). Autoimmune

response to Mycobacterial (Myc) HSP70 and human binding immunoglobulin protein (Bip), a member of the human HSP70 family, has also been reported in RA patients (43). Shoda's study showed that the similarity between Myc HSP70 287–306 and human Bip336–355 epitopes can lead to a broken immune tolerance, triggering an auto-immune response as a result of the T cells' inability to distinguish between self- and pathogens' antigens (44).

A different approach to investigate the similarities between the virulence factors of Mtb and human proteins are bioinformatics models. HLA class I and II restricted T cell epitopes from host proteins that share bacterial and homologues human HSP60 specialty KPLVIIAEDVDGEALSTLVLN, bind to many HLA class I and class II alleles, including HLA-DRB1: *01:01, *03:01, *04:01, *07:01*, 08:02, *11:01, *13:01, *15:01, A*01:01, A*02:01, A*03:01, A*011:01, A*024:02, A*07:02, A*08:01 (45).

Findings indicated the presence of matching 22 B-cell, 79 human leucocyte antigen *(*HLA*)* class II and 16 HLA class I specific predicted epitopes in these virulence factors having human homologs (46). In addition, in silico analysis showed that T cell cross-reactive epitopes between *M. tuberculosis* and the human proteome can be considered as vaccine candidates (47,48).

Examination of SNPs in *TNF-α* gene, and its receptors (TNFRSF1A/TNFRSF1B), in RA patients compared to HCs, reported that some SNPs, TNFRSF1A:rs767455 and TNFRSF1B:rs3397, are linked to TNFRSF1B downregulation, increased susceptibility to MAP infection, increased inflammation and osteocalcin deficiency, and, possibly, increased osteoporosis (49). Sharp et al. showed that the SNPs in *PTPN2/22* genes (protein tyrosine

phosphatase non-receptor type 2 and 22) are linked to increased sensitivity to MAP infection and, therefore, increased T lymphocyte response, and IFN-γ expression in RA patients (50).

1-1-5-2. *Porphyromonas gingivalis* and Rheumatoid arthritis

Epidemiological studies suggesting a potential pathogenic link between periodontitis and RA (51–53). *Porphyromonas gingivalis* (Pg) and *Aggregatibacter actinomycetecomitans* (Aa) are the most common reported pathogens in periodontitis, and they can contribute to RA autoantibody production through various mechanisms: directly by post-translation modification of human protein (by the PPAD enzyme of Pg) or indirectly by neutrophil osmotic lysis (leukotoxin of Aa) (51,54–56).

Laboratory and clinical studies have shown that pg is the most common microorganism associated with RA etiopathology (57). Of note, it has been reported a similarity of up to 82% between Pg enolase and human α-enolase within the 17-amino acid immunodominant region, and Abs levels against bacterial enolase were related to the levels of Abs against the human enolase (58).

In addition, Pg is the only bacterium that produces the peptidylarginine deiminase (PAD)-enzyme with citrullination activity. Host proteins post-translation modifications are catalyzed by this enzyme, resulting in the production of new antigens. It has also been reported that Pg, through PAD-enzyme activity, is able to generate neo-antigens in the joint, including citrullinated-fibrinogen, α-enolase and vimentin, resulting in the stimulation of the auto-immune response (59,60). Also, by producing proteinase enzymes, Pg increases apoptosis in

chondrocyte cells, thereby destroying cartilage tissue and deforming the joint, which is an important mechanism in RA pathogenesis (61).

1-1-5-3. Epstein-Barr virus (EBV) and Rheumatoid arthritis

Epstein-Barr Virus (EBV) is a member of the Human Herpes Viruses (HHVs) family and the causative agent of infectious mononucleosis (62). As previously mentioned, Abs against EBV (BOLF1 peptide) and human homologous (IRF5 epitope) were significantly higher in RA patients than healthy controls, indicating that these microorganisms may be involved in RA pathogenesis, with the production of cross-reactive Abs being a central mechanism to trigger autoimmune disease (63).

The EBV DNA increased the secretion of pro-inflammatory cytokines, such as IL-17, IL-23 and TNF-α in mice, which could lead to, or exacerbate, autoimmune diseases (64). In addition, EBV and *E. coli* DNA ligation to endosomal TLR-9 leads to increased IL-17A expression, which is an essential cytokine in the synovial environment. The EBV infection in human lymphocytes under in vitro conditions could cause the expansion of non-specific B lymphocytes and TCD8+ cells, leading to the production of polyclonal antibodies and the activation of cytotoxic T lymphocytes (65). Accordingly, T lymphocyte response to EBV has been reported in inflamed joints of RA patients (66).

1-1-6. Diagnosis and treatment of Rheumatoid arthritis

Several antibody systems have been identified in RA based on the antigens that these antibodies bind too. Among them, Serum Rheumatoid Factor (RF) and anti-CCP are currently used as biomarkers for the diagnosis of RA (5). These autoantibodies can predominantly be

detected in serum and synovial fluid (SF) of RA patients (5). They may form immune complexes in the joints, leading to the attraction of immune cells through e.g. complement activation or direct activation of immune cells leading to the secretion of chemokines and cytokines.

American College of Rheumatology–European League Against Rheumatism classification criteria; a patient with 6 or more points can be classified as having RA (Table 2) (67). There are no diagnostic criteria for RA. A diagnosis has to be established by an individual physician in an individual patient based on that patient's symptoms, which may occasionally differ from those represented in table 2 classification criteria are meant to identify patients for consideration of participation in clinical studies to provide a homogenous study population. Nevertheless, classification criteria can help in diagnosis (67).

The goal of diverse treatment strategies for rheumatoid arthritis is to relieve patients' pain and inflammation, protect the normal joint function of patients, and prevent further progression of rheumatoid arthritis and joint damage (68). Currently one of the mainly treatments is drug therapy including but not limited to the non-steroidal anti-inflammatory drugs (NSAIDs), disease modifying antirheumatic drugs (DMARDs), glucocorticoids and biological agents (68,69).

Table 2. Rheumatoid arthritis classification and follow-up

Classification	Points
Joint Distribution (0-5 points)	
1 large joint	0
2-10 large joints	1
1-3 small joints (large joints not counted)	2
4-10 small joints (large joints not counted)	3
>10 joints (≥1 small joint)	5
Serology (0-3 points)	
Negative RF and negative ACPA	0
Low positive RF or low positive ACPA	2
High positive RF or high positive ACPA	3
Symptom Duration (0-1 point), weeks	
<6	0
≥6	1
Acute Phase Reactants (0-1 point)	
Normal CRP and normal ESR	0
Abnormal CRP or abnormal ESR	1

Abbreviations: ACPA, anticitrullinated peptide antibodies; CRP, C-reactive protein; ESR, erythrocyte sedimentation rate; RF, rheumatoid factor

1-2. Parkinson's disease

1-2-1. Parkinson's disease

Parkinson's disease (PD) is the second most common neurodegenerative disorder in the world, which affects about 1% of people over the age of 60 (70). Although more than 6 million people worldwide are living with PD, it is estimated to be doubled by 2040. The death of dopaminergic neurons in the substantia nigra pars compacta (SNpc) with accumulation of misfolded and aggregated α-synuclein (α-syn) is a prominent feature of this disease (71).

Loss of vital neurotransmitters (dopamine) usually causes motor symptoms in PD patients. During the initial diagnosis of this disease, usually 50% of dopaminergic neurons have lost their activity (72). In the pathology smear from the brain autopsy (SNpc) of PD patients, dopaminergic neurons contain intracytoplasmic proteinaceous inclusions Lewy bodies (LBs) that are created from α-syn accumulation(73). Recently, electron microscopy has shown that the LBs also contains lipids, fragmented vesicles, lysosomes, and mitochondria (74).

Motor symptoms include bradykinesia, muscular rigidity, tremor, and postural instability with late appearance and generally crippling (75). In addition, non-motor symptoms of PD include as rapid eye movement (REM) sleep deficits, hyposomia, cognitive impairment, orthostatic hypotension, and most commonly, intestinal dysfunction, with ~80% of PD patients suffering from constipation (76). Autonomic dysfunction in PD includes gastrointestinal malfunction, cardiovascular dysregulation, urinary disturbance, sexual dysfunction, thermoregulatory aberrance, and pupillo-motor and tear abnormalities (76) .

1-2-2. Etiology of Parkinson's disease

Although the etiology of PD is unknown, various genetic bachground and environmental factors are known as risk factors for the disease (77). A small percentage (2-10%) of PD have a genetic background. Studies have identified approximately 24 distinct chromosomal regions related to genetic of PD (78). Interestingly, a vast number of identified PD mutations are involved in endolysosomal sorting of proteins, including α-syn. *SNCA* is the first gene linked to PD (78).

There are several environmental associated risk factors for PD etiology like, infection, cigarette smoking, caffeine intake, physical activity, plasma urate and positive associations with pesticide exposure (77).

1-2-3. Alpha-synuclein pathology in Parkinson's disease

α-syn is a small cytoplasmic protein with a molecular weight of 15 kilodaltons, which is encoded by the *SNCA* gene (79). In the past, it was believed that this protein is found only in the tissues of the nervous system, but it was later found that this protein is expressed in different parts of the body. α -syn contains two alpha-helices followed by an unstructured, acidic C-terminal tail (Figure 3). The first alpha helix (amino acid residues 1–60) is an amphipathic region that can bind to lipids due to the repeating KTKEGV motif (79). The second alpha helix (amino acid residues 61–95) is a hydrophobic sequence that required for protein aggregation (80). The tirth part of this protein (amino acid residues 96–140) is an acidic domain and contains phosphorylation sites (80).

In PD patients, α-syn pathology is not only seen in the brain, but also in the enteric nervous system (ENS) along with changes in microbiota and dysbiosis (81).

in the early stage (stage I) of PD, α-syn pathology is seen in the olfactory bulb and the medulla the brain, then spread to the the brainstem and pons (stage II) and midbrain, which includes the substantia nigra (stage III). Next, pathology propagates to the limbic lobe (stage IV), neocortex (stage V), and eventually to the primary and motor cortices at late stages of the disease (stage VI) (Figure 3). The movement of this protein from one cell to another is prion-like manner. Interestingly, the misfolded α-syn has a greater tendency to be secreted from the cell (82, 83).

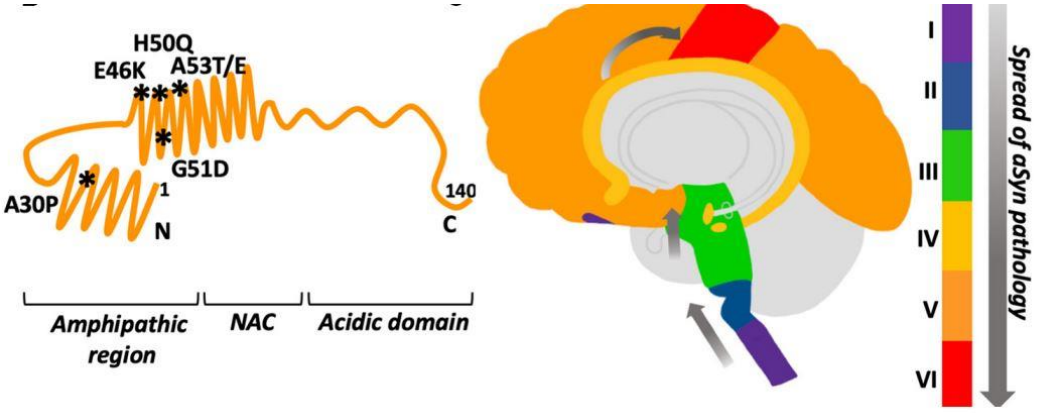

Figure 3. Alpha-synuclein structure and spreading

Evidence shows α-syn plays an important role in signaling and releasing neurotransmitters. This protein can cause the assembling of the SNAR complex (act as chaperon for SNAR protein, which plays an essential role in the release of neurotransmitters (84).

1-2-4. Infection and risk of Parkinson's disease

A variety of microbes have been described with a potential of inducing or contributing to the occurrence of parkinsonism and PD. Infection disease can cause parkinsonism symptoms in two ways: para-infection and post -infection. The term "parainfection" indicates the symptoms that develop within 15 days from the beginning of the infection (85).

Some microbes are neurotropic, which can directly cause damage to the neurons of the immune system. The microbe can reach the brain through various mechanisms through 1) peripheral neurons, 2) blood brain barrier (BBB), and 3) blood cerebrospinal fluid. In addition, microrganism can indirectly cause damage to brain neurons by inducing inflammatory, vascular and/or hypoxic injury (85,86).

Post infection parkinsonism usually occurs due to pathogen induced autoimmunity. In this mechanism, the specific immune system is activated, which targets the host's antigens. Chronic infections can cause a long-term immune response that leads to chronic inflammation and the development of the autoimmune process and damage to the neurons of the nervous system. Of course, microrgansms can cause autoimmune reactions through molecular mimicry, bystander activation, and viral persistence with or without epitope spreading (87) (Figure 4).

The molecular mimicry between the antigens of the microorganisms and the host's antigens activates the immune response mediated by B and T lymphocytes against both antigens. In addition, virus-specific T cells can surround virus-infected cells, then presentation of viral peptides by human leukocyte antigen (HLA) class I or class II molecules to virus-specifc CD8+or CD4+T cells may occur and subsequently release of cytokines such as tumour

necrosis factor (TNF), lymphotoxin (LT), and nitric oxide (NO) will lead to the killing of virus-infected cells (87).

Epitope spreading is a phenomenon related to the lymphocyte bystander activation which ultimately leads to inflammatory responses. The immune response against an antigen is initially limited to a specific peptide sequence in the target antigen, when infection persist, the immune response to other epitopes is also created, known as epitope spreading phenomenon. Persistent infections lead to polyclonal proliferation of B and T lymphocytes and thus may lead to autoimmunity (88).

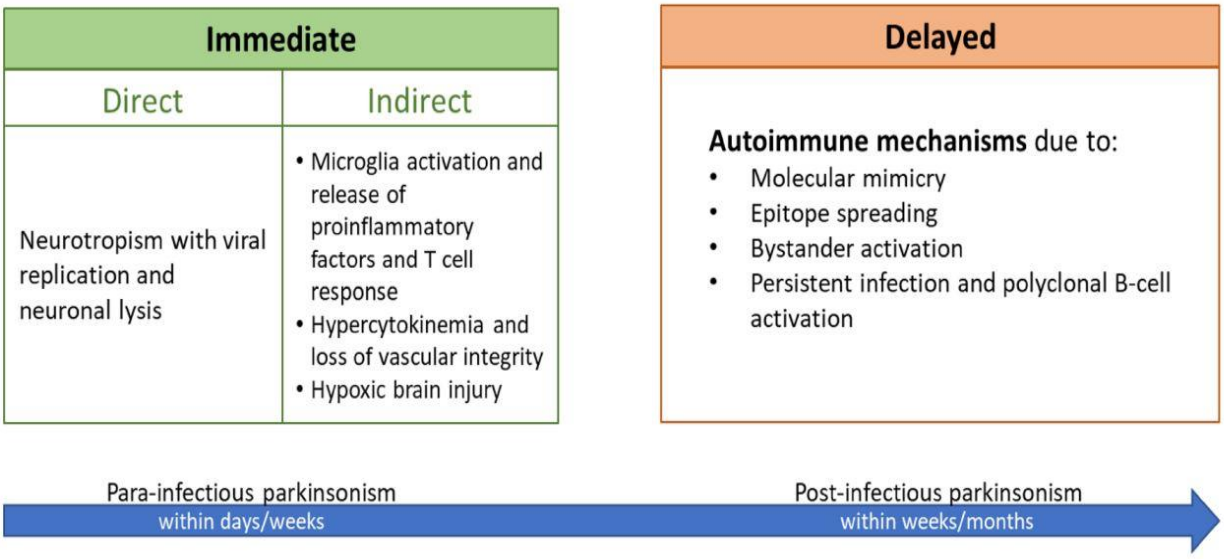

Figure 4. Putative pathophysiological mechanisms underlying infection-induced parkinsonism.

In addition, PD has been associated to the infection of different microrganisms including human herpes simplex virus type 1 (HSV-1), *Mycobacterium avium subsp. paratuberculosis*

(MAP), Epstein-Barr virus (EBV), Infuenza virus, *P. gingivalis*, hepatitis B (HBV) and C virus (HCV) and recently Coronavirus disease 2019 (COVID-19) pandemic (87,89–92).

Among herpesviruses, HSV-1 is strongly associated with PD. HSV-1 is a a neurotropic virus belonging to Herpesviridae family. After the initial infection, which usually occurs at a young age, HSV-1 can establish a latent infection in the sensory ganglia (93).

Despite the control of this virus by the immune system, reactivation and re-infection could happen many times during a person's life (94). HSV-1 can induce long-term neuroimmune activation, and this could be one of the mechanisms underlying neurodegeneration (95).

About 60% of people under the age of 50 are infected with HSV-1. Studies show that if the balance between the immune system and the virus is lost, this virus can cause inflammation of neurons and is considered as a key factor for PD (96). In vivo and in vitro studies show that HSV-1 can increase the accumulation of beta amyloid in the brain (97).

1-2-5. Gut-brain axis of Parkinson's disease

PD is a neurodegenerative disease that occurs as a result of α-syn accumulation in the brain and ultimately affects the function of the central, peripheral and enteric nervous system (98). Although the brain is the main site of aggregation of α-syn, it is also found in the peripheral nervous system and the enteric nervous system (ENS), it is produced by enteric neurons to mediate neurotransmitter release and uptake, lending support to the theory that PD pathology could be initiated in the ENS (99). Interestsingly, α-syn has also been found in the salivary glands, esophagus, and stomach (100,101). Accumulation of α-syn in ENS causes damage to

neurons and possibly intestinal dysfunction. According to the idea of gut-brain axis, α-syn accumulated in the ENS may reaches the brain through the vagus nerve (99).

Lipopolysaccharide (LPS) and bacterial metabolism can travel to the brain through the blood-brain barrier and cause inflammation and the release of cytokines and increase the inflammatory response in PD (102). LPS and curli can increase the activity of microglial cells and astrocytes. This mechanism causes inflammatory responses and increased expression of pro-inflammatory cytokines such as IL-6 and IL-8 along with increased ROS production and oxidative stress (102).

Also, microbes in the intestinal lumen cause the activation of inflammatory pathways and damage to enterocytes and ultimately increase the permeability of the intestinal epithelial membrane. Bacterial metabolites can enter the bloodstream and cause systemic inflammation (Figure 5) (102).

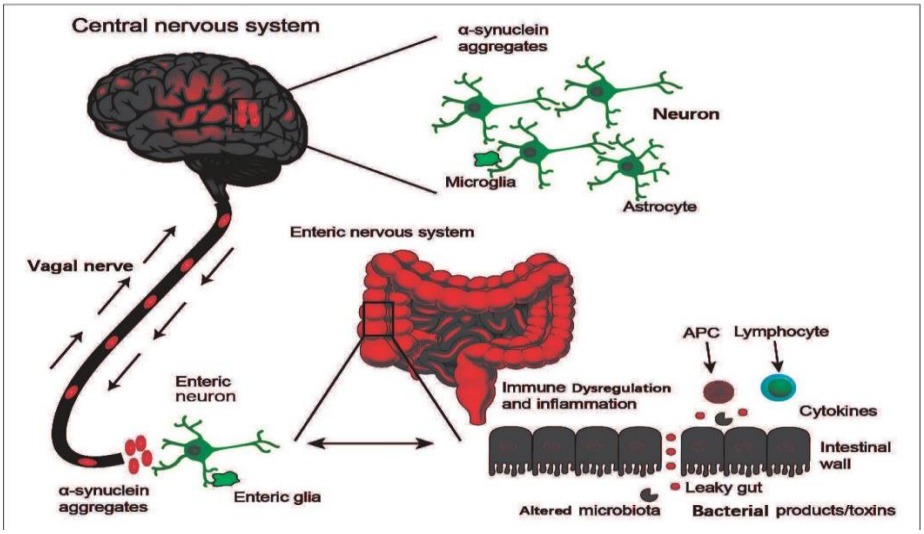

Figure 5. Schematic representation of α-synuclein accumulation and aggravation starting in the ENS to the brain.

Interesting evidence has shown that the microbial amyloid curli is structurally similar to human amyloid α-syn, which is involved in PD (103). Curli makes up as much as 85% of the extracellular matrix of enteric biofilms, which frequently contribute to cell–cell attachment and bacterial invasion in GI biofilms. This protein is expressed when enteric bacteria are grown under stressful environmental conditions (103,104). The immune system recognizes both the bacterial amyloid curli and human amyloid utilizing the same receptors, such that bacterial amyloid also stimulates the immune system and induces inflammation (105,106). However, these bacterial amyloids can initiate additional α-syn deposits through cross-seeding, potentially indirectly causing neuroinflammation and then neurodegeneration.

Moreover, dysbiosis of bacterial strains in the oral cavity has a critical role in the development of inflammatory diseases such as diabetes mellitus (107,108), rheumatoid arthritis (109,110) and neurodegenerative diseases (111).

Recent studies have shown the relationship between oral microbiota and systemic diseases such as AD and PD. One of the most common oral diseases in adults and the elderly is periodontitis, which increases the dysbiosis of the oral microbiota and the growth of pathogenic strains. Among the bacteria involved in periodontitis disease, *Porphyromonas spp.* and *Aggregatibacter spp.,* as key pathogens, can cause inflammation and biofilm formation in the oral cavity (51,54–56) There is evidence on the role of Pg and its connection with AD. Adam et al. showed the presence of Pg and its virulence factor (protease RgpA) in the PD plasma (112). Studies on animal models have showed that Pg can migrate to the brain and cause neuroinflammation and neurodegeneration (113) .

1-3. Colorectal Cancer

1-3-1. Colorectal Cancer

Colorectal cancer (CRC) is the third most common cancer among humans and the second leading cause of death in the world, two million new cases of this disease are reported every year (114). CRC is the second most common type of cancer in women and the third most common type of cancer in men (115).

In general, CRC can be divided into three subtypes, including hereditary, sporadic, and inflammation-related. Family studies have shown that heretical CRC is caused by mutations in dominant genes such as the adenomatous polyposis coli gene (APC) and mismatch repair genes. This subgroup of CRC accounts for only 10-15% of CRC. Epidemiological studies have shown that 85-95 % of CRC cases are sporadic, usually, it originates below the age of 50. The third subtype of colorectal cancer is associated with inflammatory bowel diseases such as Crohn's disease and ulcerative colitis. This subgroup of cancer comprises only 1% of CRC.

Although the anatomical location of CRC is different in people of different ages and sexes, generally 41% of CRC is in the proximal colon, 22% in the distal colon, and 28% occur in the rectum. In fact, colorectal cancer is a heterogeneous process that is influenced by various factors such as age, inflammation, obesity, physical activity, diet, microbial and environmental exposure, and host immunity.

1-3-2. Gut microbiome and its influence on the colon

As mentioned earlier, one of the key factors playing a role in colorectal carcinogenesis is the environment of the gut microbiome. The gut microbiome constitutes a rich and diverse community of microorganisms (116). This ecosystem is formed before birth and develops to become a fully functioning and stable microbiome within 2 to 3 years. The human intestine is estimated to contain more than 2000 microbial species (117). In addition, the most heavily microbial colonized section of the digestive system is the colon. It is estimated to contain around 70% of the human microbiome (118). These microbial species perform a variety of functions, some of which include metabolizing indigestible food, modulating immune response, and synthesizing nutrients(117). Moreover, it is now evident that the process of acquiring and maintaining gut microbes is fundamental for an individual's health (119). These microbes are vital in the formation of mucosal immunity(120). For example, a class of microbicidal proteins in Paneth cells known as angiogenin-4 can be secreted against microbes into the gut lumen (120). The commensal bacteria residing within the intestine can enhance the intestines' innate immunity by modulating toll-like receptors (TLRs) expression on the immune cells' surface via pathogen-associated molecular patterns leading to the expression of antimicrobial peptides (AMPs) (121). Microbes lead to the activation of T-cells by the nuclear factor-kappa B signaling pathway, which in turn leads to the stimulation of cytokine production and overexpression of costimulatory molecules on the antigen-presenting cells (APCs) (121). In turn, the TLRs activation leads to the induction of islet-derived protein 3 gamma (Reg3g) expression (121). The TLR activation induces the inhibition of inflammatory action contributing to intestinal homeostasis (121). Additionally, microbes within the gastrointestinal

tract can communicate with each other, as well as with the host (119). This communication feature may ultimately result in great effects on disease and health development (119). In addition to the immune response, this communication is also essential for appropriate mucosal function (122). Furthermore, this crosstalk is mediated by metabolites, proteins, and small RNAs (122). In this regard, since the gut microbiome interacts with the host, it contributes to the process of carcinogenesis (118). In addition, the colon is thought to be the most disposed to cancer development upon its comparison to other sections of the digestive tract (116). Alterations in the gut microbiome may contribute to various diseases. This may be due because of their role in metabolism and immune function (117). These alterations are known as dysbiosis, and changes are described in the *Mus musculus* miRNA (122) and may result in the initiation and promotion of colorectal cancer (116). *Fusobacterium nucleatum* and *Escherichia coli*, through the uptake of specific human sncRNA, regulate the expression of microbial genes, thus affecting their growth (122). *Fusobacterium nucleatum* is the most found gut bacterium in CRC patients; this bacterium is a gram-negative anaerobe (123). Furthermore, this bacterium acts as a prognostic biomarker; at higher levels it usually means a shorter overall survival (123). Based on different studies, certain bacteria are found to be greater in number in CRC patients, while others were decreased (123). Bacteria such as *Alistipes, Akkermansia* spp. *Fusobacteria*, *Porphyromonadaceae*, *Coriobacteridae,* and *Methanobacteriales* were found to be increasead in the colon microbiota of a CRC patient (124). More specifically, *Bacteroides fragilis*, *Fusobacterium nucleatum*, *Escherichia coli*, *Enterococcus faecalis*, and *Streptococcus gallolyticus* contribute to CRC (125). An increase in pks (polyketide synthase) island-positive *Escherichia coli* was found in the colon tissues isolated from CRC patients (126). Additionally,

F. nucleatum, an oral bacterium, which will be elaborated on further in the upcoming sections, was also found increased within the colorectal tumors of the patients (126). Moreover, the number of bacteria belonging to *Bifidobacterium*, *Lactobacillus*, *Ruminococcus*, *Faecalibacterium* spp., *Treponema*, and *Roseburia* were decreased (Table 3) (124). Additionally, fecal samples of patients with CRC and healthy individuals were transplanted into the mice in which cancer was promoted chemically. It was recorded that the fecal microbiota from patients with CRC can promote tumorigenesis in the germ-free mice (127,117). It is hypothesized that alterations in colonic flora may create a more favorable microenvironment for tumor development (118). Bacterial micro vesicles may play a role in tumorigenesis, and in fact, their role is underestimated (122). There is a possibility that the extracellular vesicles from the host and microbiota in the intestinal ecosystem promote tumor survival and multi-drug resistance (122). Furthermore, with changes in the gut microbiota, it may be possible to identify the precursor lesion for CRC: colorectal adenoma, for individuals at risk (117). It may be possible to modify the intestinal microbiome to prevent of CRC. The most common bacteria related to CRC are showed in Table 4.

Table 3. Various bacterial species associated with CRC

Bacterial Species	Increase or Decrease in Colorectal Cancer (CRC) Patients
Alistipes *Akkermansia spp.* *Fusobacteria* *Porphyromondaceae* *Coriobacteridae* *Methanobacterials*	Increase
Bifidobacterium *Lactobacillus* *Ruminococcus* *Faecalibacterium spp.* *Treponema Roseburia*	Decrease

Table 4. The most common bacteria related to CRC

Bacteria Related CRC	mechanism
Streptococcus gallolyticus (Sgg)	Induction of host cell proliferation and adhesion to colon cancer cells leading to tumor progression in a mouse model of CRC. Killing the related commensals (e.g., *Enterococci*) leads to microbial imbalance and the development of CRC. Accelerating transformation from pre-malignant to malignant cells by increase in oncogenic targets (c-Myc and cyclin D).
Enterococcus faecalis	Infection of macrophages and induction of aneuploidy and tetraploidy in colonic epithelial cells by release of some mediator Ability to generate reactive oxygen species (ROS) and extracellular superoxide causing damageing colonic DNA and genomic instability Production of metalloprotease resulting to compromise the intestinal epithelial barrier and induce inflammation
Fusobacterium nucleatum	Promotion of pro-inflammatory response in CRC cell lines Activation of β-catenin signaling by TLR4/p21-activated kinase 1 (PAK1) cascade leading to intestinal tumorigenesis Change in the lumen microbial structures, and also promoted colon tumorigenesis by increasing cytokine secretion of cytokines
Enterotoxigenic *Bacteroides fragilis* (ETBF)	Induction of IL17, activation of STAT3, and recruitment of immature cells to lamina propria Disruption of cytoskeleton via binding to E-cadherin
Peptostreptococcus anaerobius	Induction of cholesterol synthesis resulting from TLR2/TLR4 signaling ROS Increasing the expression of pro-inflammatory cytokines and recruiting immunosuppressive myeloid-derived suppressor cells
Escherichia coli	Promotion of DNA double-strand breaks, chromosomal instability in normal cells and inflammation

1-3-3. Oral bacteria and its role in colorectal cancer

The oral microbiome is a complex ecological system containing billions of bacteria with over 700 predominant taxa (128,129). The bacterial taxa colonizing the oral cavity are associated with oral health and oral diseases (128). Oral bacteria have been implicated in the pathogenesis of CRC (122). In fact, various studies indicate that various oral bacteria may play a critical role in the CRC development (130). The intestinal mucosa tissue samples from CRC patiens confirmed higher numbers of *Fusobacterium*, *Peptostreptococcus*, *Mogibacterium* spp., and *Porphyromonas* (129). Subsequent studies in fecal samples from patients with colonic adenomas, also, including *Actinomyces*, *Corynebacterium*, *Haemophilus*, *Mogibacterium*, and *Porphyromonas*, compared to controls. Additionally, in another study, fecal samples from CRC pateints have revealed elevated numbers of oral genera include *Actinomyces*, *Corynebacterium*, *Mogibacterium*, *Haemophilus*, and *Porphyromonas* (129). Furthermore, oral bacterial species such as *Fusobacterium* and *Bacteroides fragilis* are found in both primary and metastatic CRC in humans (122). A high abundance of *Fusobacterium* is believed to be associated with tumor location and regional lymph node metastases (130). Moreover, *Fusobacterium nucleatum* is of specific interest since it has only recently been linked to colorectal cancer (131). Associations between *F. nucleatum* and colorectal cancer in humans have been found in patients during the different disease stages (131). Changes regarding the composition and abundance of oral bacteria in CRC and healthy controls are summarized in Table 5.

Table 5. Increase of oral microbes in colorectal tissue and stool samples of CRC patients

Oral Microorganisms	Methods
Parvimonas, Fusobacterium and *Porphyromonas*	16S rRNA gene sequencing
Porphyromonas asaccharolytica, Fusobacterium nucleatum, Prevotella intermedia, and *Parvimonas micra*	Metagenomics sequencing
Fusobacteria	Next-Generation Sequencing; qPCR
Parvimonas micra, Peptostreptococcus stomatis, Solobacterium moorei, Gemella morbillorum, Fusobacterium nucleatum and *Actinomyces odontolyticus*	Metagenomics sequencing

1-3- 4. *Bacteroides fragilis,* the most important bacteria linked to CRC

The microbiota of the human digestive tract is one of the largest populations of bacteria in the human body (132). Species belonging to the genus *Bacteroides* constitute about 25% of the bacteria in the digestive tract, which are involved in the metabolism of polysaccharides and help in the protective response of the immune system in the digestive tract (133). Among the different species of this genus, *Bacteroides fragilis* is the most abundant opportunistic anaerobic bacterium isolated from clinical samples. This bacterium constitutes 0.5-1% of the natural flora of the digestive system and if it reaches other anatomical sites of the body, it causes various infections such as abdominal infections, abscesses, and bacteremia with a mortality rate of about 19% (133). During the last few years, the increase of antibiotic resistance in *Bacteroides fragilis* is considered an important health challenge worldwide (134).

Bacteroides fragilis has two variants, Enterotoxigenic *Bacteroides fragilis* (ETBF) and non-Enterotoxigenic *Bacteroides fragilis* (NTBF) (110). Outside the digestive tract, this bacterium acts as an opportunistic pathogen and causes infection (133,134) .

About 30% of *Bacteroides fragilis* strains in the digestive system have toxin coding genes. Studies show that toxin-producing strains are more pathogenic than non-toxin-producing strains and are associated with various diseases such as diarrhea, irritable bowel syndrome (IBS), and colorectal cancer (CRC) (135). This bacterium is attached to the tissue surface and causes disease through some pathogenic factors such as capsule, fimbriae, biofilm, toxin production, and some enzymes (133).

1-3-4-1. Virulence factors of *Bacteroides fragilis*

Although *B. fragilis* constitutes about 0.5% of the natural flora of the gastrointestinal tract, it is the most abundant anaerobic bacterium isolated from clinical samples (133). Recent studies show the connection of some pathogenic factors of this bacterium with diseases such as diarrhea and colorectal cancer (136). Pathogenic factors in this bacterium are divided into three general categories: a) Factors effective in binding to the host tissue, such as fimbriae and agglutinin; b) protective factors against the immune system, such as capsule and lipopolysaccharide; c) destructive factors of the host tissue, such as hyaluronidase and chondroitin sulfatase. The main important virulence factors of *Bacteroides fragilis* are toxin and biofilm (133).

1-3-4-2. The toxin of *Bacteroides fragilis*

Toxin-producing strains have a pathogenicity island (PAI) of 6 kilobases, which is inserted in the transposon (CTn86) of 65 kilobases and placed on the bacterial chromosome (135). This pathogenic island has at least two pathogenic toxin (*bft*) and metalloprotease (mpII) genes. This region is present only in toxin-producing strains and its C+G percentage (35%) is lower than other parts of the chromosome (C+G 43%), so this region (called pathogenicity island, BfPAI) was acquired by these strains (137,138).

Non-toxin-producing strains do not have the BfPAI pathogenicity island, but in some of them a flanking region is observed, which enables the transfer and displacement of the pathogenicity island from toxin-producing strains to non-toxin-producing strains. Based on chromosomal characteristics and toxin coding genes, three different patterns can be seen in *Bacteroides fragilis* strains; Pattern I: toxin-producing strains containing flanking region and *bft* gene. Pattern II: Non-toxin-producing isolates whose chromosomes are intact. This pattern lacks flanking region and *bft* gene. Pattern III: Non-toxic producing strains that contain flanking region inside the chromosome. In this pattern, there is no pathogenicity island and *bft* gene (139) (Figure 6).

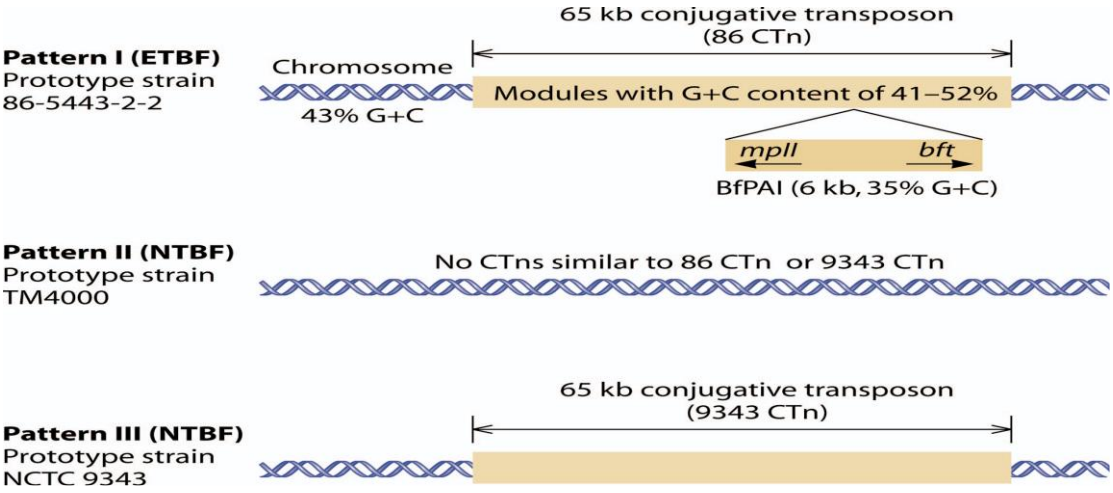

Figure 6. Pattern I, II and III of *Bacteroides fragilis*. Pattern I has CTn86, Pattern II does not have CTn86, Pattern III has CTn9343

Toxin gene (*bft*) has 1191 nucleotides and a C+G of 39%. There are three alleles of the *bft* gene (*bft-1*, *bft-2*, and *bft-3*), according to which there are three isotypes of this toxin, BFT-1, BFT-2, and BFT-3. Toxin-producing strains may have two copies of the same isotype at the same time, but the simultaneous presence of different isotypes in one strain has not been reported (137,138).

Isotype I and II of this toxin (BFT) are resistant to trypsin in a wide range of pH. The toxicity of these isotypes is different from each other; So, the highest toxicity start from BFT2>BFT1>BFT3, in order. Although isotypes have been reported from different places, isotype I and then isotype II are the most common isotypes known in different parts of the

world. Also, isotype III has been reported in some parts of the world, for example in East Asia, such as Iran, Japan, and Vietnam (133,137,138).

BFT toxin expresses a holotoxin of 397 amino acids with a molecular weight of 44.5 kilodaltons (Figure 7). This holotoxin consists of three protein domains including a signal peptide, proprotein, and mature protein.

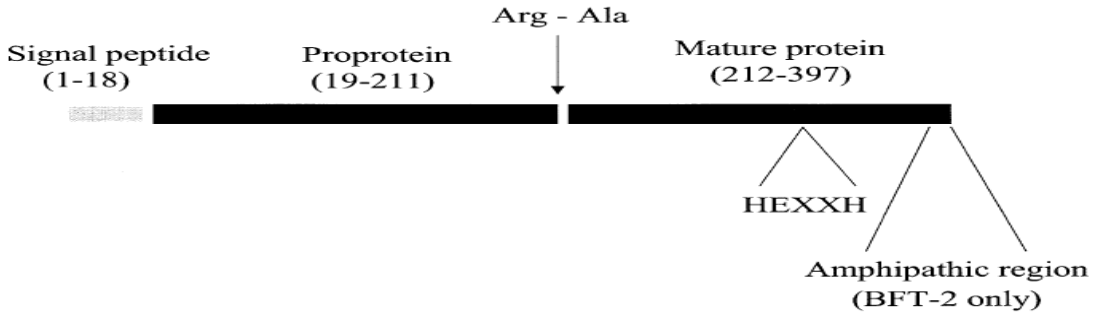

Figure 7. Structure of the BFT toxin. The toxin protein consists of three parts: signal peptide region, proprotein and mature protein.

The second signal peptide consists of 18 amino acids. This domain is necessary for the transfer of holotoxin to the bacterial membrane. Holotoxin is broken by an unknown protease in the Arg-Ala region and the mature form of the toxin is released and exits the bacterium. The mature toxin has a zinc-dependent metalloprotease motif (HEXXHXXGXXH), which confirms the proteolytic activity of this toxin. Zinc chelators can reduce its activity by 90%. In addition to autoproteolytic activity, this protein also has proteolytic activity on actin, gelatin, and casein substrates. In BFT2, there is a region containing 20 carboxyl amino acids that creates an

amphipathic structure. This region plays a role in placing the toxin in the cell membrane and creating an ion channel. The isoelectric point of pure toxin is equal to 4.5 and it is stable in a wide range of pH and temperature (137,138).

Bacteroides fragilis toxin, by binding to its unknown receptor on the surface of epithelial cells, causes rapid cleavage in the E. cadherin protein in an ATP-dependent state, which subsequently leads to a decrease in the function of membrane junctions and an increase in the permeability of barriers on the surface of epithelial cells. In the continuation of this process, β-catenin and NFκB signaling pathways are activated and increase the activation of pro-inflammatory signals. As a result of this function, the Epithelial-Mesenchymal-Transition (EMT) process is activated, which plays a key role in the stages of cancer development. Also, this toxin probably increases the level of reactive oxygen species (ROS) and damages the host's DNA (135,140).

1-3-4-3. Biofilm

In humans, about 80% of bacterial infections are caused by biofilm-forming organisms. Biofilm is a community of microbial cells surrounded by a matrix consisting of polysaccharide, protein, and nucleic acid (141,142). One species or a mixture of several microbial species is found within the biofilm community. The presence of a matrix or coating around the microbial cells makes the microorganisms have a stronger and more stable connection to living and non-living surfaces. In addition, the presence of the matrix reduces the possibility of penetration and diffusion of antibiotics and the effect on the microbes in the biofilm and reduces the replication, division of the wall and the growth of bacteria, which results in the lack of effect

of effective antibiotics on the wall and antibacterial substances (141,142). In the biofilm state, the life of bacteria changes from a free life to a closed life, which leads to a decrease in the response to environmental stress, an increase in the horizontal transfer of resistance genes between bacteria, and subsequently, an increase in the occurrence of antibiotic resistance (141).

In addition to the role of biofilm in increasing antibiotic resistance, new studies show that bacterial biofilm can make clinical manifestations more severe in patients with ascending colon cancer than in patients with descending colon cancer (143,144). The biofilm of bacteria directly destroys the connections between epithelial cells and increases the permeability of these cells, increases the metabolism of polyamines and their acetylation, increases the production of IL6, activates the STAT3 signaling pathway, and as a result increases pro-inflammatory/damaging responses. Two hypotheses have been proposed regarding the relationship between bacterial biofilm and colorectal cancer. The first hypothesis states that bacterial invasion is present in the biofilm of all colorectal cancers, while this invasion was not observed in colorectal cancer without biofilm. In the second hypothesis, electron microscopy and FISH techniques showed that biofilm formation is abundant (90-100%) in ascending colon cancer, but less biofilm is present in descending colon cancer (15 %), while patients with ascending colon cancer have more severe clinical manifestations than patients with descending colon cancer. *Bacteroides* and *Prevotella* are the most common bacteria known to create biofilm in the digestive tract (145,146).

1-3-4-4. Infection caused by *Bacteroides fragilis*

Anaerobic bacteria are the cause of 0.5-11.8% of positive blood cultures and their mortality is 35-15%. *Bacteroides fragilis* group is the most common (70%) anaerobic bacteria associated with blood infections (147). *Bacteroides fragilis* is also associated with diseases such as irritable bowel syndrome, diarrhea, and colorectal cancer (148,149).

Abdominal infection is the most common infection caused by *Bacteroides*. After the destruction of the intestinal wall due to various reasons such as rupture, surgery, malignancy, appendicitis, etc., the flora of the digestive system enters the sterile parts of the body and causes infection. In the early stages of infection (first 20 hours), aerobic bacteria such as *Escherichia coli* cause infection and by destroying tissue and reducing the oxidation-regeneration potential, they favor the growth of anaerobic bacteria (133). As a result, anaerobic bacteria play an important role in the chronic stages of the disease. Moreover, *Bacteroides fragilis* and *Escherichia coli* are the most common anaerobic and aerobic bacteria isolated from gangrenous and perforated appendicitis (133).

Inflammatory bowel disease includes Crohn's disease and ulcerative colitis, which occurs chronically in the digestive system, especially the large intestine (148). The main and exact cause of this diseases is not known, but it seems that a set of genetic, immune, microbial, or even lifestyle factors play a role in its occurrence (150). ETBF, by releasing the toxin, increases the permeability of the mucous membrane on the surface of the epithelial cells, and in the continuation of this process, the inflammatory pathway is activated (151). During this process, the entry of various gastrointestinal bacteria into the gastrointestinal epithelial cells is

increased, as a result of which, a large number of bacterial antigens are presented to the immune cells of the gastrointestinal tract and tissue invasion occurs. This process can play a role in the occurrence of IBD (151).

In 1984, Myers et al. described an association between severe diarrheal disease in lambs and enterotoxin-producing strains of *Bacteroides fragilis*. This new animal enteropathogen was detected with the ability to induce a secretory response in the ileal loops of sheep and calves. For the first time in 1987, the isolation of ETBF from human feces with diarrhea was described (152).

Bacteroides fragilis toxin affects the actin filaments (F) of the epithelial cells of the digestive tract and leads to their rearrangement; As a result, the structure of the cells is changed, the cell-to-cell connection is lost, the cells become round and swollen and the cell volume increases, cell secretory responses begin and finally diarrhea occurs (153). Studies conducted on HT29/C1 cells in laboratory conditions have shown that toxin breaks G-actin monomers, which changes the cytoskeleton and then the function of digestive epithelial cells. Also, by stimulating the secretion of IL-8, immune cells, especially leukocytes, move to the submucosa, causing an inflammatory response, fluid secretion, and diarrhea (153,154). ETBF-related diarrhea is watery and self-limiting and usually lasts between 1 and 4 weeks and is seen in all age groups, especially children (152).

Studies show that the clone's microbiota plays a significant role in the development of this disease. Bacteria such as *Bacteroides fragilis*, *Fusobacterium nucleatum*, *Clostridium septicum*, *Enterococcus faecalis*, *Helicobacter pylori*, *Streptococcus bovis,* and *Escherichia*

coli have played a role in causing colorectal cancer (155). The release of pathogenic factors and bacterial toxins through DNA damage leads to an increase in the risk of cancer. In addition, the release of reactive oxygen species (ROS) and the expression of cytokines and chemokines after bacterial infection can cause ROS-mediated DNA damage (156,157).

Studies have shown that there is a significant correlation between the presence of ETBA in stool samples and colorectal biopsies of people with colorectal cancer (139,151). *Bacteroides fragilis* toxin, by binding to its unknown receptor on the surface of epithelial cells, causes cleavage in the E. cadherin protein in an ATP-dependent manner, following this process, β signaling pathways. catenin and NFκB are activated and increase the activation of pro-inflammatory signals. As a result of this function, the Epithelial-Mesenchymal-Transition (EMT) process is activated, which plays a key role in the stages of cancer development. *Bacteroides fragilis* toxin is also effective in increasing the level of reactive oxygen species (ROS) and damaging the host's DNA. Recent studies indicate the ability of *Bacteroides fragilis* biofilm formation in the development of colorectal cancer (137,138,140). The biofilm of bacteria causes the resistance of bacteria and their attachment to the epithelium of the digestive tract. On the other hand, biofilm can change the metabolism of cancer and cause cell proliferation and growth and development of colorectal cancer (141,144).

Chapter 2: Humoral response to immunogenic microbial peptides in Rheumatoid arthritis Patients

2-1. Aim of study

Rheumatoid arthritis (RA) is a chronic systemic autoimmune disorder affecting 0.5–1% of people worldwide (158). The etiology of RA is not well understood. However, several triggers, such as microbial infection, have been identified as risk factors for initiating and exacerbating the disease in genetically susceptible individuals (159). Recent studies have suggested that mucosal surfaces, specifically the periodontium, the gut, and the lungs, might be privileged sites of autoimmunity initiation in RA (160, 161). However, a comprehensive demonstration of the role of the immune response against multiple pathogens in RA pathogenesis is still lacking. Therefore, this study aimed to evaluate the prevalence and magnitude of the immune response against different highly immunogen microbial peptides derived from *Porphyromonas gingivalis*, Pg (RgpA, Kpg), *Aggregatibacter actinomycetemcomitans*, Aa (LtxA1, LtxA2), *Mycobacterium avium* subsp. *paratuberculosis*, MAP (MAP4027), Epstein-Barr virus, EBV (EBNA1, EBVBOLF), and human endogenous retrovirus, HERV (HERV-W env-su) in RA patients and compared the results with the healthy controls (HCs).

2-2. Materials and Methods

2-2-1. Study Population and Blood Collection

Consecutive unselected RA patients attending the outpatient Rheumatology Unit at the Department of Clinical and Experimental Medicine of the University of Sassari (Italy) during the period between 2019 and 2020 and fulfilling the 2010 American College of Rheumatology classification criteria (162,163) were enrolled in the study. To evaluate the presence of correlations between humoral immune response and RA-specific features, the following disease-specific scores, disease descriptors, and treatment data were collected: current steroid treatment; cumulative dosage of steroids (last 12 months); current treatment with biological or targeted-synthetic disease-modifying anti-rheumatic drugs (b/tsDMARDs); current use of methotrexate; cumulative; C-reactive protein (CRP) concentrations, mg/dL; erythrocyte sedimentation rate (ESR), mm/h; Disease Activity Score-28 (DAS-28); Clinical Disease Activity Index (CDAI). In addition, as a control group, we enrolled age- and sex-matched healthy blood donors attending the local blood transfusion service. The Ethics Committee of the University of Cagliari approved this study (PG 2018/5643). Informed consent was obtained from all individual participants.

2-2-2. Peptides

Peptides derived from Pg ($RgpA_{800\text{-}81}$ and $Kpg_{328\text{-}339}$) and Aa ($LtxA1_{429\text{-}445}$ and $LtxA2_{64\text{-}80}$) were designed using the Immune Epitope Database and Analysis Resource (IEBD) and synthesized at >95% purity (LifeTein, South Plainfield, NJ, USA). Peptides derived from EBV ($EBNA1_{400–413}$, $BOLF1_{305–320}$), MAP ($MAP\_4027_{18\text{-}32}$), and HERV-W (HERV-W env-su 93–108) were selected from previous studies (63,164,165). All peptides were dissolved in dimethyl

sulfoxide (DMSO) and stored at −80 ◦C in single-use aliquots (10 mM). Table 6 shows the amino acid sequence of the peptides.

Table 6. Immunogenic peptides used as antigens in the ELISA assay

Peptides	Epitope Sequence	Epitope Position
$RgpA_{800-812}$	ADPVVTTQNIIVT	800-812
$Kpg_{328-339}$	VTDLYYSAVDGD	328-339
$LtxA1_{429-445}$	AWENKYGKNTFENGYDA	429-445
$LtxA2_{64-80}$	TALIKAAQKLGIEVYHE	64-80
MAP_4027_{18-32}	AVVPVLAYAAARLL	18-32
$EBNA1_{400–413}$	PGRRPFFHPVGEAD	400-413
$BOLF1_{305–320}$	AAVPVLAFDAARLRLLE	305-320
HERV-W $_{env\text{-}su\ 93–108}$:	NPSCPGGLGVTVCWTY	93-108

2-2-3. Enzyme-Linked Immunosorbent Assay (ELISA)

In brief, 50 µL of each peptide at a concentration of 10 µg/mL in 0.05 M carbonate/bicarbonate buffer, at pH 9.5 (Sigma-Aldrich, St. Louis, MO, USA), were coated in 96-well plates (Thermo Fisher Scientific, South San Francisco, CA, USA) and incubated at 4 ◦C for 1 day. The coating solution on plates was removed and blotted on paper towels. Plates were incubated for one hour at room temperature (RT) in a blocking solution with 200 µL of 5% non-fat dried milk (5 g non-fat dried milk powder in 100 mL 1× PBS; Sigma-Aldrich, St. Louis, MO, USA) and washed twice in a solution with 0.05% Tween-20 and phosphate-baffered saline (1× PBS-T; Sigma-Aldrich, St. Louis, MO, USA). Plasma samples (diluted 1:100; 1 µL plasma to 99 µL

1× PBS-T) were added, and the plates were incubated for 2 h at RT. Then, each plate was washed five times in 1× PBS-T and incubated for one hour at RT with 100 µL of PBS and anti-human IgG alkaline phosphatase conjugated antibody produced in goat (1:1000; Sigma-Aldrich, St. Louis, MO, USA). Plates were washed five times in 1× PBS-T and incubated in a dark environment for eight to ten minutes in milli-Q water and p-nitrophenyl phosphate (One p-290 nitrophenyl phosphate tablet and one Tris buffer tablet were dissolved in 20 µL of milli-Q water; Sigma-Aldrich, St. Louis, MO, USA), and the optical density (OD) was read at a wavelength of 405 nm using a microplate reader (Molecular Devices, Sunnyvale, CA, USA). All samples were repeated in duplicate, and positive controls were used for each peptide. The positive sample was a sample previously tested for strong reactivity to the selected peptides, and not reactivity to irrelevant peptides, in order to verify the binding specificity. The negative controls were samples from patients previously tested for the same peptides which had a weak reaction. Moreover, a technical negative control was added, where no sera was added into the peptide-coated wells. The OD values were normalized to a highly positive control serum with absorbance reactivity set at 1.0 OD. Results are expressed as means of duplicate 405 nm OD values. Intra-assay variation was calculated based on the mean of the CV percentages (%CVs) obtained from OD measurements repeated two times for each serum in the same plate. Inter-assay variation was calculated based on the mean of %CVs obtained from experiments repeated two times for each serum in two separate plates on two different days. Inter-assay variation was done for 30 serum samples with high, low, and moderate ODs.

2-2-4. Statistical Analysis

The results were expressed as a mean of three separate experiments, and the analysis was performed using GraphPad Prism version 8.0 software (San Diego, CA, USA). A T-test and

Fisher's exact test were performed to analyze the matching age and sex in RA patients with HC group. The Mann–Whitney test was performed for non-parametric comparisons. A value of $p < 0.05$ was considered significant. The cut-off for positivity was established in the interval 0.35–0.52 (AU)/mL based on the receiver operating characteristic (ROC) curve with ≥90% specificity and 95% confidence interval. In addition, Fisher's exact test was employed to compare the percentages of positive subjects in the two groups. The correlation between OD values obtained by the ELISA test from different peptides, and the RA features, RA activity (DAS-28), systemic inflammation (ESR, CRP), and type of immunosuppressive treatment was explored by bivariate correlation and regression analysis with Stata.

2-3. Results

This retrospective case-control study examined a set of serum samples derived from 148 RA patients (123 females, 25 males; median ± SD: 65.2 ± 9) and 148 healthy controls (120 females, 28 males; median ± SD: 63.5 ± 7). The demographic and clinical features of all subjects involved in the present study are summarized in Table 7.

Table 7. Demographic and clinical characteristics of groups

	Rheumatoid arthritis n=148	**Healthy controls n=148**	**p-value**
Age, years	65.2(0.7)		
Female, n(%)	123(83.1)		
Disease duration, months	108(8.2)		
ACPA, (%)	74.2		
RF, (%)	81.0		
DAS28	3.9(0.1)	/	
CDAI	10.9(0.7)	/	
CRP, mg/l	3.7(2.4)	/	
ESR, mm/h	32.3(1.8)	/	
Steroid use, n(%)	37.1	/	
DMARDs use, (%)	70.2	/	
Methotrexate use, (%)	55.7	/	
TNFi use, (%)	23.4	/	
Abatacept use, (%)	4.7	/	
Tocilizumab use, (%)	5.4	/	

Values are mean (1DS) and proportions. DAS28, disease activity score 28 joints; CDAI, clinical disease activity index; ACPA, anti-citrullinated peptide antibodies; RF, rheumatoid factor; CRP, C-reactive protein concentrations, mg/dL; ESR, erythrocyte sedimentation rate, mm/h; DMARDs, synthetic disease-modifying anti-rheumatic drugs; TNFi, tumor necrosis factor inhibitors. RA, rheumatoid arthritis; SLE, systemic lupus erythematosus; SSc, systemic sclerosis; HCs, healthy controls. DAS-28, disease activity score-28 joints; SLEDAI, systemic lupus erythematosus disease index 2000; ESCsG-AI, European Scleroderma Research Group Activity Index; ESSDAI, EULAR Sjogren's syndrome disease activity index.

No significant difference was observed between the age and sex of HC compared to RA patients' groups ($p > 0.077$ and $p > 0.76$). The variation was from 7.2% to 9.6% for intra-assay and from 10.1% to 13.7% for inter- assay.

Among the tested immunogen peptides, the highest titer of antibodies was observed against the MAP4027 peptide, corresponding to a seroreactivity of 30.4% (n = 45) among RA patients and 10.1% (n = 15) in HCs (AUC = 0.736, $p < 0.0001$) (Figure 8A, Figure 9). It was also reported a strong Ab response against both *P. gingivalis*-derived peptides in RA sera compared with HCs that reached statistical significance for the RgpA peptide ($p < 0.0001$) (Figure 8 B,C). Therefore, 36 (24.3%) out of 148 RA sera and 14 (9.4%) out of 148 HCs sera were anti-RgpA positive (AUC = 0.705, $p = 0.001$) (Figure 8B, Figure 9). On the contrary, the humoral immune response against *A. actinomycetecomitans*-derived peptides was not significantly different between groups (Figure 8D,E). Similarly, as expected, the titer and prevalence of Abs against EBV (EBNA1, BOLF1) was significantly higher in RA sera than in the counterpart ($p < 0.0001$) (Figure 8F,G). This corresponds to 38 (25.7%) and 28 (18.9%) of RA sera being positive to BOLF and EBNA1 compared with 12 (8.1%) and 14 (9.4%) of control sera, respectively (AUC = 0.647, and AUC = 0.736, respectively; $p < 0.0001$ and $p = 0.029$, respectively) (Figure 8F,G; Figure 9). In addition, Abs titers against peptides derived from HERV-W (HERV-W env-su) were significantly higher in RA than in HCs ($p < 0.0001$) (Figure 8H). This figure corresponds to 20.3% (n = 30) of RA sera seropositivity against anti-HERV-W env-su compared with 9.4% (n = 14) of its counterpart (AUC = 0.736, $p < 0.0001$; $p = 0.013$) (Figure 8H, Figure 9). In total, 53 (35.8%) out of 148 RA sera and 93 (62.8%) out of 148 HCs were negative for all tested peptides ($p < 0.0001$). There was no significant difference between

OD values in patients < 1 year disease duration compared with patients >1 year disease duration ($p > 0.05$).

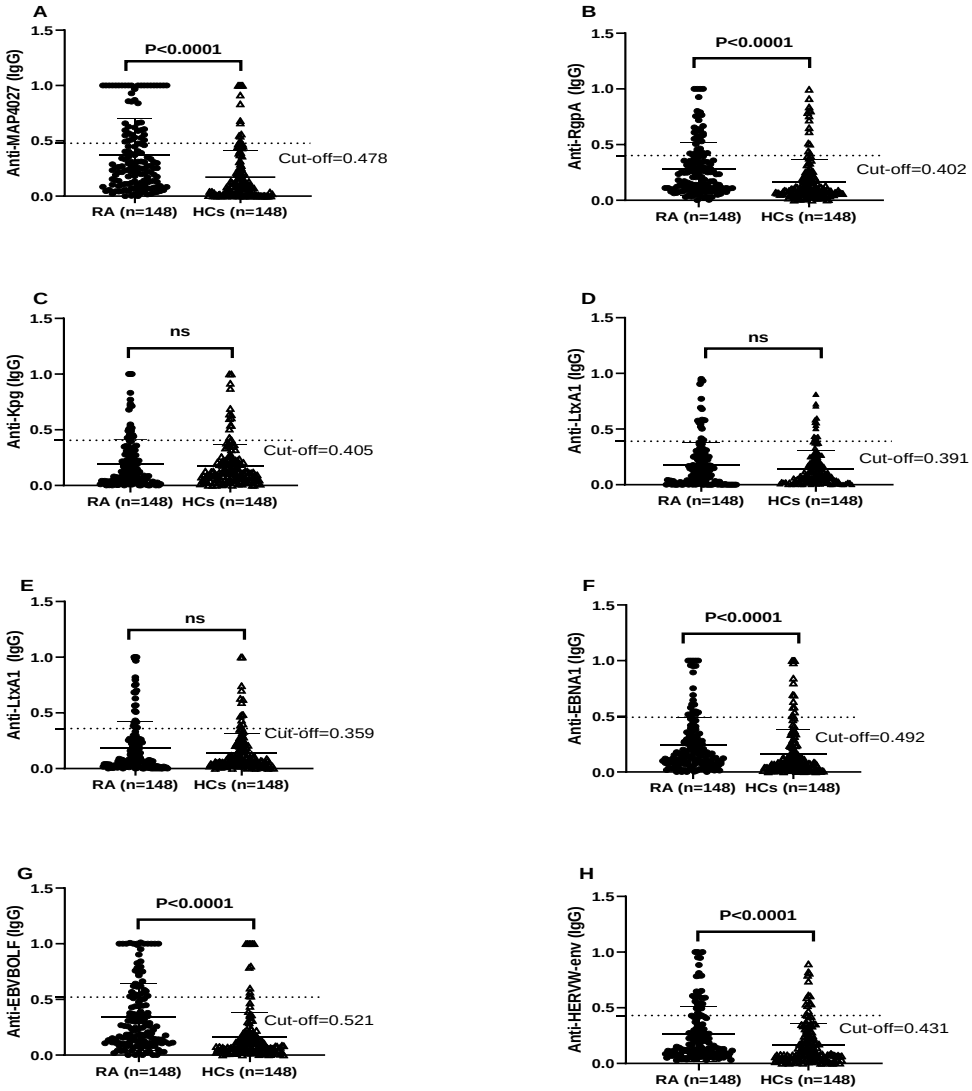

Figure 8. ELISA-based analysis of Abs reactivity against pathogenic microorganism-derived peptides in RA patients and HCs. Sera samples were tested against plate-coated (A) MAP4027, (B) RgpA, (C) Kpg, (D) LtxA1, (E) LtxA2, (F) EBNA1, (G) EBVBOLF, and (H) HERV-W env peptides. Dashed lines represent thresholds used to assess the samples' positivity (cut-off value based on the ROC curve with ≥90% specificity and 95% confidence interval).

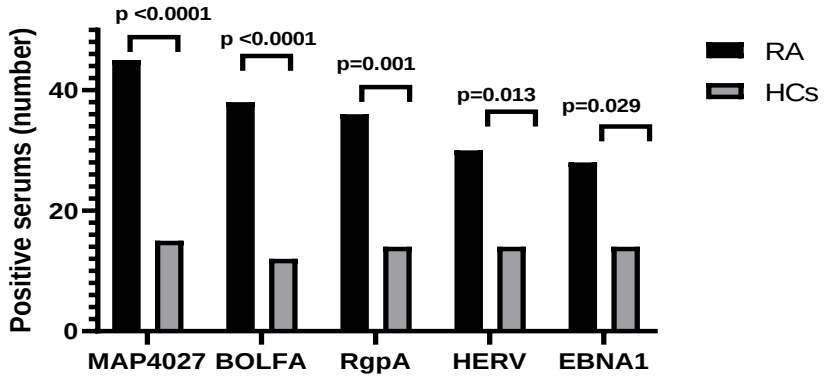

Figure 9. Serum reaction positivity (number) of MAP4027, BOLFA, RgpA, HERV and EBNA1 peptides in RA and HCs serums (Fisher's exact test: $p < 0.05$)

Of note, we found an increased titer and prevalence of antibodies against LtxA1 and LtxA2 in seropositive vs. seronegative RF among RA patients (Figure 10). The correlation analysis between remaining RA predictors and Abs was not significant.

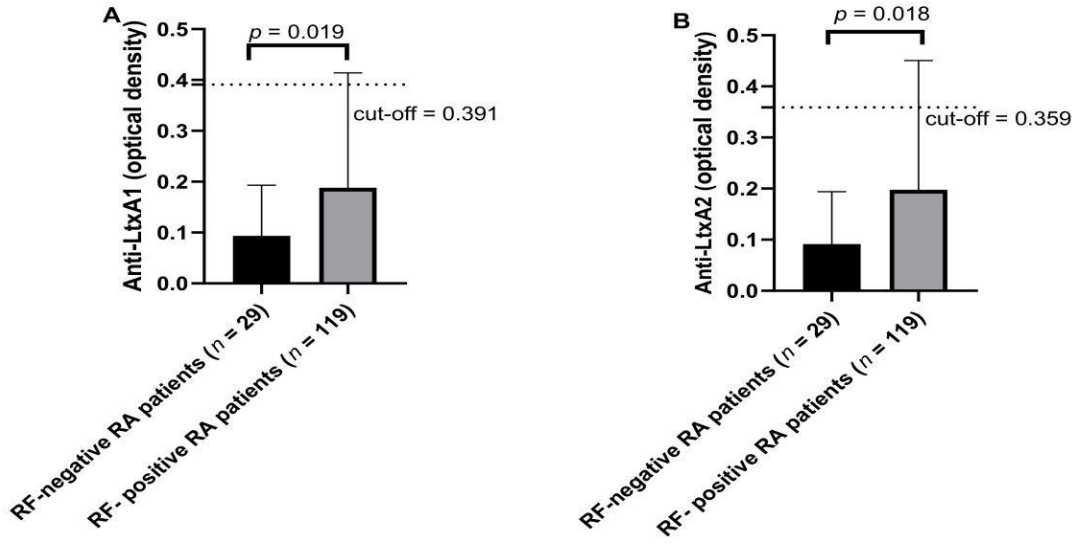

Figure 10. Abs response against LtxA1 (A) and LtxA2 (B) in RF-positive RA patients vs. RF-negative RA patients. The black bars represent the average ±S, dashed lines represent thresholds used to assess the samples' positivity.

There was a significant correlation between all Abs ($p < 0.05$). Higher correlation was observed between anti-LtxA2 and anti-Kpg (r = 0.652, $p < 0.0001$) followed anti-HERV-W andanti-LtxA2 (r = 648, $p < 0.0001$), anti-LtxA1 and anti-LtxA2 (r = 641, $p < 0.0001$), antiMAP4027 and anti-HERV-W (r = 0.637, $p < 0.0001$), anti-Kpg and anti-HERV-W (r = 0.635, $p < 0.0001$), anti-HERV-W and anti-RgpA (r = 0.632, $p < 0.0001$), anti-LtxA1 and anti-Kpg (r = 0.628, $p < 0.0001$), and anti-HERV and anti-LtxA1 (r = 0.627, $p < 0.0001$). The heatmap (Figure 11) shows the r values between pairs of epitopes.

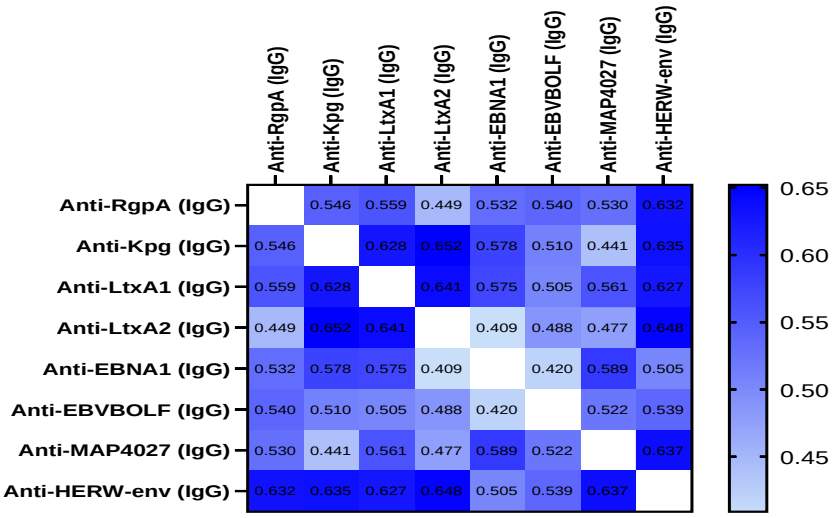

Figure 11. Heatmap displaying the r values obtained from Spearman correlation analysis performed among derived peptides.

2-4. Discussion

Several environmental factors, including infections, have been associated with an increased risk of RA (166–168). We tested the humoral response against selected peptides derived from pathogens previously associated with RA, including *P. gingivalis*, *A. actinomycetemcomitans*, MAP, EBV, and HERV-W in RA patients in comparison to HCs. We found that the highest

prevalence of humoral response was against MAP, suggesting a contributing role for this microorganism in RA development. After colonization of MAP in the host, it can evade the immune system through different mechanisms such as molecular mimicry, which is a condition that may lead to the host immune system targeting self-epitopes (166). This bacterium is the causative agent of paratuberculosis, which is a disease predominately found in ruminants that may spread to human hosts by water and foodborne transmission routes (169). This pathogen is associated with Crohn's disease and other autoimmune diseases in humans (169). The potential role of MAP in RA has been already highlighted in a previous study in which RA sera showed a remarkably frequency of reactivity against PtpA ($p < 0.001$) and PknG ($p = 0.0054$) peptides in comparison to HCs (30). A significant linear correlation between the number of swollen joints and the concentrations of antibodies against PtpA was also found ($p = 0.018$) (30). Accordingly, we previously demonstrated significant cross-reactivity between MAP (MAP4027) and interferon regulatory factor 5 peptide (IRF5424–434) in RA (63). In this study, the Ab response against peptides derived from lysogenic phase (BOLF1) and latent phase (EBNA1) proteins of EBV was significantly higher in RA patients compared with the control group. This result support previous evidence regarding the role of EBV in RA (170,171). Of note, EBV is potentially involved in the activation and stimulation of HERV-K expression (172–174). For the first time, we found a strong reactivity in RA against the selected surface epitope of HERV-W (HERV-W env-su 93–108). These results are in line with other studies reporting increased humoral responses to EBV and HERV-K peptides in Sardinian patients with different autoimmune diseases, including RA (170,175). Interestingly, our results have shown high correlation between the HERV-W env peptide and LTX2, MAP4027, Kpg, and RgpA, which probably supports the hypothesis that these pathogens might act synergically

to induce autoimmunity through a common target. Furthermore, we found that RA compared with HCs show a higher prevalence of humoral response against peptides derived by periodontal pathogens, which was statistically meaningful for the anti-RgpA IgG peptide. This is in line with findings from epidemiological studies suggesting a potential pathogenic link between periodontitis and RA (51–53). *P. gingivalis* and *A. actinomycetecomitans* are the most common reported pathogens in periodontitis, and they can contribute to RA autoantibody production through various mechanisms: directly by post-translation modification of human protein (by the PPAD enzyme of *P. gingivalis*) or indirectly by neutrophil osmotic lysis (leukotoxin of Aa) (51,54–56). In this study, we found a positive significant correlation between anti-LtxA2 and anti-Kpg, and also, anti-LtxA1 and anti-LtxA2 with RF, suggesting that *P. gingivalis* and *A. actinomycetecomitans* may cooperate in inducing immunity against periodontal and synovial self-antigens. Although data from in vitro and in vivo studies on the interaction between these two pathogens are scarce, co-infection seems to be associated with poor RA prognosis (176). One potential limitation of the current study is the absence of RA patients in the preclinical period for the evaluation of antibodies against our peptides. Moreover, a lack of anti-CCP titer and its quantitative evaluation among RA patients is another limitation of this investigation. In conclusion, this study demonstrated a link between different pathogens and RA. The exposure to these pathogens, either in the preclinical period (before the disease onset) or during the clinical phase, is likely to have a pivotal role in the emergence and maintenance of RA. Further investigations are needed to confirm these results in larger groups of RA patients.

Chapter 3: Humoral response to immunogenic microbial peptides in Parkinson's disease Patients

3-1. Aim of study

Parkinson's disease (PD) is a neurodegenerative disorder with unknown ethiology characterised by the accumulation of misfolded α-synuclein (α-syn) in substantia nigra pars compacta in brain (177,178). In the past decade, it has become increasingly apparent that gut microbiota and microbial pathogens may contribute to neurodegenerative diseases directly or via immune activation (179). Interesting evidence showed that curli-producing bacteria in the gut microbiota could promote α-syn aggregation in both the enteric nervous system (ENS) and brain through the immune system activation and cross-seeding (180).

A comprehensive demonstration of the role of the humoral immune response against bacterial amyloid and multiple pathogens in PD pathogenesis is still lacking. Therefore, this study aimed to evaluate the prevalence and magnitude of the immune response against immunogen peptides derived from human α-syn$_{100-114}$ and bacterial amyloid curli (Curli$_{133-141}$), *Porphyromonas gingivalis*, Pg (RgpA$_{800-812}$, Kpg$_{328-339}$), *Aggregatibacter actinomycetemcomitans*, Aa (LtxA1$_{429-445}$, LtxA2$_{64-80}$), *Mycobacterium avium* subsp. *paratuberculosis*, MAP (MAP3865c $_{125-133,}$ MAP1,4-a-gbp$_{157-173}$ and MAP_4027$_{18-32}$), Epstein-Barr virus (EBNA1$_{400–413}$, BOLF$_{1305–320}$), and Herpes Simplex Virus HSV-1 (UI42$_{22-36}$) in PD patients compared with the general population.

3-2. Materials and Methods

3-2-1. Study Population and Blood Collection

The current case-control study examined two populations, the PD patients, and the healthy controls (HCs) during the period between 2021 and 2022. This study was approved by the Ethics Committee of the University of Sassari in 2019 (prot 2159/CE). Informed consent was obtained from all individual participants. All patients were diagnosed based on medical history, clinical symptoms as well as neurological and physical examination. All data on age, gender, and HY scale (Hoehn and Yahr Scale) were retrieved from patients' records. During the same period, healthy controls, with no personal or familial history of diagnostic PD, whose age and gender-matched with those of the patients were included in the study as controls. Blood samples were collected from participants referred to the *Parkinson* Institute hospital at the Azienda Ospedaliera Universitaria of Sassari, and sera were separated according to the standard method (181) and preserved at a –80 ◦C freezer.

3-2-2. Peptides

Synthesis of an immunogenic peptide derived from bacterial amyloid curli (Curli $_{133\text{-}141}$: NSSVNVTQV) was designed using the Immune Epitope Database and Analysis Resource (IEBD) and synthesized at >95% purity (LifeTein, South Plainfield, NJ, USA).

Immunogenic peptides derived from human amyloid (α-syn$_{100\text{-}114}$), *Porphyromonas gingivalis*; Pg (RgpA$_{800\text{-}812}$, Kpg$_{328\text{-}339}$), *Aggregatibacter actinomycetemcomitans* (LtxA1$_{429\text{-}445}$, LtxA2$_{64\text{-}80}$), *Mycobacterium avium* subsp. *paratuberculosis* (MAP3865c$_{125\text{-}133,}$ MAP1,4-a-gbp$_{157\text{-}173}$ and MAP_4027$_{18\text{-}32}$), Epstein-Barr virus (EBNA1$_{400–413}$, BOLF$_{1305–320}$), and Herpes Simplex Virus 1 (UI42$_{22\text{-}36}$) were selected from peptides used in previous studies (182–185). All

peptides were resuspended in dimethyl sulfoxide (DMSO) at a final concentration of 10 µg/mL and stored at −80 ◦C until use.

3-2-3. Enzyme-Linked Immunosorbent Assay (ELISA)

Indirect ELISA was performed to investigate the specific IgG antibodies against the designed peptides according to the method mentioned in chapter 2, page 41.

3-2-4. Statistical Analysis

Data distribution was analyzed using the D'Agostino–Pearson omnibus normality test and therefore Shapiro–Wilk test. Non-parametric data were analyzed using the Mann–Whitney U test to compare abs against different peptides in PD patients in compared to HCs. The student's t-test and Fisher's exact test were applied to compare the matching age and sex in PD patients with the HCs group. A value of $p < 0.05$ was considered significant. Optimal cut-off points to discriminate between positive and negative samples were identified based on the receiver operating characteristic (ROC) curve with ≥ 90% specificity and 95% confidence interval. In addition, Fisher's exact test was employed to compare the percentages of positive subjects in the two groups. The correlation between OD values obtained by the ELISA test from different peptides was explored by bivariate correlation and regression analysis with Stata. In addition, the correlation analysis between the HY scale and OD values obtained by the ELISA test from different peptides was explored by bivariate correlation and regression analysis.

3-3. Results

This case-control study investigated a set of serum samples derived from 51 PD patients (27 females, 24 males; median ± SD: 74.05 ± 8.6) and compared their results with 58 HCs (30

females, 28 males; median ± SD: 72.5 ± 8.5). This study found no statistically significant difference between the age and sex of PD patients compared to HCs (p= 0.346 and p> 0.99). Optical density values (OD) at 405 nm (OD405) were obtained from the IgG indirect-ELISA protocol to 12 designed immunogenic peptides for all PD and HC sera demonstrated in Figure 12.

Based on our result, antibodies (Abs) against human amyloid-derived peptide (α-syn$_{100-114}$) were not significantly different between PD patients and HCs (Figure. 12A; p>0.05), whereas Abs level against bacterial amyloid-derived peptide (Curli $_{133-141}$) was significantly higher in PD patients (50.1%, 26 out of 51) than in HCs (22.4%, 13 out of 58) (cut-off value 0.45; AUC = 0.756; p < 0.0001 Figure 12B).

In addition, we observed a remarkable abs response against microorganism-derived peptides, Pg (Kpg$_{328-339}$, RgpA$_{800-812}$,) and HSV-1 (UI42$_{22-36}$), in PD patients' sera that were significantly higher compared to HCs. For Kpg$_{328-339}$ we found, a significant difference in the abs response between PD and HCs (Figure 12C). Totally, 82.3% (42 out of 51) of PD patients showed a positive abs response against Kpg peptide, whereas just 10.3% (6 out of 58) were positive in the HC group (cut-off value 0.39; AUC = 0.95; p < 0.0001 Figure 12C). Concerning RgpA$_{800-812}$ peptide, we found, a significantly higher abs response in PD patients (60.7%, 31 out of 51) than in HCs (24.1%, 14 out of 58) (cut-off value 0.29; AUC = 0.902; p < 0.0001 Figure 12D). The positivity and mean levels of anti- UI42$_{22-36}$ Abs showed a significant difference between PD patients (43.1%, 22 out of 51) than HCs (25.8%, 15 out of 58) (cut-off value 0.25; AUC = 0.741; p < 0.0001 Figure 12G).

Level of Abs against other immunogenic peptides ($LtxA1_{429\text{-}445}$, $LtxA2_{64\text{-}80}$, $EBNA1_{400–413}$, $BOLF_{1305–320}$, $MAP4027_{18\text{-}32}$, $MAP1,4\text{-}\alpha\text{-}gbp_{157\text{-}173}$, $MAP3865c_{125\text{-}133}$ peptides) were not statistically different in PD patients compared to those of HCs ($p > 0.05$).

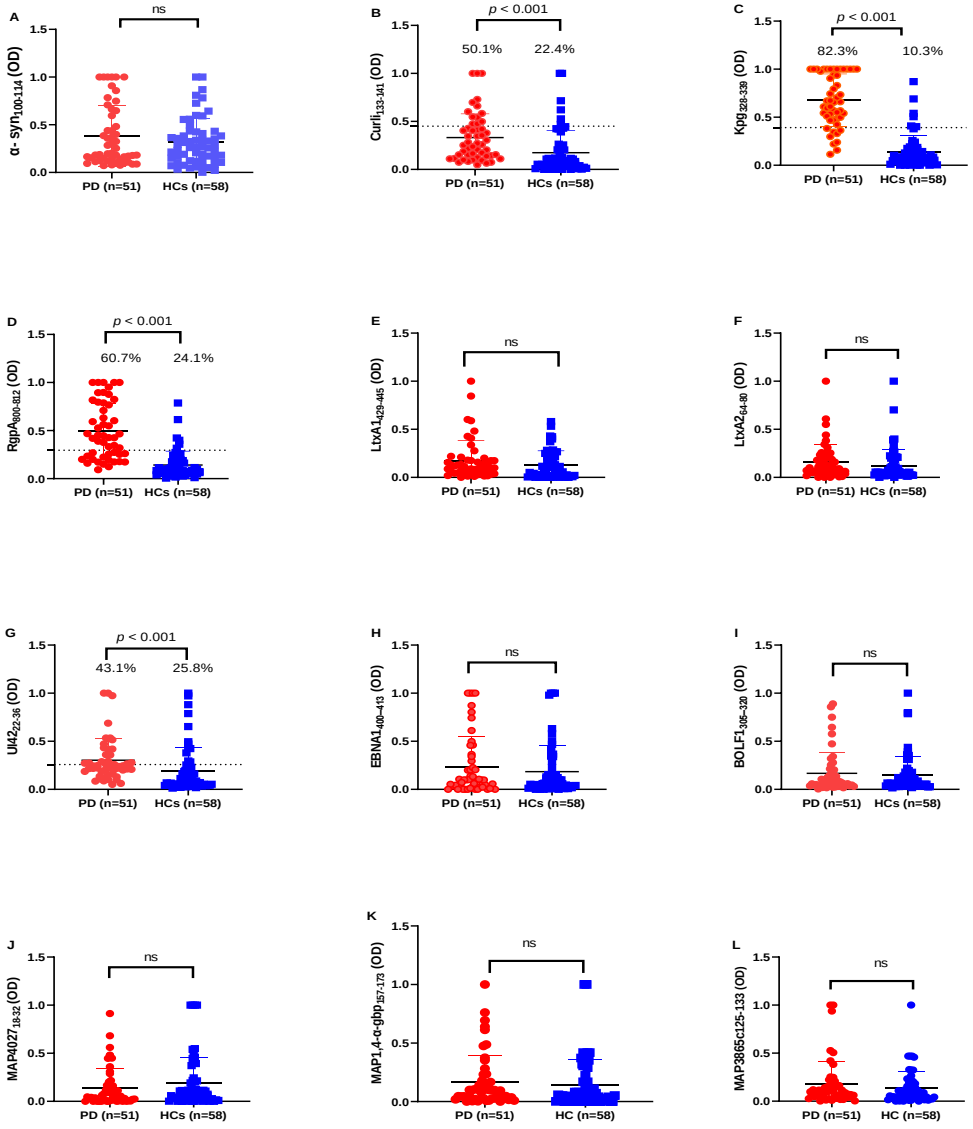

Figure 12. Analysis of Abs reactivity against human α-syn and pathogenic microorganism-derived peptides in PD patients and HCs. Serum samples were tested with indirect ELISA assay to plate-coated (A) α-syn$_{100\text{-}114}$, (B) Curli $_{133\text{-}141}$, (C) Kpg$_{328\text{-}339}$, (D) RgpA$_{800\text{-}812}$, (E) LtxA1$_{429\text{-}445}$, (F) LtxA2$_{64\text{-}80}$, (G) UI42$_{22\text{-}36}$, (H) EBNA1$_{400\text{–}413}$, (I) BOLF$_{1305\text{–}320}$, (J) MAP4027$_{18\text{-}32}$, (K) MAP1,4-α-gbp$_{157\text{-}173}$, (L) MAP3865c$_{125\text{-}133}$ peptides. The dotted lines represent the cut-off values calculated by ROC analysis; In the upper section of the graph, are indicated the Mann-Whitney *p*-value and the percentage of positive patients' values calculated by the Fisher's exact test. Statistically significant levels showed at $p < 0.05$, ns: not significant.

Spearman's correlation analysis was investigated to find a possible correlation between OD values obtained against different immunogenic peptides between PD patients and HCs. The

highest rate of correlation was observed between anti-UI42$_{22\text{-}36}$ and anti- Curli $_{133\text{-}141}$ (r = 0.811, $p < 0.0001$), followed by anti-RgpA$_{800\text{-}812}$ and anti-Kpg$_{328\text{-}339}$ (r = 0.659, $p < 0.0001$), anti-LtxA1$_{429\text{-}445}$ and anti-LtxA2$_{64\text{-}80}$ (r = 0.653, $p < 0.0001$), anti-BOLF1$_{305–320}$ and anti-LtxA1$_{429\text{-}445}$ (r = 0.513, $p < 0.0001$), and anti- Curli $_{133\text{-}141}$ and anti-RgpA $_{800\text{-}812}$ (r = 0.506, $p < 0.0001$). Figure 13 shows the r values obtained from Spearman correlation analysis performed among derived ODs against designed peptides.

In addition, Spearman correlation analysis was performed to evaluate a possible correlation between the severity of disease (HY scale 1 to 5) and ODs values derived from the indirect-ELISA assay. There was a significant correlation between ODs against LtxA1$_{429\text{-}445}$ and HY scales ($r = 0.306$, $p < 0.028$) and Kpg$_{328\text{-}339}$ and HY scales ($r = 0.290$, $p < 0.038$) in PD sera. There was no significant correlation between ODs values against other peptides and the HY scale.

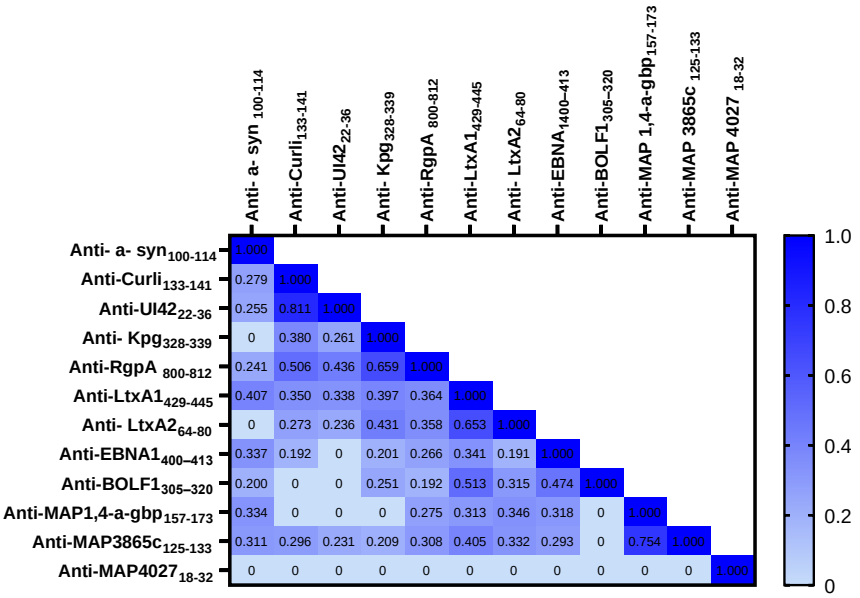

Figure 13. Heatmap shows the r values obtained from Spearman correlation analysis performed among derived peptides' ODs.

3-4. Discussion

Parkinson Disease (PD) is a complex neurodegenerative amyloid disorder with unknown cause of disease (70,178). Growing evidence has demonstrated that the gut microbiota and microbial pathogens' involvement in its etiology (103,179). In addition, novel findings emphasized that amyloid curli produced by gram-negative enteric bacteria in the biofilm state in the GI tract is linked to neurodegenerative diseases (103).

In this study, Abs against human amyloid α-syn and bacterial amyloid curli were investigated. We find for the first time, an increase in Abs level against bacterial amyloid curli in PD patients compared to HCs ($p<0.005$), whereas no significant difference was observed for anti-human amyloid between the two groups. Several studies showed no difference in serum human amyloid α-syn Abs between patients with PD and HC (186,187), which was consistent with our study. In contrast, other studies found high levels of α-syn Abs in PD patients compared to HC sera (188,189). Future investigations are necessary to determine the α-syn Abs level subclasses in a different stage of PD and compare them with HC to use them as a therapeutic or diagnostic biomarker in PD patients.

Interestingly, in our study, the Abs against bacterial amyloid curli was significantly higher in PD patients than in HCs. The presence of abs to a key biofilm component curli in 51% PD vs. 22.4% of HC sera suggests that biofilm may play a potential role in the development of PD, possibly as cryptic reservoirs of α-syn homolog curli. The recent finding demonstrates that the presence of curli-expressing *E. coli* in mice microbiota increases α-syn-mediated motor deficits and brain pathology (190). A considerable correlation between persistent bacteriuria and anti-curli/eDNA IgG levels (IgGs against curli naturally complexed with bacterial extracellular DNA), detected in lupus and HC plasma, was described in Pachucki et al. study (191). In

addition, IgA anti-curli/eDNA levels were higher in lupus donors compared to controls (191). However, detailed knowledge about the role of curli in the stimulation of the immune system and its relationship with PD requires further investigation. Moreover, this is the first report of anti-curli IgGs in PD patients, which could be a promising target for treatment and diagnostic biomarkers in PDs.

Furthermore, we found a higher prevalence of humoral response against peptides derived from periodontal pathogens Pg and Aa in PD patients compared to HCs, which was statistically meaningful in particular for the anti-RgpA and Kpg IgG peptides. Periodontal pathologies are known to be linked to systemic inflammation (192), and *P. gingivalis* (Pg) especially, is associated with different systemic diseases including PD, noninsulin-dependent diabetes mellitus (107,108), Alzheimer's disease (111), rheumatoid arthritis (109,110), and cardiovascular disease (184,193). These findings show the possible association between Pg and PD, confirming the hypothesis that Pg can induce a systemic antibody response, probably influencing the progression of PD disease. On the other hand, there was a significant relationship between the increase in the level of antibodies against this bacterium and the severity of Parkinson's disease (HY index). This relationship emphasizes the role played by oral infection during Parkinson's disease. Despite various studies on the relationship of Pg with PD, no study was found on the relationship of Aa with PD. Díaz-Zúñiga et al. study showed that Aa can increase the risk of Alzheimer's disease by specific inflammatory and immune responses in brain cells (194). Therefore, the association between periodontal pathogens, especially Aa, in the progression of neurodegenerative diseases thus needs to be further investigated. It also seems that accurate oral and dental hygiene in Parkinson's patients can be effective in prevention and reduction the symptoms of the disease. We observed a

statistically significant difference in antibody levels against a common pathogen of the central nervous system, HSV-1 (Ul4222–36) in PD patients in comparison to HCs (182), which was consistent with other studies (195). Furthermore, the antibodies able to recognize the HSV-1-Ul4222–36 peptide are able to cross-react with the homologous human α-syn100–114 epitope (182). In this study, we highlight a positive correlation between Abs against HSV-1 and curli, supporting the hypothesis that HSV-1 infection may change the composition of the gut microbiota, which may lead to dysbiosis. The results from the study of Ramakrishna et al. showed that HSV and acyclovir can disrupt the gut bacterial community in a sex-biased manner in a C57BL/6 mice model (196). In our study, the level of Abs against EBV peptides was higher in PD patients than in the healthy group; however, this difference was not statistically significant. Epidemiological studies have demonstrated that PD patients are significantly more Abs seropositive for EBV than HCs (186,197). Latent EBV infection can trigger autoantibodies that can cross-react with α-syn and elevate α-syn aggregation (186,197). Considering that EBV is one of several proposed environmental factors associated with PD, our study population is probably influenced by other genetic and environmental factors. On the other hand, to obtain more accurate epidemiological statistical results, it is suggested to investigate of Abs against other EBV-immunogenic peptides in a larger number of PD patients and comparison with HC, in future studies. As it has been reported in a previous study, a high level of Ab-mediated immune reaction was detected against MAP3865c207–219, and MAP3865c82–97 peptides, while no significant reaction was observed against MAP3865c81–95 and MAP3865c44–59 peptides (180). In this study, Abs levels against other MAP epitopes were the same in the two populations (i.e., PD and HCs). The most obvious limitation of the current study was that of small sample size for the evaluation of Abs against these peptides.

Moreover, selection of other microbial peptides with broad immunogenic potential designed from these organisms and checking Abs against them in large sample sizes is recommended. This study reports a significantly increased humoral response against curli, Pg, and HSV-1 in PD patients, implying the important role of these factors in the pathogenesis of the disease. Therefore, while the development of PD has not yet been associated with a unique microbial species and their products, more studies will be necessary to examine potential interactions between the bacterial amyloid curli and the human amyloid and to understand their relevance in PD pathogenesis.

Chapter 4: Profle patterns and bioflm formation ability of *Bacteroides fragilis* strains isolated from colorectal cancer (CRC) tissues

4-1. Aims of the study

Several genetic and environmental factors are implicated in CRC development (198). Enterotoxigenic *Bacteroides fragilis* (ETBF) is the most common carcinogenic bacteria and one of the main environmental factors involved in CRC development (198,199.) *B. fragilis* toxin (BFT) is coded by the *bft* gene with three isotypes, namely *bft-1*, *bft-2*, *bft-3*, located on a pathogenicity island (PAI). Based on this assumption, three patterns are assigned to *Bacteroides fragilis*. Enterotoxigenic *B. fragilis* strains (ETBF) with *bft* gene is defined as pattern I and nontoxigenic strains (NTBF) are defined as Pattern II and III. Pattern II defined as strains without the pathogenicity island region and flanking region and pattern III defined as strains without the pathogenicity island and with flanking region (137). At the same time, studies suggest that bioflm formation by *B. fragilis* is closely related to CRC, and *B. fragilis* in bioflms can be a diffusion barrier that causes antibiotic access limitation and survive in hostile environments (200). Due to the importance of toxin and bioflm formation in pathogenicity of *B. fragilis* and development of CRC, we have investigated the profle patterns of *bft* gene I, II, and III and bioflm formation ability in *B. fragilis* isolated from colorectal cancer (CRC) tissues in this study.

4-2. Materials and Methods

4-2-1. Patient population

In this study, 31 patients with a mean age of 59.03 (SD±11.18) with a clinically diagnosed CRC confirmed by radiographic, pathologic, and colonoscopy examination were enrolled.

Patients had not received any antibiotic treatment for three months prior to the experiment. Thirty-one healthy individuals with age-matched control (Mean± SD, 57.35 ± 10.79) whit no intentional disorders were also recruited in this study. This study was approved by the Ethics Committee of Tehran University of Medical Sciences and Sassari university (NO. 9421133003).

4-2-2. Inclusion criteria and exclusion criteria

Colorectal cancer tissues biopsy was collected from patients whose presence of colorectal cancer was confirmed using radiography, pathology, and colonoscopy methods. We excluded biopsy samples from colorectal cancer tissue of people who were subjected to radiation therapy, chemotherapy, and antibiotic therapy.

4-2-3. Sample collection

Biopsy samples were obtained from each participant over 6 months by a gastroenterologist. Samples were taken from the colon and rectum. 80.6% of tumor samples were in stage II. Samples were placed in thioglycolate broth (THIO) transport medium containing vitamin K1 (0.5mg/l), and hemin (5mg/l) and sent to the microbiology laboratory within 30 minutes.

4-2-4. Samples preparation and isolation of *Bacteroides fragilis*

Samples were homogenized using a mortar and pestle upon arrival at the lab. Homogenized samples were transferred to inoculate Bacteroides Bile Esculin Agar (BBE) and Brucella Blood Agar (BBA) containing 5% sheep blood, 0.5mg/l vitamin K1, and 5mg/l hemin and incubated for 48-72 hours at 37°C under anaerobic condition. Dark colonies grown on BBE and BBA were re-cultured in a BBA medium. Anaerobic respiration was double-checked using an

aerotolerance test. Anaerobic coccobacilli with positive bile esculin and negative catalase tests were transferred to BHI broth containing 15% glycerol and stored at -80°C.

4-2-5. Bacterial species identification

To determine type and species of *Bacteroides fragilis*, two polymerase chain reactions were used for amplifcation of 16S rRNA gene region. First reaction was reserved to verify *Bacteroides fragilis* group and the second to determining its species. PCR primers and product size are presented in Table 8. The 16S rRNA gene was sequenced for some strains and submitted in GenBank.

Table 8. Primers and 16S PCR product size for *B.fragilis* identification

Target region	Primer	Sequence 5' to 3'	Amplicon size (bp)
16S rRNA (*Bacteroides fragilis group*)	g-Bfra148-F g-Bfra626-R	ATAGCCTTTCGAAAGRAAGAT CCAGTATCAACTGCAATTTTA	495
16S rRNA *(Bacteroides fragilis)*	Bf.specific-F Bf-specific-R	TCRGGAAGAAAGCTTGCT CATCCTTTACCGGAATCCT	163

The PCR reaction materials included distilled water and a final concentration of 1.5 mM MgCl2, 1x buffer, 0.2 mM dNTP, 0.25 mM Forward primer, 0.25 mM Reverse primer, 0.5 units of Taq polymerase enzyme, and 10 nanograms of DNA. The temperature and times of the PCR steps are shown in Table 9. The 16S rRNA gene was sequenced for some strains and submitted to GenBank.

Table 9. 16S rRNA gene PCR reaction conditions

PCR Steps		Temperature (°C) Time
Denaturation		95 5 minutes
35 cycles	**Denaturation**	95 30 second
	Annealing	54 30 second
	Extension	72 20 second

To observe the PCR product, 1% agarose gel was used. To prepare agarose gel, 0.5 X- TAE and safety dye were used 0.5 X- TAE was also used for the electrophoresis buffer. In order to estimate the size of the obtained band, electrophoresis of the PCR product was performed in the presence of a 100 bp marker with a voltage of 90-100.

Then, the gel was observed by transilluminator, and imaging was done by gel documentation. Then, 30 microliters of PCR products along with 10 picomoles of forward primer were sent for sequencing. Results were checked in https://blast.ncbi.nlm.nih.gov/Blast.cgi site.

4-2-6. Identification of the *bft* gene and its isotypes

PCR was used to detect *bft* gene and the isotypes as previously described by Odamaki T et al (201). Primers properties are presented in Table 10. *Bacteroides fragilis* strain whose *bft* gene was sequenced (GenBank: Mk792343.1) was used as a positive control. The temperature and times of the PCR steps are shown in Table 11.

Table 10. Sequence of *bft* gene isotypes primers

Target region	Sequence 5' to 3'	size (bp) Amplicon
All *bft* gene	F: GGATACATCAGCTGGGTTGTAG R: GCGAACTCGGTTTATGCAGT	296
bft-1	F: TCTTTTGAATTATCCGTATGCTC R: CTTGGGATAATAAAATCTTAGGGATG	169
bft-2	F: ATTTTTAGCGATTCTATACATGTTCTC R: GGGCATATATTGGGTGCTAGG	114
bft-3	F: TGGATCATCCGCATGGTTA R: TTTGGGCATATCTTGGCTCA	148

Table 11. *bft* gene PCR reaction conditions

PCR Steps		Temperature (°C) Time	
Denaturation		95	5 minutes
35 cycles	**Denaturation**	95	25 second
	Annealing	54	25 second
	Extension	72	30 second

After amplifying the *bft* gene fragment and observing its target band in 1% agarose gel, 30 microliters of PCR products along with 10 picomoles of forward primer were sequenced. The obtained data were checked for reading accuracy at https://blast.ncbi.nlm.nih.gov/Blast.cgi. After ensuring the accuracy of the readings, the chromatogram data were checked with Chromas software (version 2.6.4), then the obtained sequences were analyzed with Bio Edit (version 7.2.6.0) and ClustalX2 (version 2.1) software.

4-2-7. Identification of patterns I, II, and III

Based on the evidence provided by previous studies (9), ETBF strains exhibit pattern I. Hence, pattern I consist of strains of *Bacteroides fragilis* that possess *bft* gene. NEBF strains exhibit patterns II and III. To separate pattern II from pattern III, the selected section of the flanking region was amplified by PCR. Primers sequence is presented in Table 12. One of the strains that was positive for this gene was used as positive control. The reaction conditions of this PCR are given in Table 13.

Table 12. Flanking region primers

Target region	**Sequence 5' to 3'**	**Amplicon size (bp)**
Flanking region	F: TTCAACCTGATCGATCCGGAAGATCCG R: GCTGGTAGACTACCTGAGTAAGGAGTC	1600

Table 13. PCR reaction conditions of Flanking region

PCR Steps		**Temperature (°C)** **Time**
Denaturation	95	5 minutes
35 cycles **Denaturation**	95	60 second
Annealing	65	65 second
Extension	72	2 minutes

After amplifying the flanking region gene fragment and observing their target band in 1% agarose gel, 30 microliters of PCR products along with 10 picomoles of forward primer were sent to Pishgam company for sequencing as one-way reading. The obtained data were checked for reading accuracy at https://blast.ncbi.nlm.nih.gov/Blast.cgi. After ensuring the accuracy of

the readings, the chromatogram data were checked with Chromas software (version 2.6.4), then the obtained sequences were analyzed with Bio Edit (version 7.2.6.0) and ClustalX2 (version 2.1) software.

4-2-8. Biofilm formation in vitro test (microtiter method)

Microtiter plate assay was used to investigate bioflm formation ability in vitro. Briefy, several colonies from the fresh culture were diluted in BHIS broth to obtain a microbial suspension with a concentration of OD=0.08–0.1. Once done, 20 µl of the microbial suspension was added to a microplate containing 180 µl of BHIS broth. Te same procedure was repeated for each strain in three separate wells, and cultures were incubated for 24 h at 37 °C under anaerobic condition. At the subsequent stage, the upper layer medium of wells was disposed, and the wells were rinsed with 100 ml of PBS (pH=7.2). Microplates were left for 10 min at 65 °C to dry. Ten, 200 µl of crystal violet (1%) was added and incubated for 5 min at room temperature. To dissolve the colour attached to bioflm, 150 µl of acetic acid at 30% concentration was added to each well and absorbed crystal violet was measured at 570 nm by an ELISA reader. The obtained results were interpreted as follows:

Based on the OD obtained from the negative control, the OD obtained from the isolates was categorized into four levels:

• Negative (OD control ≥ OD sample)

• Weak (OD2 control ≥ OD sample ≥ OD control)

Average (OD 4 control ≥ OD sample ≥ OD 2 control)

Strong (OD4 sample ≥ OD control)

4-2-9. *bft* gene expression under planktonic and biofilm conditions with Real-time PCR

To determine *bft*-gene expression under planktonic condition, *Bacteroides fragilis* strains were cultured in Brucella Blood agar (BBA) and incubated for 24 h at 37 °C. Then, several colonies from the fresh culture were diluted in BHIS broth and incubated for 16 h at 37 °C under anaerobic condition. To examine *bft* expression under bioflm condition, colonies from the fresh culture were diluted in BHIS broth to obtain a microbial suspension with a concentration of OD=0.8–0.1. Once done, 20 µl of the microbial suspension was added to a microplate containing 180 µl of BHIS broth and incubated for 24 h at 37 °C under anaerobic condition. At the subsequent stage, the upper layer medium of wells was disposed, and the wells were rinsed with 100 ml of PBS (pH=7.2). Using a sterile pipette and pipette tip, cells were scraped of the base and walls of the well, diluted in 100 µl of PBS, and collected.

RNA was extracted subsequently using an RNX-Plus solution kit (Sinaclon-Iran) according to the instruction protocol. DNase I, RNase free kit (Sinaclon-Iran) was used to avoid possible genomic DNA contamination. Finally, cDNA was synthesized using a Reverse Transcription kit (Sinaclon-Iran) with random hexamer primers. Real-time PCR Expression of *bft* gene was quantifed by specifc primers and SYBR Green real-time PCR (202). Primer properties is presented in Table 14. PCR conditions included an initial denaturation at 95 °C for 5 min, followed by a 40-cycle amplifcation consisting of denaturation at 95 °C for 20 s and annealing and extension at 59 °C for 30. Specifcity of PCR reactions was verifed by melt graph analysis. Gene expression level was normalized by 16S rRNA sequence, and gene expression was quantifed by ΔΔCT method.

Table 14. The sequence of primers used for *bft* gene expression.

Target region	Primer	Sequence 5' to 3'
bft	BFT qRT-PCR	F: AAGGGCTGGATGGCTTTACT R: GGGATACATCAGCTGGGTTG
16srRNA	16S qRT-PCR	F: CAGTCTTGAGTACAGTAGAGGTGG R: GTGGACTACCAGGGTATCTAATCC

4-2-10. Data collection and statistical analysis

To analyze data from SPSS ver. 18.0 (SPSS Inc., Chicago, IL) was used. Quantitative data results were statistically analyzed based on the average of three repetitions.

1) Chi-square test was used to check the significance of the difference in the frequency of toxin-producing strains in people with colorectal cancer compared to healthy people.

2) Independent t-test was used to check the significance of biofilm formation ability among strains isolated from people with colorectal cancer compared to healthy people.

3) Paired t-test was used to check the significance of *bft* gene expression difference in the planktonic state compared to the biofilm state.

For all statistical tests, $P \geq 0.5$ was considered significant.

4-3. Result.

4-3-1. Patient population

In this case–control study, 62 biopsy samples were collected from patients and healthy individuals referring to the colonoscopy Unit of Tehran's Imam Khomeini Hospital. 31 (50%) biopsy samples were extracted from CRC tissue, and 31 (50%) from normal colorectal tissue. Patient demographics are presented in Table 15.

Table 15. Characteristics of Patient population and controls.

Population characteristic	CRC N (%) 31(50)	NT N (%) 31(50)
Age median (%) Mean±SD	58 59.03±11.18	58 57.35± 10.79
Gender n (%) Female Male	 13 (41.9) 18 (58.1)	 16 (51.6) 15 (48.4)

CRC, Colorectal cancer tissue; NC, Normal Colorectal tissue; N, Number of patients

4-3-2. Identification of *Bacteroides fragilis* by molecular method

In order to identify *Bacteroides fragilis*, two PCRs were used. In the first PCR, species belonging to the *Bacteroides fragilis* group were differentiated from other bacteria, and in the second PCR, *Bacteroides fragilis* was differentiated from the *Bacteroides fragilis* group.

Identification of *Bacteroides fragilis* group and *Bacteroides fragilis* species were confirmed by PCR method using specific primers of 16srRNA gene fragment. The presence of the 501 bp band (Figure 14) confirmed the identity of the *Bacteroides fragilis* group. The presence of a band of 163 base pairs (Figure 15) confirmed the identity of *Bacteroides fragilis*. 82 isolates

belonged to the *Bacteroides fragilis* group, of which 68 isolates were confirmed as *Bacteroides fragilis*. The frequency of isolates from different clinical samples is given in Table 16.

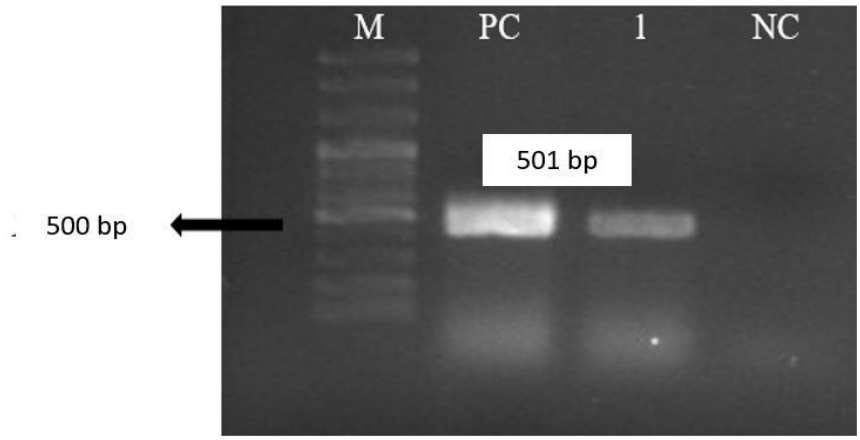

Figure 14. 501 base pair PCR product display of 16srRNA gene, M: 100 base pair marker, PC: positive control (*Bacteroides fragilis*; Accession number in NCBI= MN955544.1), NC: negative control and 1: isolate belonging to *Bacteroides fragilis* group

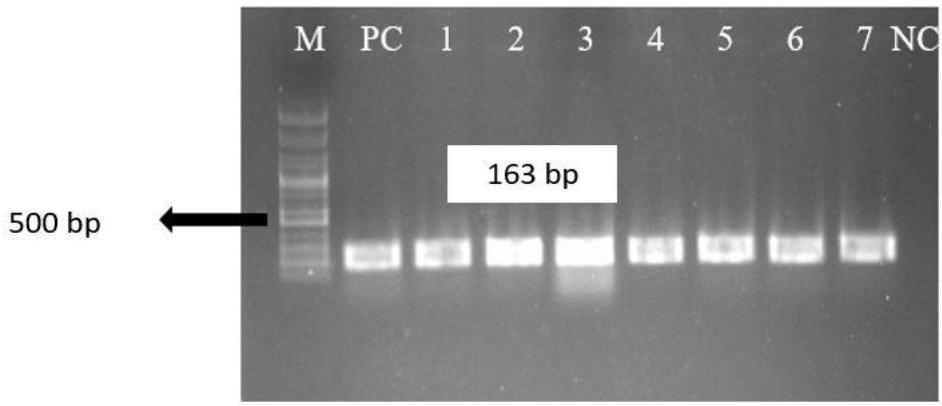

Figure 15. Display of 163 bp PCR product of 16srRNA gene, M: 100 bp marker, PC: positive control (*Bacteroides fragilis*; Accession number in NCBI = MN955544.1), NC: negative control and 1-7: related isolates to *Bacteroides fragilis*

Table 16. Frequency of *Bacteroides fragilis* group and *Bacteroides fragilis* species from different clinical samples

Biopsy N (%)	*B.fragilis* N (%)	*bft* gene N (%)	PatternI	PatternII	PatternIII
NC biopsy 31 (50)	32 (47.1)	2 (6.25)	**2**	**23**	**12**
CRC biopsy 31 (50)	36 (52.9)	11 (30.5)	11	8	12
62 (100)	68 (100)	13 (19.1)	13 (19.1)	31 (45.6)	24 (35.3)

CRC Colorectal cancer, NC Normal Colorectal tissue, N Number of patients

4-3-3. Checking the presence of the *bft* gene

The presence of *bft* gene was confirmed by PCR method using fragment-specific primers for this gene. The presence of a band of 197 base pairs confirmed the presence of this gene Figure 16. Out of 68 isolates of *Bacteroides fragilis* group, 13 (19.1%) isolates were positive for this gene. Eleven *bft* gene positive stains were isolated from CRC patients just 2 strains were from healthy individuals. This difference was statistically significant (*p*:0.004) (Table 16).

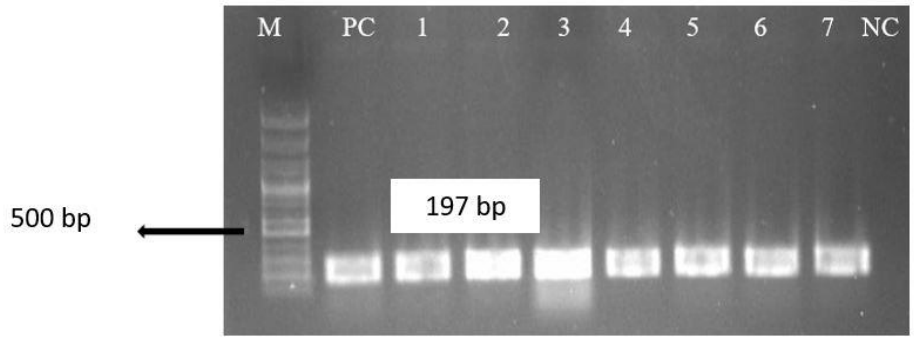

Figure 16. Display of 197 bp *bft* gene PCR product, M: 100 bp marker, PC: positive control (*Bactroides fragilis*; Accession number in NCBI = MK792343.1), NC: negative control and 1-7: isolates Belonging to *Bacteroides fragilis*

4-3-4. Investigation of *bft* gene isotypes

Using appropriate primers, toxin isotypes (*bft-1*, *bft-2*, and *bft-3*) in *Bacteroides fragilis* isolates were investigated by PCR method. The results of this test are shown as a product of 169 base pairs for the *bft-1* gene isotype (Figure 17a), 114 base pairs for the *bft-2* gene isotype (Figure 17b). Among the 13 isolates with *bft* gene, 12 isolates belonged to isotypes 1 and 1 isolate belonged to isotype 2. In this study, isotype 3 was not found.

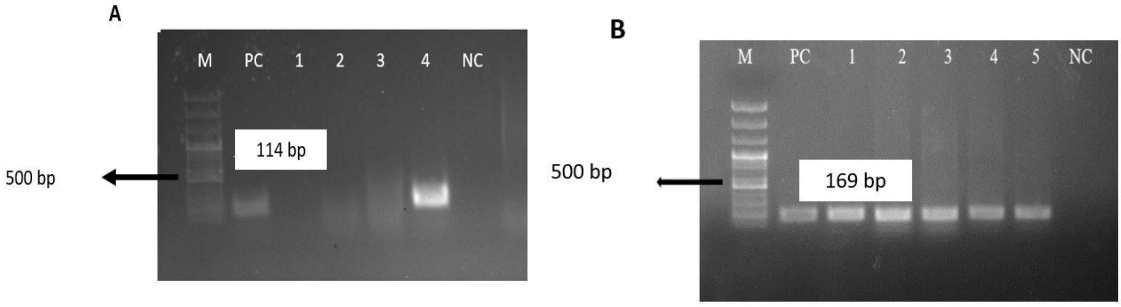

Figure 17. Product display (a) 114 bp PCR gene *bft2*, M: 100 bp marker, PC: positive control, NC: negative control and 4-1: *Bacteroides fragilis* isolates, (b) 169 bp PCR *bft1* gene, M: 100 bp marker, PC: positive control, NC: negative control and 5-1: *Bacteroides fragilis* isolates

4-3-5. Identification of patterns I, II, and III

Considering that pattern I, *Bacteroides fragilis* strains have toxin gene. Therefore, the strains with the *bft* gene follow pattern I. Strains lacking the *bft* gene follow pattern II or III. A pair of specific primers for the flanking region (transposon CTn86) was used to separate patterns II and III. Amplification of a part of these gene fragments was done using PCR. The results of this test are shown as a product of 1577 game pairs (Figure 18) for the flanking region. Table 16 shows the absolute and relative frequency of pattern I, II, and III among *Bacteroides fragilis*

isolates. Pattern I ETBF was detected in 13 isolates. Twenty-four (35.3%) NTBF isolates were flanking region-PCR positive, suggesting pattern III in these strains, and 31 (45.6%) were flanking region-PCR negative, indicating pattern II in these strains. Table 13 displays the abundance of patterns for the isolated strains of *Bacteroides fragilis* extracted from CRC and normal colorectal tissues.

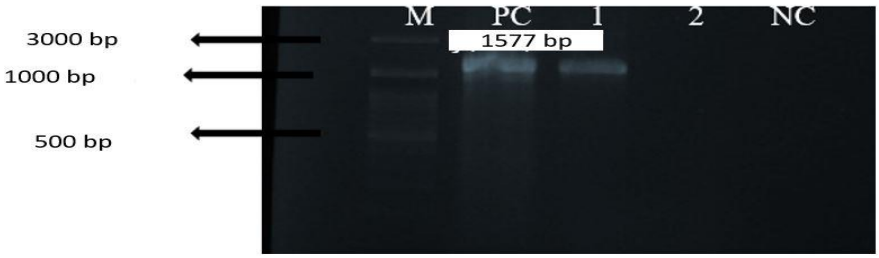

Figure 18- 1577 bp PCR product display of CTn86 region, M: 100 bp marker, PC: positive control, NC: negative control and 1-2: *Bacteroides fragilis* isolates.

4-3-6. Biofilm production test in vitro

Biofilm formation was monitored by means of OD measurements of individual strains. According to the classification of the isolates based on the ability to adhere to the base of the wells and produce biofilm, 5 isolates (7.4%) showed "weak" (+1), 36 isolates (52.9%) exhibited "medium" (+2), and 27 isolates (39.7%) showed "strong" (+3) biofilm-forming ability. All *Bacteroides fragilis* isolates derived from CRC tissue possessed a medium to strong biofilm-producing ability. The ability of biofilm formation in strains isolated from colorectal cancer and normal tissues is shown in Table 17 .

Table 17. Biofilm formation ability in *Bacteroides fragilis* isolates.

Biopsy **N (%)**	**Weak** N (%)	**Moderate** N (%)	**Strong** N (%)
NC biopsy 31 (50)	5	18	9
CRC biopsy 31 (50)	0	18	18
62 (100)	5 (7.4)	36 (52.9)	27 (39.7)

There was a meaningful difference in the ability of biofilm formation of CRC-extracted *Bacteroides fragilis* isolates as compared to those derived from normal tissue (*P*=.000). isolated from colorectal cancer had more ability to form biofilm than healthy individuals. Also, ETBF strains had more biofilm formation ability than NEBF strains. This difference was statistically significant (*p*:0.01) (Figure 19).

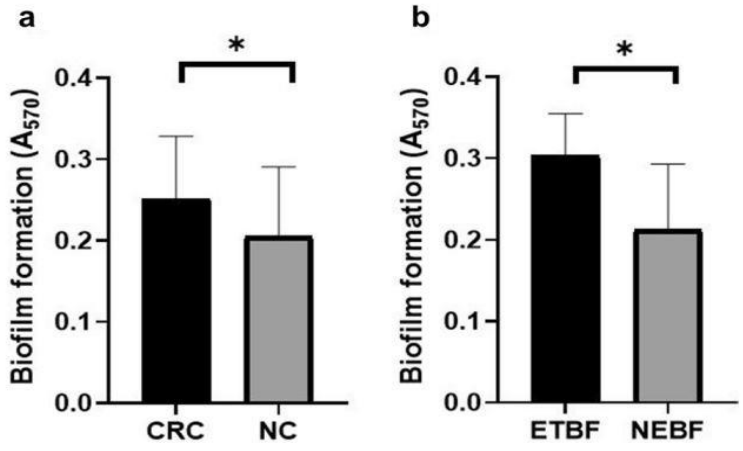

Figure 19. Bioflms of *B. fragilis* strains were stained with 1% crystal violet and evaluated by measuring the absorbance at A570. a) The black bars represent the average±SD (0.25±0.07) of in *B. fragilis* strains isolated from CRC and gray bars represent the average±SD (0.20±0.08) of in *B. fragilis* strains isolated from NC. *Indicates statistical signifcance (*P*=0.022). b) The black bars represent the average±SD (0.30±0.05) of ETBF strains and gray bars represent the average±SD (0.21±0.08) of in NEBF strains. *Indicates statistical significance (*P*=0.001)

4-3-7. Toxin expression in ETBF isolates in planktonic and biofilm mode using real-time PCR

In this study, the 16srRNA gene was used as a housekeeping gene to normalize the test. The results of the amplification of *bft* and 16srRNA genes and the melting curve of these genes are shown in Figures 20 and 21.

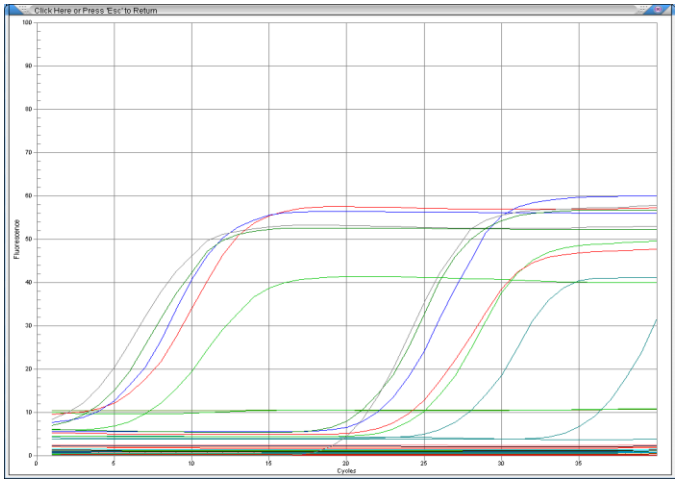

Figure 20. Real-time PCR amplification of bft and 16srRNA genes

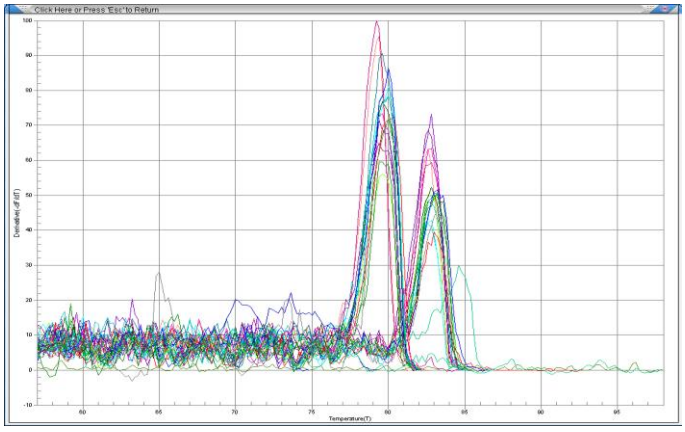

Figure 21. Melting curve diagram of *bft* and 16srRNA genes

The *bft* gene expression was investigated by real-time PCR method in planktonic and biofilm conditions. Statistical analysis of *bft* gene expression data was done by GraphPad Prism version 8 software and fold change was calculated. The *bft* gene was more expressed in the planktonic state than in the biofilm state, and this difference was statistically significant (Figure 22).

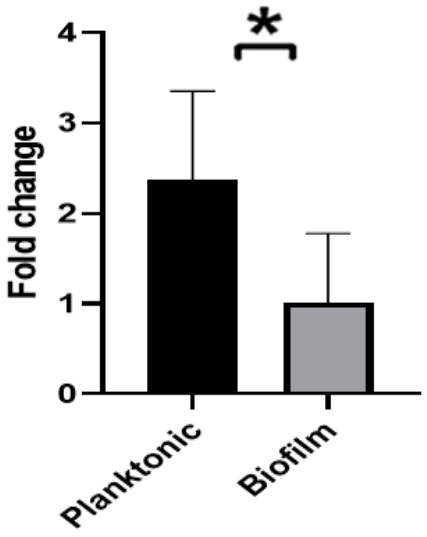

Figure 22. Comparison of *bft* gene expression in *Bacteroides fragilis* strains under planktonic and biofilm conditions. The black bars represent the average fold-change±SD (1.64±0.96) of *bft* gene expression under planktonic condition and the gray bars represent the average fold-change±SD (0.50±0.38) of *bft* gene expression under biofilm condition. *Indicates statistical significance (*P*=0.001)

4-4. Discussion

In the present study, we have investigated the profile patterns I, II, and III and the biofilm-forming ability in CRC-extracted *Bacteroides fragilis* isolates and normal tissue. To the best of our knowledge it was the first study to evaluate biofilm-forming ability and toxin expression of CRC-extracted *Bacteroides fragilis* isolates under planktonic and biofilm conditions in our region.

The study suggests a meaningful difference between the presence of *bft* gene in CRC-derived isolates compared to isolated strains from normal tissue (p=0.02). Several studies have also supported the existence of a meaningful relation between the presence of *bft* gene and CRC (154,203). Few studies have conducted in Iran to study the relationship between ETBF and CRC (204). For instance, Haghi et al., examined 60 faeces samples in patients diagnosed with CRC and 60 faeces samples in healthy individuals to identify ETBF via direct PCR. ETBF strains were detected with higher frequency among CRC patients than healthy controls.

The relationship between *Bacteroides fragilis* and CRC has been studied in other parts of the world. In the study conducted by Boleiji *et al.*, all "stage III" (severe infection) CRC samples were *bft*-positive (205). The prevalence of "stage I" and "stage II" was 72%.

Topark *et al*. (2006) also demonstrated a meaningful difference in *bft* gene presence in faeces samples of CRC patience compared to normal individuals (38% and 12% respectively) (154). *bft* gene has three isotype variants, pathologically expressed as *bft-2*>*bft-1*>*bft-3*. In the present study, ETBF strains were examined in terms of isotype toxin. Twelve isolates possessed *bft-1* and in a single isolate the presence of *bft-2* was confirmed. None of the isolates exhibited *bft-3*. Based on previous findings in various geographic regions such as Iran, Turkey, and the USA *bft*-1 was the most common isotype toxin (151,154,206).

In this study, the majority of CRC-derived *Bacteroides fragilis* isolates exhibited pattern I (ETBF strains). In contrast, this pattern was the least common pattern detected in healthy individuals. These findings underline the significant role of PAI and its flanking region in CRC pathogenesis and their correlation with this disease.

In the majority of isolates collected from normal tissue, *Bacteroides fragilis* isolates exhibited pattern II which lack PAI and flanking region. Pattern III (strains lacking PAI but possessing flanking region) was observed in CRC-extracted NTBF isolates in 11 isolates and from 8 isolates from normal tissues. Phylogenic studies suggest the possibility of PAI transfer to other isolates and subsequent transformation to ETBF over time. Meanwhile, no study was discovered to evaluate the distribution of these patterns in CRC-extracted isolates in Iran.

In a study conducted by Claros et al., 63 *Bacteroides fragilis* isolates extracted from blood and 197 isolates derived from other clinical samples were investigated. In blood samples, 43%, 38%, and 19% of isolates exhibited patterns II, III, and I respectively. In other clinical samples, the frequency of patterns II, III, and I was as follows the result was 47%, 43%, and 10% respectively which is similar to the patterns discovered in our study in normal tissues. Different studies have revealed a direct correlation between ETBF (pattern I) and CRC development. In other words, the presence of *bft* gene (pattern I) has been associated with CRC development.

Concurrently, the biofilm-forming ability of *Bacteroides fragilis* was detected by staining the bacteria attached to the base of the microplate with crystal violet dye. Results indicated a high biofilm formation ability in ETBF strains compared to NTBF, which was statistically meaningful (p=0.00).

In the study conducted by Pierce et al., several NCTC strains were examined. They showed that toxin-generating strains were more capable of biofilm formation compared to non-toxin

generating strains (207). Biofilm-forming ability is a crucial feature of bacteria which is involved in antibiotic resistance, ETBF colonization, adherence to the epithelial surface, and prevention of toxin dissemination (207).

In the present study, strains isolated from CRC tissue showed higher biofilm-forming ability compared to isolates of normal tissue, which was also a statistically meaningful finding (p=0.000). Based on the obtained results, biofilm-forming ability, with or without toxin, may be associated with CRC development. Studies have also demonstrated the effect of multi-bacterial biofilms on the increase of polyamine metabolites which may intensify CRC growth, invasion, and metastasis (144).

Changes in *bft* gene expression under planktonic and biofilm growth was also considered in this study. The *bft* expression showed a statistically meaningful reduction under biofilm condition. Meantime, no studies were found to compare *bft* gene expression under biofilm and planktonic conditions so far.

The findings possibly suggest that *bft* gene has no significant role in the biofilm formation process. Similarly, other studies also show that the absence of *bft* gene in non-toxin generating strains does not reduce biofilm formation, which suggests that toxin may not be a crucial factor for the formation of this phenotype (144). Studies have also identified the impact of toxin-regulating two-component system RprXY on *bft*-gene expression in vivo and in vitro (202). This system regulates the expression of *bft*-gene. Although, 30% of *Bacteroides fragilis* in the gastrointestinal system have *bft* gene, it is in suppressed state (135). *bft* gene expression may increase depending on dynamic interaction between intestinal mucosa with toxin and the two-component system. Hence, further investigation in vivo and in vitro is required to quantify *bft*-gene expression in the CRC tissues under biofilm condition.

In the present study, pattern I, II, and III profiles among CRC-extracted *Bacteroides fragilis* isolates were different from isolates obtained from normal individuals. Pattern I was the most common pattern in CRC isolates and exhibited greater biofilm-forming ability compared to patterns II and III. These findings suggest a possible correlation between *bft* gene presence and biofilm-forming ability in *Bacteroides fragilis* and CRC development. However, further studies are needed to evaluate the role of pattern I and biofilm in the development of CRC and to target toxin-expression and bacterial biofilm more effectively as an efficient strategy in the treatment of colorectal cancer.

Chapter 5: 16s RNA analysis of the oral and fecal microbiome in colorectal cancer patients versus normal subjects as potential screening tests

5-1. Aim of the study

When CRC is detected in the early stages, the five-year survival rate is above 80%, while, in advanced stages, this rate reaches less than 10% (208). Today, the fecal immunochemical test (FIT), as a non-invasive screening method, is applied to find high-risk individuals who are then referred for CRC screening. However, the sensitivity of this test is low and produces variable results among different studies and populations (209). Hence, more accurate and non-invasive screening is needed to determine patients with early stages of CRC. Over the years, the relationship between gut microbiota and various diseases has become the focus of many researchers (210,211), including those studying CRC (212). In CRC cases, altered gut microbiome hints at a possible role of the host–microbial interaction in the initiation and progression of CRC (208,213). The changes of gut microbial composition may be considered an accurate test in CRC screening with appropriate specificity and sensitivity (214,215). Previously, studies have shown changes of colonic mucosal and fecal microbiome in CRC cases (213,214,216) and also the suitability of fecal microbiome analysis as a powerful method for CRC diagnosis (213,214,216), especially in combination with the FIT (214). In addition, the distinct profiles of microbiota in saliva have been previously correlated to oral (217,218), esophageal (219), and pancreatic cancers (PCs) (220,221). In addition, the microbiome related to the oral cavity can also be found in the mucosa and feces and is associated with CRC (208,215,216,222–225). This encouraged us to evaluate oral microbiome in CRC as a viable alternative and to determine whether saliva sampling can be used as a convenient and readily available methodology for CRC screening. In this work, our aim was to utilize metagenomics

analyses in order to compare the oral and fecal microbiome composition and diversity between CRC patients and HCs in the Iranian population. This has allowed us to develop a classifier of saliva and fecal microbiome assessment with the goal of finding novel biomarkers for noninvasive CRC screening. This study also supplements the current literature in which there is a lack of studies regarding gut microbiota in several underdeveloped countries.

5-2. Material and methouds

5-2-1. Inclusion and exclusion criteria:

We collected saliva and stool samples from patients whose presence of colorectal cancer was confirmed using radiography, pathology, and colonoscopy methods.

Exclusion criteria were as follows:

1) Using antibiotics, prebiotics, and probiotics within the past 3 months;

2) Having a vegetarian diet or high consumption of red and processed meat (because of its direct impact on microbiota composition;

3) Having an invasive medical intervention within the past 3 months,

4) Having a past history of any cancer, inflammatory or infectious diseases of the intestine,

5) Having other GI disorders, including Crohn's disease, inflammatory bowel disease, irritable bowel syndrome, CRC, ulcerative colitis, liver disorder, and nonalcoholic fatty liver disease

6) Having high risk for CRC, such as patients with familial adenomatous polyposis and cancer syndrome. In addition, demographic information, such as age, sex, height, weight, diabetes mellitus history, physical activity, GI disease history, and alcohol consumption was collected by questionnaire forms.

5-2-2. Saliva and stool Samples collection

Saliva samples (n = 20, CRC patients and n= 20 HCs) were gathered, in the current case-control investigation from Taleghani hospital, affiliated with Shahid Beheshti University of Medical Sciences, Tehran–Iran, consisting of CRC TNM stage 0, I, and HC groups (between 2020 and 2021). Saliva specimens were collected between 08:00 am and 12:00 noon and eating and drinking at least 2 h prior to sampling was not permitted. Saliva was provided in a 20 mL falcon tube on ice. About 1 mL of unstimulated saliva was collected over 5–10 min. Then, specimens were transferred to new 2 mL microtubes and frozen at −80 °C for further evaluation. Cases were precisely identified using the colonoscopy procedure and histopathology results of biopsies.

Fecal samples were taken from the same patients and healthy individuals whose saliva was collected; (n = 20, CRC patients and n= 20 HCs) including CRC stage 0 and I and HC groups. As above, cases were precisely identified by colonoscopy procedure and histopathology results of biopsies.

5-2-3. DNA extraction from fecal and saliva samples

Oral specimens were thawed, and Genomic DNA was extracted using the QIAamp DNA Microbiome Kit from Qiagen (Hilden, Germany) according to the manufacturer's instructions. Fecal samples were thawed on ice and DNA extraction was performed using the QIAamp DNA Fecal Mini Kit according to manufacturer's instructions (Qiagen). Extracts were then treated with DNase-free RNase to eliminate RNA contamination. DNA quality and quantity were determined using a NanoDrop2000 spectrophotometer (Thermo Fisher Scientific, Waltham, MA, USA).

5-2-4. PCR Amplification and Sequencing

The gene-specific sequences applied in the current study target the 16S ribosomal RNA V3 and V4 regions using two primers: a forward (5'TCGTCGGCAGCGTCAGATGTGTATAAGAGACAGCCTACGGGNGGCWGCAG 3') and a reverse (5'GTCTCGTGGGCTCGGAGATGTGTATAAGAGACAGGACTACHVGGGTATCTAA TCC3'). The PCR (25 μL) was set up as follows: 12.5 μL per sample 2xKAPA HiFi HotStart Ready Mix, 5 μL primer of forward (1 μM), 5 μL primer of reverse (1 μM), and 2.5 μL bacterial genomic DNA (5 ng/μL in 10 mM Tris pH 8.5) in a 96-well 0.2 mL PCR plate. The thermal cycling situation for amplification of PCR was as follows: initial incubation step at 98 °C for 3 min, then 30 denaturation cycles at 94 °C for 30 s, annealing at 55 °C for 30 s, extension at 72 °C for 30 s, and a final extension step at 72 °C for 5 min. Next, 1 μL of PCR product was run on a BioanalyzerDNA 1000 chip to confirm the size.

Utilizing the V3 and V4 primer pairs in the study, the expected size on a Bioanalyzer trace after the Amplicon PCR step is ~550 bp.

Amplicon product purification was performed with AMPure XP beads based on the manufacturer's recommendations to remove all remaining contaminants or PCR artifacts. Purified amplicons were applied to construct the library based on standard protocols, and sequencing was performed using the Nextera XT Index Kiton on an Illumina NovaSeq platform (Illumina, San Diego, CA, USA).

5-2-5. 16S rRNA Sequence Preprocessing and Analysis

Demultiplexed raw sequences were imported into QIIME2 v.2022-2 (226) and were denoised and clustered using DADA2 (227). Taxonomy classification was conducted using the pre-

trained, via scikit-learn (228), SILVA (229)with 138 99% full-length sequences. The resulting amplicon sequence variant (ASV) table, taxonomy assignment, and appropriate metadata were used as input for the Marker Data Profiling module of the online platform Microbiome Analyst (230). Features with low counts (<4 and <20% prevalence in samples, n = 1815) along with those with low variance (based on interquartile range, n = 25) were excluded from the downstream analysis's counts were normalized using Total Sum Scaling (TSS); moreover, based on their poor quality, 2 samples (1 saliva and 1 fecal, both from the same patient) were excluded from the dataset. Alpha diversity (α-diversity) metric was calculated using the Chao1 index, and the statistical differences between groups were explored using the Mann–Whitney test. Beta microbial diversity (β-diversity) was analyzed using the non-metric multidimensional scaling (NMDS) ordination method, the Bray–Curtis distance, and Analysis of Similarities (ANOSIM). Both alpha and beta microbial diversity analyses were applied on the feature level. Clustering heatmaps were produced on the genus level using the Ward clustering and Euclidean distance methods. Univariate analysis for detecting differentially abundant features between conditions was performed on the genus level (on raw and log-transformed counts) using the Mann–Whitney test, filtering for results with adjusted p values less than 0.05 (p.adjust < 0.05). The Linear Discriminant Analysis (LDA) Effect Size (LEfSe) method (231) was employed to detect genera with biomarker potential. Finally, Random Forest (RF) classification was applied using 1000 tree permutations to test for genera that can serve as explanatory variables for the models. The models' robustness was evaluated using a calculation of the Out- Of-Bag (OOB) error rates.

5-3-Results

5-3-1. Composition of bacteria and the relative differential abundance of the bacterial genera in fecal and saliva samples

The oral and fecal microbiota composition from CRC patients and HCs were identified and quantified as previously described in order to be used as input for further analyses. Differences between saliva and fecal specimens were investigated by focusing on the composition of the bacterial population and the relative abundance of each genus. The relative abundance at the genus bacterial level (%) of both types of specimens (fecal and saliva samples) revealed similar but perturbed profiles between CRC patients and HCs (Figure 23). In detail, in the fecal specimens of CRC cases, *Bacteroides* had the highest abundance across genera with 28.61%, followed by *Escherichia_Shigella* (18.68%), *Faecalibacterium* (7.51%), and *UGG-002* (4.83%), while, in the HCs' individual fecal samples, *Bacteroides* was the most abundant feature, with an average relative abundance of 31.49%, followed by *Escherichia-Shigella* (16.28%), *Dialister* (10.32%), *Roseburia* (5.77%), and *Faecalibacterium* (4.79%). Moreover, in CRC patient saliva samples, *Streptococcus* (34.34%) was the most abundant genus, followed by *Prevotella* (17.31%), *Veillonella* (14.43%), *Neisseria* (11.61%), and *Rothia* (5.91%). Finally, in the HCs' individual saliva samples, *Streptococcus* (42.10%) *Veillonella* (15.28%), *Prevotella* (14.55%), *Neisseria* (10.60%), and *Haemophilus* (4.06%) were the most frequent taxa.

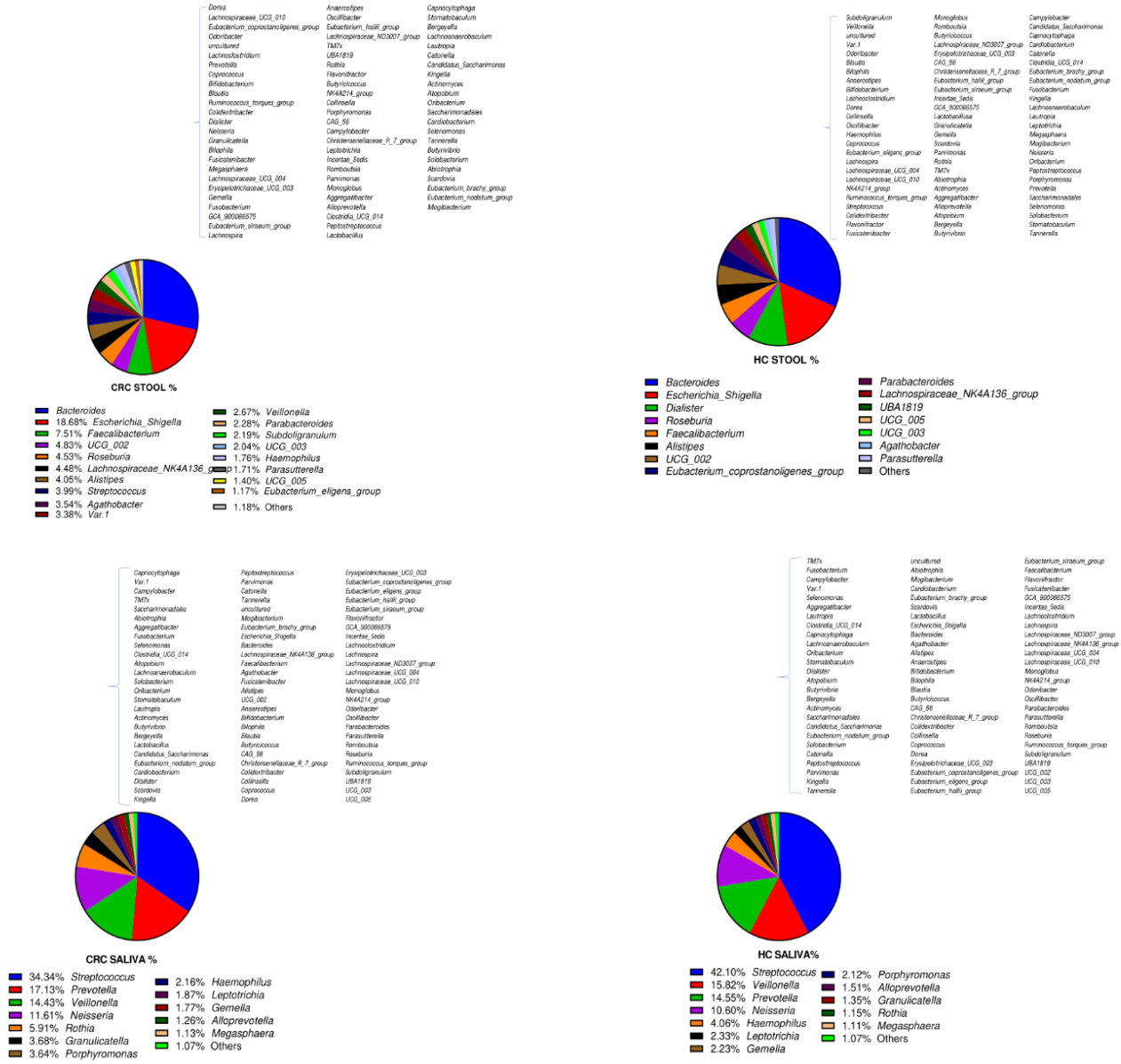

Figure 23. Composition of bacteria and the relative differential abundance of the bacterial genera in fecal and saliva samples of colorectal cancer (CRC) patients and healthy controls (HCs).

5-3-2. Microbial Community Diversity

α-diversity index differentiated between the microbiome of HC saliva compared to CRC patient saliva was found to be statistically significant using the CHAO1 method (p = 0.003) (Figure 24A) but not between the CRC and HC fecal samples (p = 0.56) (Figure 24B). A direct comparison of α-diversity between the fecal and saliva samples of CRC patients only also yielded statistical significance (p = 0.03) (Figure 24C). As a baseline, the α- diversity of fecal and saliva samples of HCs was calculated and revealed that the saliva samples of HCs are statistically and significantly (p = 0.0002) different than HC fecal samples (Figure 24D). Comparing biodiversity in raw numbers between the tested groups resulted in a several observations. HC saliva samples are more biodiverse than CRC saliva ones, whereas CRC fecal samples appear to be more enriched than their HC counterparts. In addition, fecal samples appear to be richer in microbial taxa than saliva samples in CRC patients, whereas, in HCs, these findings are reversed.

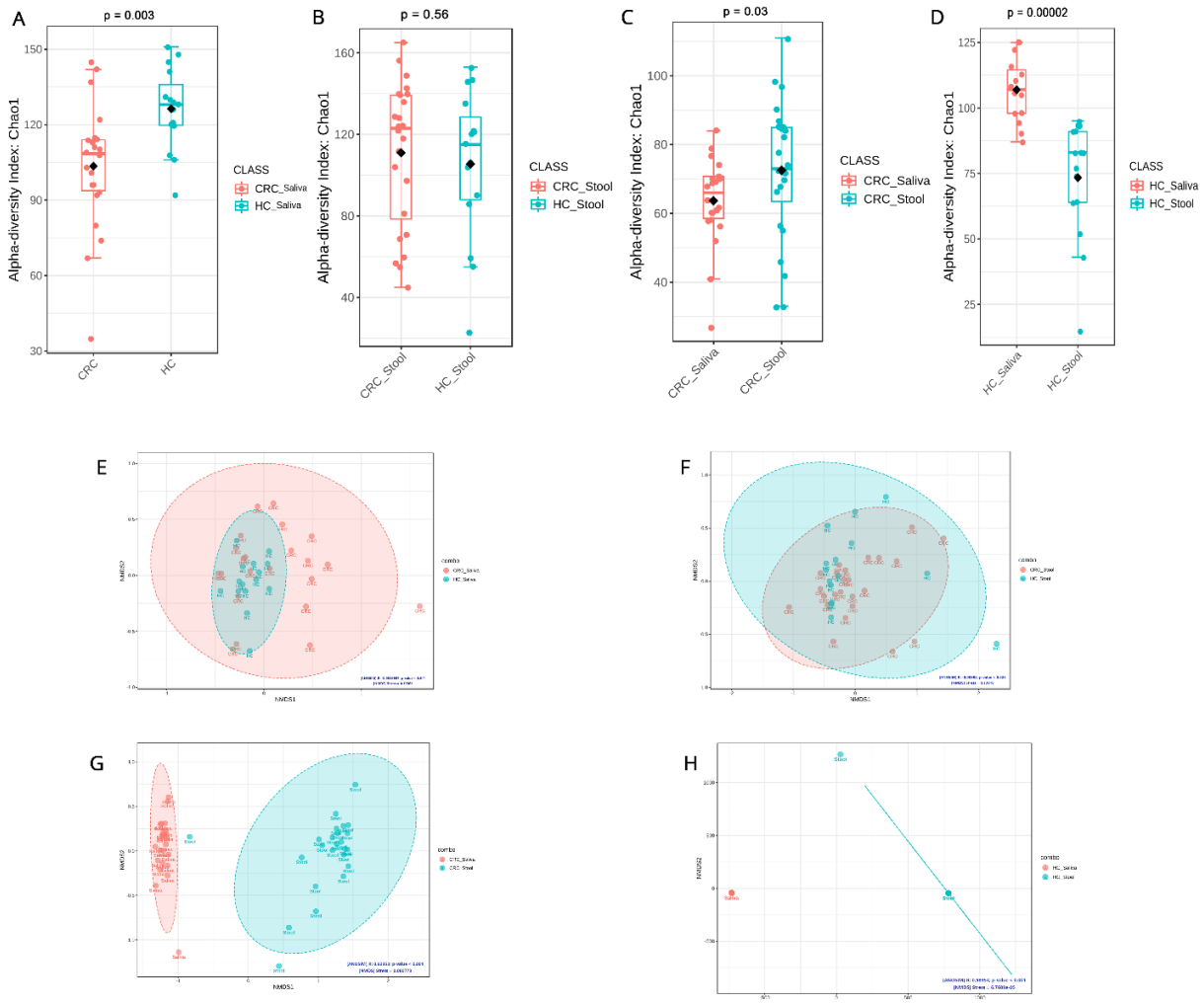

Figure 24. Microbial community diversity across our study groups using the Chao1 approach for α- diversity and NMDS metric for β-diversity: (**A**) α-diversity of saliva samples from CRC patients and healthy controls; (**B**) α-diversity of stool samples from CRC patients and healthy controls; (**C**) α-diversity of saliva and stool samples from CRC patients; (**D**) α-diversity using CHAO1 of saliva and stool samples from healthy controls; (**E**) β-diversity of saliva samples from CRC patients and healthy controls; (**F**) β-diversity of stool samples from CRC patients and healthy controls; (**G**) β- diversity of saliva and stool samples from CRC patients; (**H**) β-diversity of saliva and stool samples from healthy controls.

NMDS analysis using the Bray–Curtis distance was applied to study saliva microbial β-diversity in HCs compared to CRC patients, and it depicted a dense clustering of the microbiome in HC saliva but more dispersed patterns in CRC saliva, while significant overlaps were detected between the microbiome diversity clusters in CRC with the HC of both sample

types (Figures 23E and 23F). On the other hand, the β-diversity differences between saliva and fecal in both CRC and HC samples are distinct and reveal unique localized microbiomes (Figures 23G and 23H).

5-3-3. Phenotype–Microbial Associations

Clustered heatmaps, for differentially abundant bacterial genera in the saliva of CRC patients and HCs (Figure 25A) and the fecal samples of CRC patients and HCs (Figure 25B), were created. There appears to be no clear clustering of genera associated with CRC or HC in the saliva (Figure 25A) or fecal samples (Figure 25B), respectively; however, certain strong associations can be ascertained in the smaller subclusters of samples.

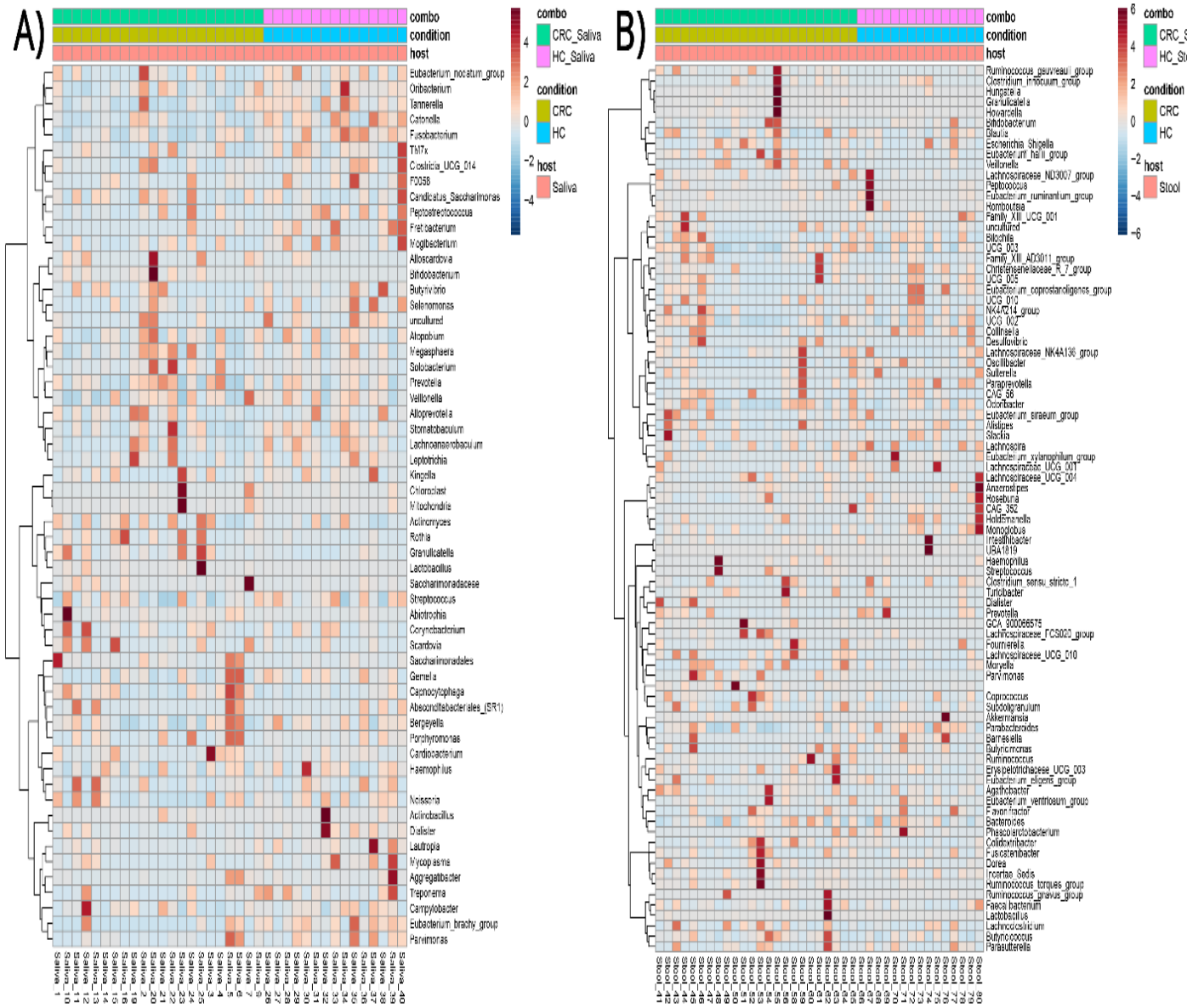

Figure 25. Clustered heatmap of bacterial genera–sample group associations in (**A**) saliva samples of colorectal cancer (CRC) patients and healthy controls (HCs) and (**B**) stool samples of colorectal cancer (CRC) patients and healthy controls (HCs).

On the other hand, in the clustered heatmaps of genera–group associations, and using all samples, regardless of phenotype and collection source, there appears to be a clear clustering of genera associated with saliva and fecal samples, respectively, whereas the condition appears

to affect composition only (Figure 26). These findings appear to be in agreement with the previous β-diversity observations.

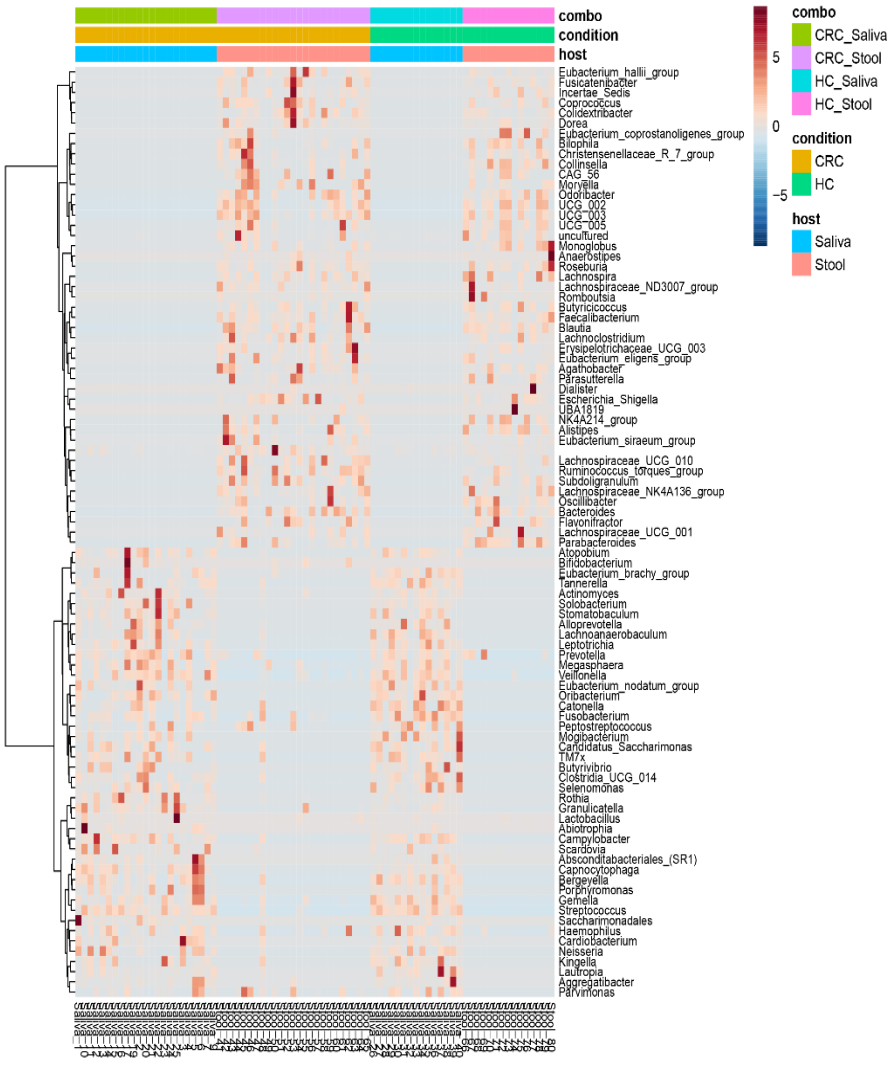

Figure 26- Clustered heatmap of bacterial genera–sample group associations regardless of explanatory variable. The heatmap shows a clear distinction between saliva and stool samples while the the disease creates different association patterns versus healthy controls.

5-3-4. Classification and Biomarker Discovery

By employing a Random Forest (RF) model, a robust supervised classification algorithm was created to detect features that can differentiate between phenotypes and provide some predictive power. The analyses were based on bacterial genera' relative abundances in the saliva of CRC patients and the HC group (Figure 27A) and in the fecal samples of CRC individuals and the HC group (Figure 27B). This has allowed for testing of the respective predictive powers of saliva and fecal microbiomes in CRC detection while highlighting specific features (microbial genera) that are important for each model. The model based on the saliva microbiome outperformed the fecal one based on the OOB error of the models (21.6% for saliva and 43.6% for fecal) along the correctly classified samples. The saliva model highlighted features such as the *Eubacterium_brachy_group, Bifidobacterium, Fusobacterium, Catonella,* and others while the fecal model based its classification decisions on features such as the *Ruminococcus_torques_group, Collinsela, Ruminococcus_ gauvreauii_group, Monoglobus,* and *Parabacteroides*.

To supplement and further validate the classification approach, Linear discriminant analysis Effect Size (LEfSe) was used to detect and highlight potential diagnostic microbial biomarkers. From the findings of the LEfSe for the saliva microbiome in CRC and the HC (Figure 27C), a total of seven genera were highlighted: six in HC saliva and one in CRC saliva, which can help us differentiate between phenotypes. The HC saliva samples were identified using the genera *Fusobacterium, Dialister, Catonella, Tennerella, Eubacteriumbrachy- group,* and *Fretibacterium,* while the CRC saliva was characterized by the genus *Bifidobacterium.*

A similar analysis of the fecal microbiome in CRC and the HC (Figure 27D) showed a total of six genera, three of which are associated with HC fecal and three with CRC fecal.

As depicted in Figure 27D, HC fecal samples were identified using the genera *Parabacteroides*, *Barnesiella*, and *Collinsella*, while the CRC fecal samples were characterized by the genera *Ruminococcus-torques-group*, *Granulicatella*, and *Ruminococcus-gauvreauii*-group.

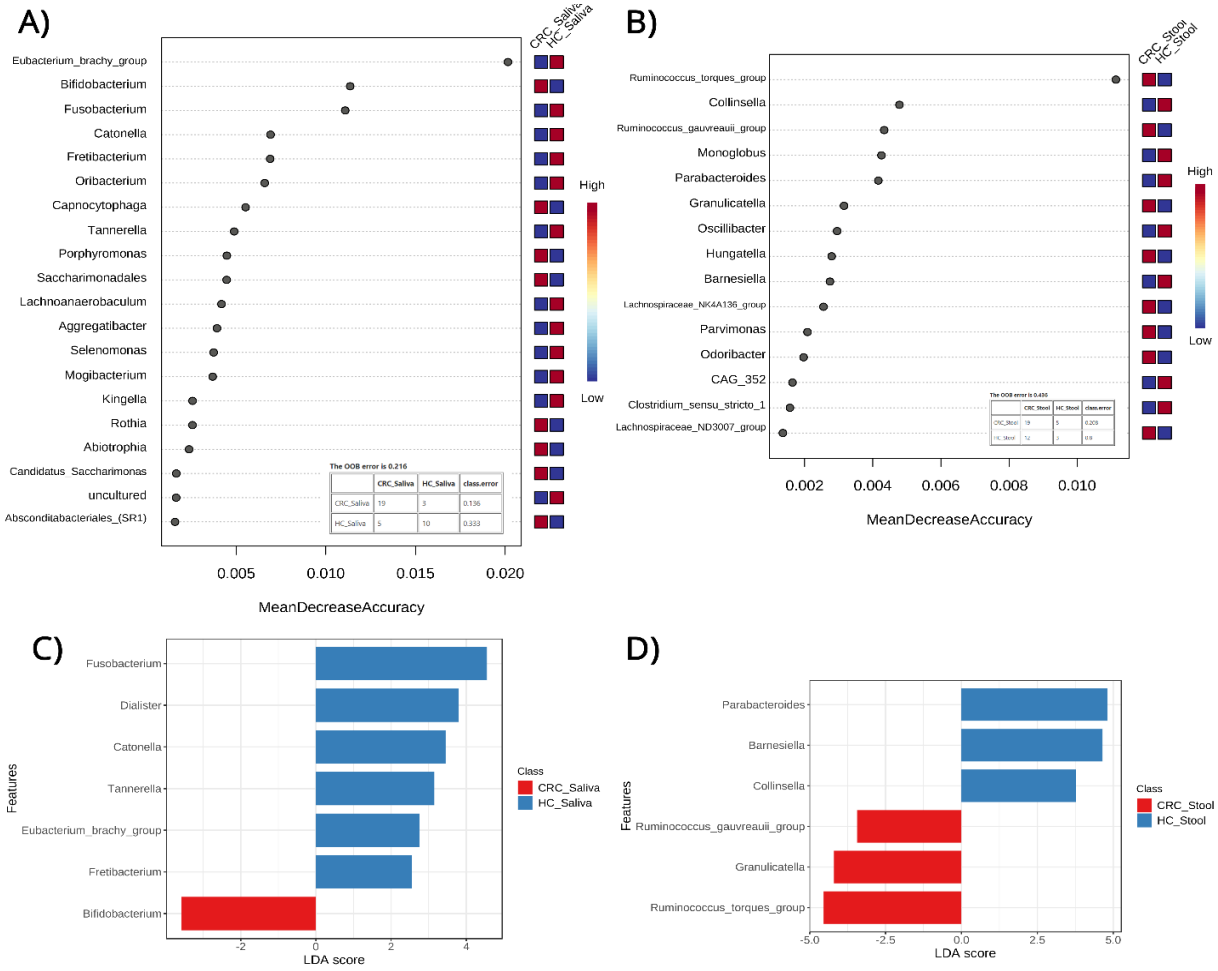

Figure 27. Top features (bacterial genera) in Random Forest (RF) models using (**A**) saliva samples of CRC (Colorectal cancer) patients and healthy controls (HC); (**B**) stool samples of CRC patients and healthy controls to predict sample classification into the patient and control groups. Figures also include Out-Of-Bag error and classification matrices for each model. In addition, Linear Discriminant Analysis (LDA) (18C) and (18D) between the same sample groups reveals bacterial genera which can serve as biomarkers for possible sample classification in CRC. Both approaches highlight, through different statistical methodologies, specific bacterial genera.

5-4. Discussion

The present study describes a combined analysis of the microbiome in saliva and fecal samples of CRC Iranian patients. Using abundance metrics, classification models, and biomarker discovery approaches, based on bacterial genera relative abundances, in the CRC saliva, HC saliva, CRC fecal, and HC fecal samples, our findings indicate certain features as potential bacterial biomarkers for the early diagnosis of CRC.

In the present study, we found that there is a clear clustering of genera associated with the saliva and fecal samples of CRC patients and the HC, respectively, pointing to distinct microbial signatures in both conditions. The most abundant microbial genera among saliva specimens were *Streptococcus* followed by *Prevotella, Veillonella, Neisseria*, and *Rothia* in CRC cases, while, in the HC, *Streptococcus* followed by *Veillonella, Prevotella, Neisseria,* and *Haemophilus* were the most frequent. Our analysis of the similarity between saliva and fecal samples in CRC and the HC showed distinct bacterial taxonomic compositions.

Even though, statistically, the differences on the genera level do not show any significance between CRC and HC using univariate methodologies, they highlight the distinct compositional profiles of saliva and fecal samples and point to their individual ability to provide unique insights during dysbiosis. These findings also underline the need for the more complex statistical analyses, such as the LEfSe and ML approaches employed in our subsequent analyses. The latter analyses also reveal the top three genera that were differentially abundant–*Eubacterium spp, Bifidobacterium spp,* and *Fusobacterium spp*–in the saliva of CRC patients vs. healthy controls. *Eubacterium* and *Fusobacterium* species might contribute to cancer initiation via promoting inflammation (232). *Bifidobacterium* species might exhibit anticancer activity on CRC by decreasing and boosting anti-apoptotic and pro-apoptotic genes

(233). These differences in saliva microbial composition between the CRC and controls further strengthens the theory that saliva microbiota could be a possible diagnostic biomarker in the future. Regarding the fecal samples, the top three differentially abundant genera were the *Ruminococcus torques* group and *Collinsella* and *Ruminococcus gauvreauii* group. Our results are in agreement with previous findings (234–236) that suggest that the *Ruminococcus torques* group, and *Collinsella* could be novel fecal biomarkers for CRC diagnosis. The low OOB error values exhibited by our predictive models encourage the use of saliva-based prediction for the occurrence of CRC. Previous studies are also in agreement with our results (205,237). Furthermore, Boleij et al. reported an increased risk of CRC and colorectal adenomas particularly in patients with *Streptococcus*-associated endocarditis and bacteremia (238). Additionally, our results supported the findings of Guven et al. that also reported a higher amount of *Streptococcus* in CRC patients, even if the role of *Streptococcus* in the carcinogenesis process is debatable (238).

There are studies supporting the idea that *Streptoccocus* is implicated in the inflammatory process of CRC pathogenesis (239,240); however, there are those that support the idea that *Streptococcus* is more likely an opportunist pathogen benefiting from a favorable oncogenic environment (241). Nevertheless, the increased amount of *Streptococcus* in the saliva of CRC patients is an interesting finding. Furthermore, the increased abundance of *Prevotella*, *Veillonella*, *Neisseria*, and *Rothia* in cancer saliva samples has been confirmed in a number of studies (242,243), indicating their potential contribution in the carcinogenesis process. Regarding the fecal samples compared to the literature, we surprisingly found that the CRC patients were more diverse than the HC in all alpha diversity indices (244). This observation may be related to ethnic nutritional habits and the genetic background, since it has been

observed in the Iranian CRC population. However, it is well known that changes over time in the gut microbiome can occur during the course of the disease and of therapy and in other types of cancers (i.e., metastatic kidney cancer, cervical cancer); moreover, it has been reported that the patients with the highest benefit from cancer treatment were those with higher microbial diversity (245,246). For example, the increased biodiversity of the cervical microbiome is associated with cervical cancer (246). Another notable finding of our research is that the saliva microbiome can predict CRC more accurately than the fecal microbiome. Six genera in HC saliva samples and one in the CRC saliva samples can accurately differentiate the two phenotypes. CRC saliva samples were characterized by the genus *Bifidobacterium,* a finding which is supported by previous studies that reported, in mouth rinse samples, oral pathogenic taxa such as *Treponema denticola*, *Bifidobacteriaceae*, and *Prevotella* (*P. denticola, P. intermedia, P. oral taxon 300*), which were positively associated with an increased risk of CRC (247).

Our study has some limitations that need to be considered when interpreting the results. First, the sample size of this work can potentially be hindering since no statistical power calculations had been applied when designing the study, which could have led to more accurate conclusions. Moreover, based on the current study, α and β diversity of fecal microbiome in the HC and CRC patients showed no statistically significant differences, suggesting that the microbial diversity and abundance in the HC group are the same as in the CRC group. Flemer et al. confirmed these results regarding the microbiota in fecal samples (224). They claimed that similar bacterial networks in CRC or HC colon biopsies and saliva samples indicate that these bacterial networks existed before CRC progression and can hypothetically be associated with CRC development. Furthermore, they reported that these bacterial communities were just

partially distinguishable in the fecal specimens of healthy people or those with CRC, which proves that these networks establish a strong and tight relationship with the intestinal mucosa, which shows the limitations of examining fecal to identify the microbiome in CRC (224). Similar bacterial networks from the oral cavity were found more in the colon tissues than in the fecal samples. In fact, colonic mucosal samples help to better detect gut microbiota, although its preparation is invasive, while the fecal samples are easily obtained, and its evaluation is considered non-invasive (222). Our future studies will merge oral, mucosal, and fecal samples to better clarify whether saliva bacterial communities exist before CRC progression and if they can hypothetically be responsible for CRC formation. Finally, while we found alterations of the saliva and fecal microbiota compositions, our approach was based on 16S rRNA amplicons instead of using metagenomic sequencing, thus limiting our capability to identify specific bacteria at the species level and report on bacterial function and their potential metabolites, whose mechanisms of function are uncertain.

It must be noted that this non-invasive diagnostic test, which contains the results of the microbiome of saliva and feces, can increase sensitivity in combination with the noninvasive FIT. It is well known that FIT is able to only identify advanced CRC stages (III and IV) by tracing the blood from intestinal lesions into the feces and that it is not able to identify primary lesions and CRC in stages 0, I, and II with sufficient sensitivity (209). Moreover, the identification of methylated and tumor DNA in fecal samples in addition to occult blood detection seems to be a promising strategy to increase the sensitivity of FIT.

However, there are disadvantages in these methods, such as the complicated requirement of fecal collection, the technical complexity requiring multistep lab analysis, and the false positive rate, leaving colonoscopy as the gold standard tests for screening. Thus, new

noninvasive strategies, to the benefit of patients, need to be developed in order to improve CRC screening, and the present work provides a possible solution. In our previous works, we investigated the fecal microbiota in cases with various types of colon polyps and reported that the gut microbiome can intervene in CRC early stages through adenoma polyps (AP) development but not hyperplastic polyp (HP) and sessile serrated adenoma (SSA). We also found that AP is an intermediate stage between healthy people and those with CRC, therefore gut microbiota can be considered as possible biomarkers for CRC early detection that may occur later in these patients (216,249). Based on those results, we concluded that the study of healthy microbiota that are reduced in patients with AP might promote the implementation of nutritional intervention and prebiotic and probiotic treatments to stimulate their growth again some years before the development of this malignancy (216,249). However, oral cavity microbiota also plays an important role in maintaining homeostasis and may indicate the oral, and general health status. The significant differences in the saliva and fecal microbiota of CRC patients, compared to the HC, would provide new insights for the disease pathogenesis and prognosis. As we mentioned above, the sensitivity of FIT is low and it could miscategorize onethird of CRC 0, I, and II stages (209). Therefore, more reliable biomarkers are required besides the FIT.

One of the strong points of this study is that the samples were collected in Taleghani hospital, which is the second center of the country for GI disorders patients. Hence, this study is population-based, and all people who had digestive problems and came to this institute for their first visit were considered for our investigation. Therefore, group studies had higher background similarities to each other. As genetics, lifestyle, dietary habits, and body mass index (BMI) differ between various people, the microbial biomarkers identified in the current

research must be tested in other studies for validation. Our results revealed that saliva microbiome can be considered as a novel biomarker in CRC's early diagnosis. If the applicability of the saliva microbiome for early CRC diagnosis could be confirmed in a larger population, this might permanently progress the present screening program and subsequently impact clinical practice and guidelines. Additional studies exploring microbial richness and diversity based on lifestyle choices such as eating habits, smoking, and exercise are necessary to enhance the concept of "healthy" living and its impact on CRC prevalence, as well as to promote the finding of novel diagnostics and open up new interventional treatment approaches.

References

1. Luna F, Luyckx VA. Why have Non-communicable Diseases been Left Behind? Asian Bioeth Rev. 2020 Mar 20;12(1):5–25.
2. https://www.who.int/news-room/fact-sheets/detail/noncommunicable-diseases.
3. Huizinga TWJ, Pincus T. Rheumatoid Arthritis. Ann Intern Med. 2010 Jul 6;153(1):ITC1-1.
4. Grassi W, de Angelis R, Lamanna G, Cervini C. The clinical features of rheumatoid arthritis. Eur J Radiol. 1998 May;27:S18–24.
5. van Delft MAM, Huizinga TWJ. An overview of autoantibodies in rheumatoid arthritis. J Autoimmun. 2020 Jun;110:102392.
6. MA X, XU S. TNF inhibitor therapy for rheumatoid arthritis. Biomed Rep. 2013;1(2):177–84.
7. de Brito Rocha S, Baldo DC, Andrade LEC. Clinical and pathophysiologic relevance of autoantibodies in rheumatoid arthritis. Advances in Rheumatology. 2019 Dec 17;59(1):2.
8. Finckh A, Gilbert B, Hodkinson B, Bae SC, Thomas R, Deane KD, et al. Global epidemiology of rheumatoid arthritis. Nat Rev Rheumatol. 2022 Sep 6; 18(10):591-602.
9. Croia C, Bursi R, Sutera D, Petrelli F, Alunno A, Puxeddu I. One year in review 2019: pathogenesis of rheumatoid arthritis. Clin Exp Rheumatol. 2019;37(3):347–57.

10. Klareskog L, Catrina AI, Paget S. Rheumatoid arthritis. The Lancet. 2009 Feb;373(9664):659–72.

11. McInnes IB, Schett G. The Pathogenesis of Rheumatoid Arthritis. New England Journal of Medicine. 2011 Dec 8;365(23):2205–19.

12. Calabresi E, Petrelli F, Bonifacio AF, Puxeddu I, Alunno A. One year in review 2018: pathogenesis of rheumatoid arthritis. Clin Exp Rheumatol. 2018;36(2):175–84.

13. Kowalski ML, Wolska A, Grzegorczyk J, Hilt J, Jarzebska M, Drobniewski M, et al. Increased Responsiveness to Toll-Like Receptor 4 Stimulation in Peripheral Blood Mononuclear Cells from Patients with Recent Onset Rheumatoid Arthritis. Mediators Inflamm. 2008;2008:1–7.

14. Huang Q, Ma Y, Adebayo A, Pope RM. Increased macrophage activation mediated through toll-like receptors in rheumatoid arthritis. Arthritis Rheum. 2007 Jul;56(7):2192–201.

15. Paulissen SMJ, van Hamburg JP, Dankers W, Lubberts E. The role and modulation of CCR6+ Th17 cell populations in rheumatoid arthritis. Cytokine. 2015 Jul;74(1):43–53.

16. Hussein HM, Rahal EA. The role of viral infections in the development of autoimmune diseases. Crit Rev Microbiol. 2019 Jul 4;45(4):394–412.

17. Oldstone MBA. Molecular mimicry and autoimmune disease. Cell. 1987 Sep;50(6):819–20.

18. Venigalla SSK, Premakumar S, Janakiraman V. A possible role for autoimmunity through molecular mimicry in alphavirus mediated arthritis. Sci Rep. 2020 Jan 22;10(1):938.

19. Root-Bernstein R, Fairweather D. Complexities in the Relationship Between Infection and Autoimmunity. Curr Allergy Asthma Rep. 2014 Jan 19;14(1):407.

20. Thaper D, Prabha V. Molecular mimicry: An explanation for autoimmune diseases and infertility. Scand J Immunol. 2018 Aug;88(2):e12697.

21. Ercolini AM, Miller SD. The role of infections in autoimmune disease. Clin Exp Immunol. 2008 Dec 2;155(1):1–15.

22. Arleevskaya MI, Kravtsova OA, Lemerle J, Renaudineau Y, Tsibulkin AP. How Rheumatoid Arthritis Can Result from Provocation of the Immune System by Microorganisms and Viruses. Front Microbiol. 2016 Aug 17;7.

23. Fujinami RS, von Herrath MG, Christen U, Whitton JL. Molecular Mimicry, Bystander Activation, or Viral Persistence: Infections and Autoimmune Disease. Clin Microbiol Rev. 2006 Jan;19(1):80–94.

24. Benedek TG. The History of Bacteriologic Concepts of Rheumatic Fever and Rheumatoid Arthritis. Semin Arthritis Rheum. 2006 Oct;36(2):109–23.

25. Yinshi Yue YY. Microbial Infection and Rheumatoid Arthritis. J Clin Cell Immunol. 2013;04(06).

26. Totaro M, Cattani P, Ria F, Tolusso B, Gremese E, Fedele A, et al. *Porphyromonas gingivalis* and the pathogenesis of rheumatoid arthritis: analysis of various compartments including the synovial tissue. Arthritis Res Ther. 2013;15(3):R66.

27. Sorgato CC, Lins-e-Silva M, Leão JC, Vasconcelos LR, Romão TP, Duarte AL, et al. EBV and CMV viral load in rheumatoid arthritis and their role in associated Sjögren's syndrome. Journal of Oral Pathology & Medicine. 2020 Aug 10;49(7):693–700.

28. Cronan MR, Beerman RW, Rosenberg AF, Saelens JW, Johnson MG, Oehlers SH, et al. Macrophage Epithelial Reprogramming Underlies Mycobacterial Granuloma Formation and Promotes Infection. Immunity. 2016 Oct;45(4):861–76.

29. Rook GAW. Rheumatoid Arthritis, Mycobacterial Antigens and Agalactosyl IgG. Scand J Immunol. 1988 Oct;28(4):487–93.

30. Bo M, Erre GL, Bach H, Slavin YN, Manchia PA, Passiu G, et al. <p>PtpA and PknG Proteins Secreted by *Mycobacterium avium subsp. paratuberculosis* are Recognized by Sera from Patients with Rheumatoid Arthritis: A Case–Control Study. J Inflamm Res. 2019 Dec;Volume 12:301–8.

31. van der Heijden IM, Wilbrink B, Schouls LM, van Embden JD, Breedveld FC, Tak PP. Detection of *mycobacteria* in joint samples from patients with arthritis using a genus-specific polymerase chain reaction and sequence analysis. Rheumatology. 1999 Jun 1;38(6):547–53.

32. Erre GL, Cossu D, Masala S, Mameli G, Cadoni ML, Serdino S, et al. *Mycobacterium tuberculosis* lipoarabinomannan antibodies are associated to rheumatoid arthritis in Sardinian patients. Clin Rheumatol. 2014 Dec 25;33(12):1725–9.

33. Holoshttz J, Strober S, Koning F, Coligan JE, de Bruyn J. Isolation of CD4-CD8-mycobacteria-reactive T lymphocyte clones from rheumatoid arthritis synovial fluid. Nature. 1989 May;339(6221):226–9.

34. Brand DD, Latham KA, Rosloniec EF. Collagen-induced arthritis. Nat Protoc. 2007 May 17;2(5):1269–75.

35. Celis L, Vandevyver C, Geusens P, Dequeker J, Raus J, Zhang J. Clonal expansion of mycobacterial heat-shock protein–reactive T lymphocytes in the synovial fluid and blood of rheumatoid arthritis patients. Arthritis Rheum. 1997 Mar;40(3):510–9.

36. Esaguy N, Aguas AP, van Embden JD, Silva MT. *Mycobacteria* and human autoimmune disease: direct evidence of cross-reactivity between human lactoferrin and the 65-kilodalton protein of tubercle and leprosy bacilli. Infect Immun. 1991 Mar;59(3):1117–25.

37. Elkayam O, Segal R, Bendayan D, van Uitert R, Onnekink C, Pruijn GJ. The anti-cyclic citrullinated peptide response in tuberculosis patients is

not citrulline-dependent and sensitive to treatment. Arthritis Res Ther. 2010;12(1):R12.

38. Lim MK, Shim TS, Sheen DH, Na DJ, Min SS, Shim SC. Anti-cyclic citrulline peptide antibody in non-tuberculous mycobacteria sera: a negative association. Clin Rheumatol. 2010 Mar 6;29(3):335–6.

39. Aguas A, Esaguy N, Sunkel CE, Silva MT. Cross-reactivity and sequence homology between the 65-kilodalton mycobacterial heat shock protein and human lactoferrin, transferrin, and DR beta subsets of major histocompatibility complex class II molecules. Infect Immun. 1990 May;58(5):1461–70.

40. Esaguy N, Aguas AP, van Embden JD, Silva MT. *Mycobacteria* and human autoimmune disease: direct evidence of cross-reactivity between human lactoferrin and the 65-kilodalton protein of tubercle and leprosy bacilli. Infect Immun. 1991 Mar;59(3):1117–25.

41. Valdez MM, Clark JI, Wu GJS, Muchowski PJ. Functional similarities between the small heat shock proteins *Mycobacterium tuberculosis* HSP 16.3 and human αB-crystallin. Eur J Biochem. 2002 Apr;269(7):1806–13.

42. Zügel U, Kaufmann SHE. Role of Heat Shock Proteins in Protection from and Pathogenesis of Infectious Diseases. Clin Microbiol Rev. 1999 Jan;12(1):19–39.

43. van Eden W, van der Zee R, Prakken B. Heat-shock proteins induce T-cell regulation of chronic inflammation. Nat Rev Immunol. 2005 Apr 1;5(4):318–30.

44. Shoda H, Hanata N, Sumitomo S, Okamura T, Fujio K, Yamamoto K. Immune responses to Mycobacterial heat shock protein 70 accompany self-reactivity to human BiP in rheumatoid arthritis. Sci Rep. 2016 Mar 1;6(1):22486.

45. Babu Chodisetti S, Rai PK, Gowthaman U, Pahari S, Agrewala JN. Potential T cell epitopes of *Mycobacterium tuberculosis* that can instigate molecular mimicry against host: implications in autoimmune pathogenesis. BMC Immunol. 2012 Dec 21;13(1):13.

46. Gutlapalli VR, Sykam A, Nayarisseri A, Suneetha S, Suneetha LM. Insights from the predicted epitope similarity between *Mycobacterium tuberculosis* virulent factors and its human homologs. Bioinformation. 2015 Dec 31;11(12):517–24.

47. Mustafa AS. In silico Binding Predictions for Identification of HLA-DR-Promiscuous Regions and Epitopes of *Mycobacterium tuberculosi*s; Protein MPT64 (Rv1980c) and Their Recognition by Human Th1 Cells. Medical Principles and Practice. 2010;19(5):367–72.

48. Gowthaman U, Agrewala JN. *In silico* methods for predicting T-cell epitopes: Dr Jekyll or Mr Hyde? Expert Rev Proteomics. 2009 Oct 9;6(5):527–37.

49. Qasem A, Ramesh S, Naser SA. Genetic polymorphisms in tumour necrosis factor receptors (*TNFRSF1A/1B*) illustrate differential

treatment response to TNFα inhibitors in patients with Crohn's disease. BMJ Open Gastroenterol. 2019 Feb 1;6(1):e000246.

50. Sharp RC, Beg SA, Naser SA. Polymorphisms in Protein Tyrosine Phosphatase Non-receptor Type 2 and 22 (PTPN2/22) Are Linked to Hyper-Proliferative T-Cells and Susceptibility to *Mycobacteria* in Rheumatoid Arthritis. Front Cell Infect Microbiol. 2018 Jan 25;8.

51. Yamakawa M, Ouhara K, Kajiya M, Munenaga S, Kittaka M, Yamasaki S, et al. *Porphyromonas gingivalis* infection exacerbates the onset of rheumatoid arthritis in SKG mice. Clin Exp Immunol. 2016 Oct 7;186(2):177–89.

52. Ceccarelli F, Saccucci M, di Carlo G, Lucchetti R, Pilloni A, Pranno N, et al. Periodontitis and Rheumatoid Arthritis: The Same Inflammatory Mediators? Mediators Inflamm. 2019 May 5;2019:1–8.

53. Mikuls TR, Thiele GM, Deane KD, Payne JB, O'Dell JR, Yu F, et al. *Porphyromonas gingivalis* and disease-related autoantibodies in individuals at increased risk of rheumatoid arthritis. Arthritis Rheum. 2012 Nov;64(11):3522–30.

54. Johansson L, Sherina N, Kharlamova N, Potempa B, Larsson B, Israelsson L, et al. Concentration of antibodies against *Porphyromonas gingivalis* is increased before the onset of symptoms of rheumatoid arthritis. Arthritis Res Ther. 2016 Dec 7;18(1):201.

55. Lange L, Thiele GM, McCracken C, Wang G, Ponder LA, Angeles-Han ST, et al. Symptoms of periodontitis and antibody responses to Porphyromonas gingivalis in juvenile idiopathic arthritis. Pediatric Rheumatology. 2016 Dec 9;14(1):8.

56. Cheng Z, Meade J, Mankia K, Emery P, Devine DA. Periodontal disease and periodontal bacteria as triggers for rheumatoid arthritis. Best Pract Res Clin Rheumatol. 2017 Feb;31(1):19–30.

57. Rojas M, Restrepo-Jiménez P, Monsalve DM, Pacheco Y, Acosta-Ampudia Y, Ramírez-Santana C, et al. Molecular mimicry and autoimmunity. J Autoimmun. 2018 Dec;95:100–23.

58. Lundberg K, Kinloch A, Fisher BA, Wegner N, Wait R, Charles P, et al. Antibodies to citrullinated α-enolase peptide 1 are specific for rheumatoid arthritis and cross-react with bacterial enolase. Arthritis Rheum. 2008 Oct;58(10):3009–19.

59. Kinloch AJ, Alzabin S, Brintnell W, Wilson E, Barra L, Wegner N, et al. Immunization with *Porphyromonas gingivalis* enolase induces autoimmunity to mammalian α-enolase and arthritis in DR4-IE-transgenic mice. Arthritis Rheum. 2011 Dec;63(12):3818–23.

60. Maresz KJ, Hellvard A, Sroka A, Adamowicz K, Bielecka E, Koziel J, et al. *Porphyromonas gingivalis* Facilitates the Development and Progression of Destructive Arthritis through Its Unique Bacterial Peptidylarginine Deiminase (PAD). PLoS Pathog. 2013 Sep 12;9(9):e1003627.

61. Röhner E, Detert J, Kolar P, Hocke A, N'Guessan P, Matziolis G, et al. Induced Apoptosis of Chondrocytes by *Porphyromonas gingivalis* as a

Possible Pathway for Cartilage Loss in Rheumatoid Arthritis. Calcif Tissue Int. 2010 Oct 26;87(4):333–40.

62. Houen G, Trier NH. Epstein-Barr Virus and Systemic Autoimmune Diseases. Front Immunol. 2021 Jan 7;11.

63. Bo M, Erre GL, Niegowska M, Piras M, Taras L, Longu MG, et al. Interferon regulatory factor 5 is a potential target of autoimmune response triggered by Epstein-barr virus and *Mycobacterium avium subsp. paratuberculosis* in rheumatoid arthritis: investigating a mechanism of molecular mimicry. Clin Exp Rheumatol. 2018;36(3):376–81.

64. Shehab M, Sherri N, Hussein H, Salloum N, Rahal EA. Endosomal Toll-Like Receptors Mediate Enhancement of Interleukin-17A Production Triggered by Epstein-Barr Virus DNA in Mice. J Virol. 2019 Oct 15;93(20).

65. Salloum N, Hussein HM, Jammaz R, Jiche S, Uthman IW, Abdelnoor AM, et al. Epstein-Barr virus DNA modulates regulatory T-cell programming in addition to enhancing interleukin-17A production via Toll-like receptor 9. PLoS One. 2018 Jul 11;13(7):e0200546.

66. Lünemann JD, Frey O, Eidner T, Baier M, Roberts S, Sashihara J, et al. Increased Frequency of EBV-Specific Effector Memory CD8+ T Cells Correlates with Higher Viral Load in Rheumatoid Arthritis. The Journal of Immunology. 2008 Jul 15;181(2):991–1000.

67. Radner H, Neogi T, Smolen JS, Aletaha D. Performance of the 2010 ACR/EULAR classification criteria for rheumatoid arthritis: a systematic literature review. Ann Rheum Dis. 2014 Jan;73(1):114–23.

68. Köhler, Günther, Kaudewitz, Lorenz. Current Therapeutic Options in the Treatment of Rheumatoid Arthritis. J Clin Med. 2019 Jun 28;8(7):938.

69. Yi J, Liu Y, Xie H, An H, Li C, Wang X, et al. Hydrogels for the treatment of rheumatoid arthritis. Front Bioeng Biotechnol. 2022 Oct 12;10.

70. Gouda NA, Elkamhawy A, Cho J. Emerging Therapeutic Strategies for Parkinson's Disease and Future Prospects: A 2021 Update. Biomedicines. 2022 Feb 3;10(2):371.

71. Öksüz N, Öztürk Ş, Doğu O. Future Prospects in Parkinson's Disease Diagnosis and Treatment. Archives of Neuropsychiatry. 2022;

72. Cheng HC, Ulane CM, Burke RE. Clinical progression in Parkinson disease and the neurobiology of axons. Ann Neurol. 2010 Jun;67(6):715–25.

73. Vidović M, Rikalovic MG. Alpha-Synuclein Aggregation Pathway in Parkinson's Disease: Current Status and Novel Therapeutic Approaches. Cells. 2022 May 24;11(11):1732.

74. Smith JK, Mellick GD, Sykes AM. The role of the endolysosomal pathway in α-synuclein pathogenesis in Parkinson's disease. Front Cell Neurosci. 2023 Jan 10;16.

75. Poewe W, Seppi K, Tanner CM, Halliday GM, Brundin P, Volkmann J, et al. Parkinson disease. Nat Rev Dis Primers. 2017 Mar 23;3(1):17013.

76. Chen Z, Li G, Liu J. Autonomic dysfunction in Parkinson's disease: Implications for pathophysiology, diagnosis, and treatment. Neurobiol Dis. 2020 Feb;134:104700.

77. Chen H, Ritz B. The Search for Environmental Causes of Parkinson's Disease: Moving Forward. J Parkinsons Dis. 2018 Dec 18;8(s1):S9–17.

78. Day JO, Mullin S. The Genetics of Parkinson's Disease and Implications for Clinical Practice. Genes (Basel). 2021 Jun 30;12(7):1006.

79. Zarbiv Y, Simhi-Haham D, Israeli E, Elhadi SA, Grigoletto J, Sharon R. Lysine residues at the first and second KTKEGV repeats mediate α-Synuclein binding to membrane phospholipids. Neurobiol Dis. 2014 Oct;70:90–8.

80. Hernandez SM, Tikhonova EB, Karamyshev AL. Protein-Protein Interactions in Alpha-Synuclein Biogenesis: New Potential Targets in Parkinson's Disease. Front Aging Neurosci. 2020 Mar 17;12.

81. Sampson TR, Challis C, Jain N, Moiseyenko A, Ladinsky MS, Shastri GG, et al. A gut bacterial amyloid promotes α-synuclein aggregation and motor impairment in mice. Elife. 2020 Feb 11;9.

82. Woerman AL, Stöhr J, Aoyagi A, Rampersaud R, Krejciova Z, Watts JC, et al. Propagation of prions causing synucleinopathies in cultured cells. Proceedings of the National Academy of Sciences. 2015 Sep 18;112(35).

83. Smith JK, Mellick GD, Sykes AM. The role of the endolysosomal pathway in α-synuclein pathogenesis in Parkinson's disease. Front Cell Neurosci. 2023 Jan 10;16.

84. Yoo G, Shin YK, Lee NK. The Role of α-Synuclein in SNARE-mediated Synaptic Vesicle Fusion. J Mol Biol. 2023 Jan;435(1):167775.

85. Bozzola E, Spina G, Valeriani M, Papetti L, Ursitti F, Agostiniani R, et al. Management of pediatric post-infectious neurological syndromes. Ital J Pediatr. 2021 Dec 25;47(1):17.

86. Ghosn J, Taiwo B, Seedat S, Autran B, Katlama C. HIV. The Lancet. 2018 Aug;392(10148):685–97.

87. Leta V, Urso D, Batzu L, Lau YH, Mathew D, Boura I, et al. Viruses, parkinsonism and Parkinson's disease: the past, present and future. J Neural Transm. 2022 Sep 29;129(9):1119–32.

88. Blackburn KM, Wang C. Post-infectious neurological disorders. Ther Adv Neurol Disord. 2020;13:1756286420952901.

89. Liu Z, Xu E, Zhao HT, Cole T, West AB. LRRK2 and Rab10 coordinate macropinocytosis to mediate immunological responses in phagocytes. EMBO J. 2020 Oct 15;39(20).

90. Caggiu E, Paulus K, Galleri G, Arru G, Manetti R, Sechi GP, et al. Homologous HSV1 and alpha-synuclein peptides stimulate a T cell

response in Parkinson's disease. J Neuroimmunol. 2017 Sep;310:26–31.

91. Ghosh R, Ray A, Roy D, Das S, Dubey S, Benito-León J. Parkinsonism with akinetic mutism following osmotic demyelination syndrome in a SARS-CoV-2 infected elderly diabetic woman: A case report. Neurología. 2022 Oct;37(8):706–8.

92. Patrick KL, Bell SL, Weindel CG, Watson RO. Exploring the "Multiple-Hit Hypothesis" of Neurodegenerative Disease: Bacterial Infection Comes Up to Bat. Front Cell Infect Microbiol. 2019 May 28;9.

93. Sharma P, Kapoor D, Shukla D. Role of Heparanase and Syndecan-1 in HSV-1 Release from Infected Cells. Viruses. 2022 Sep 30;14(10):2156.

94. Traylen CM, Patel HR, Fondaw W, Mahatme S, Williams JF, Walker LR, et al. Virus reactivation: a panoramic view in human infections. Future Virol. 2011 Apr;6(4):451–63.

95. Laval K, Enquist LW. The Potential Role of Herpes Simplex Virus Type 1 and Neuroinflammation in the Pathogenesis of Alzheimer's Disease. Front Neurol. 2021 Apr 6;12.

96. Marcocci ME, Napoletani G, Protto V, Kolesova O, Piacentini R, Li Puma DD, et al. Herpes Simplex Virus-1 in the Brain: The Dark Side of a Sneaky Infection. Trends Microbiol. 2020 Oct;28(10):808–20.

97. Yu H, Wu J. Amyloid-β: A double agent in Alzheimer's disease? Biomedicine & Pharmacotherapy. 2021 Jul;139:111575.

98. Moin K, Funk C, Josephs M. Gut-brain axis: Review on the association between Parkinson's disease and plant lectins. Archive of Clinical Cases. 2022 Dec 17;9(4):177–83.

99. Chao YX, Gulam MY, Chia NSJ, Feng L, Rotzschke O, Tan EK. Gut–Brain Axis: Potential Factors Involved in the Pathogenesis of Parkinson's Disease. Front Neurol. 2020 Aug 25;11.

100. Fayyad M, Salim S, Majbour N, Erskine D, Stoops E, Mollenhauer B, et al. Parkinson's disease biomarkers based on α-synuclein. J Neurochem. 2019 Sep 28;150(5):626–36.

101. Beach TG, Adler CH, Sue LI, Shill HA, Driver-Dunckley E, Mehta SH, et al. "Body-First" Hypothesis Running Title: Vagus and Stomach Synucleinopathy. Available from: https://doi.org/10.1101/2020.09.29.20204248

102. Klann EM, Dissanayake U, Gurrala A, Farrer M, Shukla AW, Ramirez-Zamora A, et al. The Gut–Brain Axis and Its Relation to Parkinson's Disease: A Review. Front Aging Neurosci. 2022 Jan 7;13.

103. Miller AL, Bessho S, Grando K, Tükel Ç. Microbiome or Infections: Amyloid-Containing Biofilms as a Trigger for Complex Human Diseases. Front Immunol. 2021 Feb 26;12.

104. Barnhart MM, Chapman MR. Curli Biogenesis and Function. Annu Rev Microbiol. 2006 Oct 1;60(1):131–47.

105. Tursi SA, Tükel Ç. Curli-Containing Enteric Biofilms Inside and Out: Matrix Composition, Immune Recognition, and Disease Implications. Microbiology and Molecular Biology Reviews. 2018 Dec;82(4).

106. Tükel Ç, Nishimori JH, Wilson RP, Winter MG, Keestra AM, van Putten JPM, et al. Toll-like receptors 1 and 2 cooperatively mediate immune responses to curli, a common amyloid from enterobacterial biofilms. Cell Microbiol. 2010 Oct;12(10):1495–505.

107. Makiura N, Ojima M, Kou Y, Furuta N, Okahashi N, Shizukuishi S, et al. Relationship of *Porphyromonas gingivalis* with glycemic level in patients with type 2 diabetes following periodontal treatment. Oral Microbiol Immunol. 2008 Aug;23(4):348–51.

108. Blasco-Baque V, Garidou L, Pomié C, Escoula Q, Loubieres P, le Gall-David S, et al. Periodontitis induced by *Porphyromonas gingivalis* drives periodontal microbiota dysbiosis and insulin resistance via an impaired adaptive immune response. Gut. 2017 May;66(5):872–85.

109. Okada M, Kobayashi T, Ito S, Yokoyama T, Abe A, Murasawa A, et al. Periodontal Treatment Decreases Levels of Antibodies to *Porphyromonas gingivalis* and Citrulline in Patients With Rheumatoid Arthritis and Periodontitis. J Periodontol. 2013 Dec;84(12):e74–84.

110. Jasemi S, Erre GL, Cadoni ML, Bo M, Sechi LA. Humoral Response to Microbial Biomarkers in Rheumatoid Arthritis Patients. J Clin Med. 2021 Nov 2;10(21):5153.

111. Dominy SS, Lynch C, Ermini F, Benedyk M, Marczyk A, Konradi A, et al. *Porphyromonas gingivalis* in Alzheimer's disease brains: Evidence for disease causation and treatment with small-molecule inhibitors. Sci Adv. 2019 Jan 4;5(1).

112. Adams B, Nunes JM, Page MJ, Roberts T, Carr J, Nell TA, et al. Parkinson's Disease: A Systemic Inflammatory Disease Accompanied by Bacterial Inflammagens. Front Aging Neurosci. 2019 Aug 27;11.

113. González-Sanmiguel J, Schuh CMAP, Muñoz-Montesino C, Contreras-Kallens P, Aguayo LG, Aguayo S. Complex Interaction between Resident Microbiota and Misfolded Proteins: Role in Neuroinflammation and Neurodegeneration. Cells. 2020 Nov 13;9(11):2476.

114. Rebersek M. Gut microbiome and its role in colorectal cancer. BMC Cancer. 2021 Dec 11;21(1):1325.

115. Cheng Y, Ling Z, Li L. The Intestinal Microbiota and Colorectal Cancer. Front Immunol. 2020 Nov 30;11.

116. Saus E, Iraola-Guzmán S, Willis JR, Brunet-Vega A, Gabaldón T. Microbiome and colorectal cancer: Roles in carcinogenesis and clinical potential. Mol Aspects Med. 2019 Oct;69:93–106.

117. Song M, Chan AT, Sun J. Influence of the Gut Microbiome, Diet, and Environment on Risk of Colorectal Cancer. Gastroenterology. 2020 Jan;158(2):322–40.

118. la Vecchia S, Sebastián C. Metabolic pathways regulating colorectal cancer initiation and progression. Semin Cell Dev Biol. 2020 Feb;98:63–70.

119. Hold GL, Hansen R. Impact of the Gastrointestinal Microbiome in Health and Disease: Co-evolution with the Host Immune System. In 2019. p. 303–18.

120. Shi N, Li N, Duan X, Niu H. Interaction between the gut microbiome and mucosal immune system. Mil Med Res. 2017 Dec 27;4(1):14.

121. Azimi M, Keshavarz Shahbaz S, Mansourabadi AH, Mohamed Khosroshahi L, Pourkalhor S, Rezakhani M, et al. Intestinal Microbiota: Novel Personalized Cancer Immunotherapy in Colorectal Cancer. Int Arch Allergy Immunol. 2022;183(11):1147–65.

122. Ekine-Afolabi BA, Njan AA, Rotimi SO, R. I. A, Elbehi AM, Cash E, et al. The Impact of Diet on the Involvement of Non-Coding RNAs, Extracellular Vesicles, and Gut Microbiome-Virome in Colorectal Cancer Initiation and Progression. Front Oncol. 2020 Dec 14;10.

123. Temraz S, Nassar F, Nasr R, Charafeddine M, Mukherji D, Shamseddine A. Gut Microbiome: A Promising Biomarker for Immunotherapy in Colorectal Cancer. Int J Mol Sci. 2019 Aug 25;20(17):4155.

124. O'Keefe SJD. Diet, microorganisms and their metabolites, and colon cancer. Nat Rev Gastroenterol Hepatol. 2016 Dec 16;13(12):691–706.

125. Alhinai, Walton, Commane. The Role of the Gut Microbiota in Colorectal Cancer Causation. Int J Mol Sci. 2019 Oct 24;20(21):5295.

126. Chen G. The Role of the Gut Microbiome in Colorectal Cancer. Clin Colon Rectal Surg. 2018 May 1;31(03):192–8.

127. Wong SH, Zhao L, Zhang X, Nakatsu G, Han J, Xu W, et al. Gavage of Fecal Samples From Patients With Colorectal Cancer Promotes Intestinal Carcinogenesis in Germ-Free and Conventional Mice. Gastroenterology. 2017 Dec;153(6):1621-1633.e6.

128. Krishnan K, Chen T, Paster B. A practical guide to the oral microbiome and its relation to health and disease. Oral Dis. 2017 Apr;23(3):276–86.

129. Koliarakis I, Messaritakis I, Nikolouzakis TK, Hamilos G, Souglakos J, Tsiaoussis J. Oral Bacteria and Intestinal Dysbiosis in Colorectal Cancer. Int J Mol Sci. 2019 Aug 25;20(17):4146.

130. Karpiński T. Role of Oral Microbiota in Cancer Development. Microorganisms. 2019 Jan 13;7(1):20.

131. Brennan CA, Garrett WS. *Fusobacterium nucleatum* — symbiont, opportunist and oncobacterium. Nat Rev Microbiol. 2019 Mar 13;17(3):156–66.

132. Wick EC, Sears CL. *Bacteroides spp*. and diarrhea. Curr Opin Infect Dis. 2010 Oct;23(5):470–4.

133. Wexler HM. *Bacteroides* : the Good, the Bad, and the Nitty-Gritty. Clin Microbiol Rev. 2007 Oct;20(4):593–621.

134. Jasemi S, Emaneini M, Ahmadinejad Z, Fazeli MS, Sechi LA, Sadeghpour Heravi F, et al. Antibiotic resistance pattern of *Bacteroides fragilis* isolated from clinical and colorectal specimens. Ann Clin Microbiol Antimicrob. 2021 Dec 23;20(1):27.

135. Sears CL, Geis AL, Housseau F. *Bacteroides fragilis* subverts mucosal biology: from symbiont to colon carcinogenesis. Journal of Clinical Investigation. 2014 Oct 1;124(10):4166–72.

136. Buckwold SL, Shoemaker NB, Sears CL, Franco AA. Identification and Characterization of Conjugative Transposons CTn86 and CTn9343 in *Bacteroides fragilis* Strains. Appl Environ Microbiol. 2007 Jan;73(1):53–63.

137. Sears CL. The toxins of *Bacteroides fragilis*. Toxicon. 2001 Nov;39(11):1737–46.

138. Holton J. Enterotoxigenic *Bacteroides fragilis*. Curr Infect Dis Rep. 2008 Mar 9;10(2):99–104.

139. Jasemi S, Emaneini M, Fazeli MS, Ahmadinejad Z, Nomanpour B, Sadeghpour Heravi F, et al. Toxigenic and non-toxigenic patterns I, II and III and biofilm-forming ability in *Bacteroides fragilis* strains isolated from patients diagnosed with colorectal cancer. Gut Pathog. 2020 Dec 5;12(1):28.

140. Remacle AG, Shiryaev SA, Strongin AY. Distinct Interactions with Cellular E-Cadherin of the Two Virulent Metalloproteinases Encoded by a *Bacteroides fragilis* Pathogenicity Island. PLoS One. 2014 Nov 20;9(11):e113896.

141. Costerton JW, Stewart PS, Greenberg EP. Bacterial Biofilms: A Common Cause of Persistent Infections. Science (1979). 1999 May 21;284(5418):1318–22.

142. Römling U, Balsalobre C. Biofilm infections, their resilience to therapy and innovative treatment strategies. J Intern Med. 2012 Dec;272(6):541–61.

143. Johnson CH, Dejea CM, Edler D, Hoang LT, Santidrian AF, Felding BH, et al. Metabolism Links Bacterial Biofilms and Colon Carcinogenesis. Cell Metab. 2015 Jun;21(6):891–7.

144. Dejea CM, Sears CL. Do biofilms confer a pro-carcinogenic state? Gut Microbes. 2016 Jan 2;7(1):54–7.

145. Drewes JL, Housseau F, Sears CL. Sporadic colorectal cancer: microbial contributors to disease prevention, development and therapy. Br J Cancer. 2016 Jul 5;115(3):273–80.

146. Li S, Konstantinov SR, Smits R, Peppelenbosch MP. Bacterial Biofilms in Colorectal Cancer Initiation and Progression. Trends Mol Med. 2017 Jan;23(1):18–30.

147. BROOK I, FRAZIER EH. Aerobic and anaerobic microbiology in intra-abdominal infections associated with diverticulitis. J Med Microbiol. 2000 Sep 1;49(9):827–30.

148. Rabizadeh S, Rhee KJ, Wu S, Huso D, Gan CM, Golub JE, et al. Enterotoxigenic *Bacteroides fragilis*: A potential instigator of colitis. Inflamm Bowel Dis. 2007 Dec;13(12):1475–83.

149. Boleij A, Hechenbleikner EM, Goodwin AC, Badani R, Stein EM, Lazarev MG, et al. The *Bacteroides fragilis* Toxin Gene Is Prevalent in the Colon Mucosa of Colorectal Cancer Patients. Clinical Infectious Diseases. 2015 Jan 15;60(2):208–15.

150. Basset C, Holton J, Bazeos A, Vaira D, Bloom S. Are Helicobacter Species and Enterotoxigenic *Bacteroides fragilis* Involved in Inflammatory Bowel Disease? Dig Dis Sci. 2004 Sep;49(9):1425–32.

151. Zamani S, Hesam Shariati S, Zali MR, Asadzadeh Aghdaei H, Sarabi Asiabar A, Bokaie S, et al. Detection of enterotoxigenic *Bacteroides fragilis* in patients with ulcerative colitis. Gut Pathog. 2017 Dec 15;9(1):53.

152. Myers LL, Firehammer BD, Shoop DS, Border MM. *Bacteroides fragilis*: a possible cause of acute diarrheal disease in newborn lambs. Infect Immun. 1984 May;44(2):241–4.

153. Koshy SS, Montrose MH, Sears CL. Human intestinal epithelial cells swell and demonstrate actin rearrangement in response to the metalloprotease toxin of *Bacteroides fragilis*. Infect Immun. 1996 Dec;64(12):5022–8.

154. Ulger Toprak N, Yagci A, Gulluoglu BM, Akin ML, Demirkalem P, Celenk T, et al. A possible role of *Bacteroides fragilis* enterotoxin in the aetiology of colorectal cancer. Clinical Microbiology and Infection. 2006 Aug;12(8):782–6.

155. Hale VL, Jeraldo P, Chen J, Mundy M, Yao J, Priya S, et al. Distinct microbes, metabolites, and ecologies define the microbiome in deficient and proficient mismatch repair colorectal cancers. Genome Med. 2018 Dec 31;10(1):78.

156. Bundgaard-Nielsen C, Baandrup UT, Nielsen LP, Sørensen S. The presence of bacteria varies between colorectal adenocarcinomas, precursor lesions and non-malignant tissue. BMC Cancer. 2019 Dec 29;19(1):399.

157. Purcell R v., Pearson J, Aitchison A, Dixon L, Frizelle FA, Keenan JI. Colonization with enterotoxigenic *Bacteroides fragilis* is associated with early-stage colorectal neoplasia. PLoS One. 2017 Feb 2;12(2):e0171602.

158. Guo Q, Wang Y, Xu D, Nossent J, Pavlos NJ, Xu J. Rheumatoid arthritis: pathological mechanisms and modern pharmacologic therapies. Bone Res. 2018 Apr 27;6(1):15.

159. Kronzer VL, Davis JM. Etiologies of Rheumatoid Arthritis: Update on Mucosal, Genetic, and Cellular Pathogenesis. Curr Rheumatol Rep. 2021 Apr 1;23(4):21.

160. Holers VM, Demoruelle MK, Kuhn KA, Buckner JH, Robinson WH, Okamoto Y, et al. Rheumatoid arthritis and the mucosal origins

hypothesis: protection turns to destruction. Nat Rev Rheumatol. 2018 Sep 15;14(9):542–57.

161. Firestein GS, McInnes IB. Immunopathogenesis of Rheumatoid Arthritis. Immunity. 2017 Feb;46(2):183–96.

162. Aletaha D, Neogi T, Silman AJ, Funovits J, Felson DT, Bingham CO, et al. 2010 Rheumatoid arthritis classification criteria: an American College of Rheumatology/European League Against Rheumatism collaborative initiative. Ann Rheum Dis. 2010 Sep 1;69(9):1580–8.

163. Aletaha D, Neogi T, Silman AJ, Funovits J, Felson DT, Bingham CO, et al. 2010 Rheumatoid arthritis classification criteria: An American College of Rheumatology/European League Against Rheumatism collaborative initiative. Arthritis Rheum. 2010 Sep;62(9):2569–81.

164. Mameli G, Cocco E, Frau J, Marrosu MG, Sechi LA. Epstein Barr Virus and *Mycobacterium avium subsp. paratuberculosis* peptides are recognized in sera and cerebrospinal fluid of MS patients. Sci Rep. 2016 Mar 9;6(1):22401.

165. Mameli G, Cossu D, Cocco E, Frau J, Marrosu MG, Niegowska M, et al. Epitopes of HERV-Wenv induce antigen-specific humoral immunity in multiple sclerosis patients. J Neuroimmunol. 2015 Mar;280:66–8.

166. Bo M, Jasemi S, Uras G, Erre GL, Passiu G, Sechi LA. Role of Infections in the Pathogenesis of Rheumatoid Arthritis: Focus on Mycobacteria. Microorganisms. 2020 Sep 23;8(10):1459.

167. Karlson EW, Deane K. Environmental and Gene-Environment Interactions and Risk of Rheumatoid Arthritis. Rheumatic Disease Clinics of North America. 2012 May;38(2):405–26.

168. Ercolini AM, Miller SD. The role of infections in autoimmune disease. Clin Exp Immunol. 2008 Dec 2;155(1):1–15.

169. Garvey M.; *Mycobacterium avium subspecies paratuberculosis*: A possible causative agent in human morbidity and risk to public health safety. Open Vet J. 2018 Jun 4;8(2):172.

170. Erre GL, Mameli G, Cossu D, Muzzeddu B, Piras C, Paccagnini D, et al. Increased Epstein-Barr Virus DNA Load and Antibodies Against EBNA1 and EA in Sardinian Patients with Rheumatoid Arthritis. Viral Immunol. 2015 Sep;28(7):385–90.

171. Bo M, Niegowska M, Erre GL, Piras M, Longu MG, Manchia P, et al. Rheumatoid arthritis patient antibodies highly recognize IL-2 in the immune response pathway involving IRF5 and EBV antigens. Sci Rep. 2018 Jan 29;8(1):1789.

172. Nelson PN. Demystified . Human endogenous retroviruses. Molecular Pathology. 2003 Feb 1;56(1):11–8.

173. Arru G, Sechi E, Mariotto S, Zarbo IR, Ferrari S, Gajofatto A, et al. Antibody response against HERV-W in patients with MOG-IgG associated disorders, multiple sclerosis and NMOSD. J Neuroimmunol. 2020 Jan;338:577110.

174. Grandi N, Tramontano E. HERV Envelope Proteins: Physiological Role and Pathogenic Potential in Cancer and Autoimmunity. Front Microbiol. 2018 Mar 14;9.

175. Mameli G, Erre GL, Caggiu E, Mura S, Cossu D, Bo M, et al. Identification of a HERV-K env surface peptide highly recognized in Rheumatoid Arthritis (RA) patients: a cross-sectional case–control study. Clin Exp Immunol. 2017 Jun 6;189(1):127–31.

176. Rodríguez-Lozano B, González-Febles J, Garnier-Rodríguez JL, Dadlani S, Bustabad-Reyes S, Sanz M, et al. Association between severity of periodontitis and clinical activity in rheumatoid arthritis patients: a case–control study. Arthritis Res Ther. 2019 Dec 18;21(1):27.

177. Han MN, Finkelstein DI, McQuade RM, Diwakarla S. Gastrointestinal Dysfunction in Parkinson's Disease: Current and Potential Therapeutics. J Pers Med. 2022 Jan 21;12(2):144.

178. Lotz SK, Blackhurst BM, Reagin KL, Funk KE. Microbial Infections Are a Risk Factor for Neurodegenerative Diseases. Front Cell Neurosci. 2021 Jul 7;15.

179. Smeyne RJ, Noyce AJ, Byrne M, Savica R, Marras C. Infection and Risk of Parkinson's Disease. J Parkinsons Dis. 2021 Feb 2;11(1):31–43.

180. Arru G, Caggiu E, Paulus K, Sechi G pietro, Mameli G, Sechi LA. Is there a role for *Mycobacterium avium subspecies paratuberculosis* in Parkinson's disease? J Neuroimmunol. 2016 Apr;293:86–90.

181. Tuck MK, Chan DW, Chia D, Godwin AK, Grizzle WE, Krueger KE, et al. Standard Operating Procedures for Serum and Plasma Collection: Early Detection Research Network Consensus Statement Standard Operating Procedure Integration Working Group. J Proteome Res. 2009 Jan 2;8(1):113–7.

182. Caggiu E, Paulus K, Galleri G, Arru G, Manetti R, Sechi GP, et al. Homologous HSV1 and alpha-synuclein peptides stimulate a T cell response in Parkinson's disease. J Neuroimmunol. 2017 Sep;310:26–31.

183. Noli M, Meloni G, Manca P, Cossu D, Palermo M, Sechi LA. HERV-W and *Mycobacterium avium subspecies paratuberculosis* Are at Play in Pediatric Patients at Onset of Type 1 Diabetes. Pathogens. 2021 Sep 3;10(9):1135.

184. Chistiakov DA, Orekhov AN, Bobryshev Y v. Links between atherosclerotic and periodontal disease. Exp Mol Pathol. 2016 Feb;100(1):220–35.

185. Mameli G, Cocco E, Frau J, Marrosu MG, Sechi LA. Epstein Barr Virus and *Mycobacterium avium subsp. paratuberculosis* peptides are recognized in sera and cerebrospinal fluid of MS patients. Sci Rep. 2016 Mar 9;6(1):22401.

186. Woulfe J, Gray MT, Ganesh MS, Middeldorp JM. Human serum antibodies against EBV latent membrane protein 1 cross-react with α-

synuclein. Neurology - Neuroimmunology Neuroinflammation. 2016 Aug 10;3(4):e239.

187. Smith LM, Schiess MC, Coffey MP, Klaver AC, Loeffler DA. α-Synuclein and Anti-α-Synuclein Antibodies in Parkinson's Disease, Atypical Parkinson Syndromes, REM Sleep Behavior Disorder, and Healthy Controls. PLoS One. 2012 Dec 17;7(12):e52285.

188. Li QX, Mok SS, Laughton KM, McLean CA, Cappai R, Masters CL, et al. Plasma α-synuclein is decreased in subjects with Parkinson's disease. Exp Neurol. 2007 Apr;204(2):583–8.

189. Yanamandra K, Gruden MA, Casaite V, Meskys R, Forsgren L, Morozova-Roche LA. α-Synuclein Reactive Antibodies as Diagnostic Biomarkers in Blood Sera of Parkinson's Disease Patients. PLoS One. 2011 Apr 25;6(4):e18513.

190. Sampson TR, Debelius JW, Thron T, Janssen S, Shastri GG, Ilhan ZE, et al. Gut Microbiota Regulate Motor Deficits and Neuroinflammation in a Model of Parkinson's Disease. Cell. 2016 Dec;167(6):1469-1480.e12.

191. Pachucki RJ, Corradetti C, Kohler L, Ghadiali J, Gallo PM, Nicastro L, et al. Persistent Bacteriuria and Antibodies Recognizing Curli/eDNA Complexes From *Escherichia coli* Are Linked to Flares in Systemic Lupus Erythematosus. Arthritis & Rheumatology. 2020 Nov 11;72(11):1872–81.

192. Martínez-García M, Hernández-Lemus E. Periodontal Inflammation and Systemic Diseases: An Overview. Front Physiol. 2021 Oct 27;12.

193. Deshpande RG, Khan M, Genco CA. Invasion Strategies of the Oral Pathogen;*Porphyromonas gingivalis*; Implications for Cardiovascular Disease. Invasion Metastasis. 1998;18(2):57–69.

194. Díaz-Zúñiga J, Muñoz Y, Melgar-Rodríguez S, More J, Bruna B, Lobos P, et al. Serotype b of *Aggregatibacter actinomycetemcomitans* triggers pro-inflammatory responses and amyloid beta secretion in hippocampal cells: a novel link between periodontitis and Alzheimer´s disease? J Oral Microbiol. 2019 Jan 1;11(1):1586423.

195. Agostini S, Mancuso R, Costa AS, Citterio LA, Guerini FR, Meloni M, et al. A Possible Role for HSV-1-Specific Humoral Response and PILRA rs1859788 Polymorphism in the Pathogenesis of Parkinson's Disease. Vaccines (Basel). 2021 Jun 22;9(7):686.

196. Ramakrishna C, Mendonca S, Ruegger PM, Kim JH, Borneman J, Cantin EM. Herpes simplex virus infection, Acyclovir and IVIG treatment all independently cause gut dysbiosis. PLoS One. 2020 Aug 6;15(8):e0237189.

197. Woulfe JM, Gray MT, Gray DA, Munoz DG, Middeldorp JM. Hypothesis: A role for EBV-induced molecular mimicry in Parkinson's disease. Parkinsonism Relat Disord. 2014 Jul;20(7):685–94.

198. Wong SH, Yu J. Gut microbiota in colorectal cancer: mechanisms of action and clinical applications. Nat Rev Gastroenterol Hepatol. 2019 Nov 25;16(11):690–704.

199. Viljoen KS, Dakshinamurthy A, Goldberg P, Blackburn JM. Quantitative Profiling of Colorectal Cancer-Associated Bacteria Reveals Associations between Fusobacterium spp., Enterotoxigenic *Bacteroides fragilis* (ETBF) and Clinicopathological Features of Colorectal Cancer. PLoS One. 2015 Mar 9;10(3):e0119462.

200. Macfarlane S, Woodmansey EJ, Macfarlane GT. Colonization of Mucin by Human Intestinal Bacteria and Establishment of Biofilm Communities in a Two-Stage Continuous Culture System. Appl Environ Microbiol. 2005 Nov;71(11):7483–92.

201. Odamaki T, Sugahara H, Yonezawa S, Yaeshima T, Iwatsuki K, Tanabe S, et al. Effect of the oral intake of yogurt containing *Bifidobacterium longum* BB536 on the cell numbers of enterotoxigenic Bacteroides fragilis in microbiota. Anaerobe. 2012 Feb;18(1):14–8.

202. Hecht AL, Casterline BW, Earley ZM, Goo YA, Goodlett DR, Bubeck Wardenburg J. Strain competition restricts colonization of an enteric pathogen and prevents colitis. EMBO Rep. 2016 Sep 18;17(9):1281–91.

203. Viljoen KS, Dakshinamurthy A, Goldberg P, Blackburn JM. Quantitative Profiling of Colorectal Cancer-Associated Bacteria Reveals Associations between Fusobacterium spp., Enterotoxigenic *Bacteroides fragilis* (ETBF) and Clinicopathological Features of Colorectal Cancer. PLoS One. 2015 Mar 9;10(3):e0119462.

204. Haghi F, Goli E, Mirzaei B, Zeighami H. The association between fecal enterotoxigenic *B. fragilis* with colorectal cancer. BMC Cancer. 2019 Dec 5;19(1):879.

205. Boleij A, van Gelder MMHJ, Swinkels DW, Tjalsma H. Clinical Importance of *Streptococcus gallolyticus* Infection Among Colorectal Cancer Patients: Systematic Review and Meta-analysis. Clinical Infectious Diseases. 2011 Nov 1;53(9):870–8.

206. Merino VRC, Nakano V, Liu C, Song Y, Finegold SM, Avila-Campos MJ. Quantitative Detection of Enterotoxigenic *Bacteroides fragilis* Subtypes Isolated from Children with and without Diarrhea. J Clin Microbiol. 2011 Jan;49(1):416–8.

207. Pierce J v., Bernstein HD. Genomic Diversity of Enterotoxigenic Strains of *Bacteroides fragilis*. PLoS One. 2016 Jun 27;11(6):e0158171.

208. Zeller G, Tap J, Voigt AY, Sunagawa S, Kultima JR, Costea PI, et al. Potential of fecal microbiota for early-stage detection of colorectal cancer. Mol Syst Biol. 2014 Nov 28;10(11):766.

209. Niedermaier T, Tikk K, Gies A, Bieck S, Brenner H. Sensitivity of Fecal Immunochemical Test for Colorectal Cancer Detection Differs According to Stage and Location. Clinical Gastroenterology and Hepatology. 2020 Dec;18(13):2920-2928.e6.

210. Bu F, Yao X, Lu Z, Yuan X, Chen C, Li L, et al. Pathogenic or Therapeutic: The Mediating Role of Gut Microbiota in Non-Communicable Diseases. Front Cell Infect Microbiol. 2022 Jul 7;12.

211. Durack J, Lynch S v. The gut microbiome: Relationships with disease and opportunities for therapy. Journal of Experimental Medicine. 2019 Jan 7;216(1):20–40.

212. Jia W, Rajani C, Xu H, Zheng X. Gut microbiota alterations are distinct for primary colorectal cancer and hepatocellular carcinoma. Protein Cell. 2021 May 14;12(5):374–93.

213. Megat Mohd Azlan P, Chin S, Low TY, Neoh H, Jamal R. Analyzing the Secretome of Gut Microbiota as the Next Strategy For Early Detection of Colorectal Cancer. Proteomics. 2019 May 25;19(10):1800176.

214. Liang Q, Chiu J, Chen Y, Huang Y, Higashimori A, Fang J, et al. Fecal Bacteria Act as Novel Biomarkers for Noninvasive Diagnosis of Colorectal Cancer. Clinical Cancer Research. 2017 Apr 15;23(8):2061–70.

215. Rezasoltani S, Sharafkhah M, Asadzadeh Aghdaei H, Nazemalhosseini Mojarad E, Dabiri H, Akhavan Sepahi A, et al. Applying simple linear combination, multiple logistic and factor analysis methods for candidate fecal bacteria as novel biomarkers for early detection of adenomatous polyps and colon cancer. J Microbiol Methods. 2018 Dec;155:82–8.

216. Rezasoltani S, Asadzadeh Aghdaei H, Dabiri H, Akhavan Sepahi A, Modarressi MH, Nazemalhosseini Mojarad E. The association between fecal microbiota and different types of colorectal polyp as precursors of colorectal cancer. Microb Pathog. 2018 Nov;124:244–9.

217. Pushalkar S, Ji X, Li Y, Estilo C, Yegnanarayana R, Singh B, et al. Comparison of oral microbiota in tumor and non-tumor tissues of patients with oral squamous cell carcinoma. BMC Microbiol. 2012 Dec 20;12(1):144.

218. Schmidt BL, Kuczynski J, Bhattacharya A, Huey B, Corby PM, Queiroz ELS, et al. Changes in Abundance of Oral Microbiota Associated with Oral Cancer. PLoS One. 2014 Jun 2;9(6):e98741.

219. Chen X, Winckler B, Lu M, Cheng H, Yuan Z, Yang Y, et al. Oral Microbiota and Risk for Esophageal Squamous Cell Carcinoma in a High-Risk Area of China. PLoS One. 2015 Dec 7;10(12):e0143603.

220. Farrell JJ, Zhang L, Zhou H, Chia D, Elashoff D, Akin D, et al. Variations of oral microbiota are associated with pancreatic diseases including pancreatic cancer. Gut. 2012 Apr;61(4):582–8.

221. Torres PJ, Fletcher EM, Gibbons SM, Bouvet M, Doran KS, Kelley ST. Characterization of the salivary microbiome in patients with pancreatic cancer. PeerJ. 2015 Nov 5;3:e1373.

222. Flemer B, Lynch DB, Brown JMR, Jeffery IB, Ryan FJ, Claesson MJ, et al. Tumour-associated and non-tumour-associated microbiota in colorectal cancer. Gut. 2017 Apr;66(4):633–43.

223. Baxter NT, Ruffin MT, Rogers MAM, Schloss PD. Microbiota-based model improves the sensitivity of fecal immunochemical test for detecting colonic lesions. Genome Med. 2016 Dec 6;8(1):37.

224. Flemer B, Warren RD, Barrett MP, Cisek K, Das A, Jeffery IB, et al. The oral microbiota in colorectal cancer is distinctive and predictive. Gut. 2018 Aug;67(8):1454–63.

225. Kato I, Vasquez AA, Moyerbrailean G, Land S, Sun J, Lin HS, et al. Oral microbiome and history of smoking and colorectal cancer. J Epidemiol Res. 2016 Apr 22;2(2).

226. Bolyen E, Rideout JR, Dillon MR, Bokulich NA, Abnet CC, Al-Ghalith GA, et al. Reproducible, interactive, scalable and extensible microbiome data science using QIIME 2. Nat Biotechnol. 2019 Aug 24;37(8):852–7.

227. Callahan BJ, McMurdie PJ, Rosen MJ, Han AW, Johnson AJA, Holmes SP. DADA2: High-resolution sample inference from Illumina amplicon data. Nat Methods. 2016 Jul 23;13(7):581–3.

228. Pedregosa FABIANPEDREGOSA F, Michel V, Grisel OLIVIERGRISEL O, Blondel M, Prettenhofer P, Weiss R, et al. Scikit-learn: Machine Learning in Python Gaël Varoquaux Bertrand Thirion Vincent Dubourg Alexandre Passos PEDREGOSA, VAROQUAUX, GRAMFORT ET AL. Matthieu Perrot [Internet]. Vol. 12, Journal of Machine Learning Research. 2011. Available from: http://scikit-learn.sourceforge.net.

229. Pruesse E, Quast C, Knittel K, Fuchs BM, Ludwig W, Peplies J, et al. SILVA: a comprehensive online resource for quality checked and aligned ribosomal RNA sequence data compatible with ARB. Nucleic Acids Res. 2007 Nov 14;35(21):7188–96.

230. Dhariwal A, Chong J, Habib S, King IL, Agellon LB, Xia J. Microbiome Analyst: a web-based tool for comprehensive statistical, visual and meta-analysis of microbiome data. Nucleic Acids Res. 2017 Jul 3;45(W1):W180–8.

231. Chang F, He S, Dang C. Assisted Selection of Biomarkers by Linear Discriminant Analysis Effect Size (LEfSe) in Microbiome Data. Journal of Visualized Experiments. 2022 May 16;(183).

232. Wang Y, Wan X, Wu X, Zhang C, Liu J, Hou S. Eubacterium rectale contributes to colorectal cancer initiation via promoting colitis. Gut Pathog. 2021 Dec 12;13(1):2.

233. Faghfoori Z, Faghfoori MH, Saber A, Izadi A, Yari Khosroushahi A. Anticancer effects of *bifidobacteria* on colon cancer cell lines. Cancer Cell Int. 2021 Dec 12;21(1):258.

234. Park J, Kim NE, Yoon H, Shin CM, Kim N, Lee DH, et al. Fecal Microbiota and Gut Microbe-Derived Extracellular Vesicles in Colorectal Cancer. Front Oncol. 2021 Sep 14;11.

235. Sobhani I, Bergsten E, Couffin S, Amiot A, Nebbad B, Barau C, et al. Colorectal cancer-associated microbiota contributes to oncogenic epigenetic signatures. Proceedings of the National Academy of Sciences. 2019 Nov 26;116(48):24285–95.

236. Sheng Q, Du H, Cheng X, Cheng X, Tang Y, Pan L, et al. Characteristics of fecal gut microbiota in patients with colorectal cancer at different stages and different sites. Oncol Lett. 2019 Sep 10;

237. Segata N, Haake S, Mannon P, Lemon KP, Waldron L, Gevers D, et al. Composition of the adult digestive tract bacterial microbiome based on seven mouth surfaces, tonsils, throat and stool samples. Genome Biol. 2012;13(6):R42.

238. Guven DC, Dizdar O, Alp A, Akdoğan Kittana FN, Karakoc D, Hamaloglu E, et al. Analysis of *Fusobacterium nucleatum* and *Streptococcus gallolyticus* in saliva of colorectal cancer patients. Biomark Med. 2019 Jun;13(9):725–35.

239. Abdulamir AS, Hafidh RR, Bakar F. Molecular detection, quantification, and isolation of *Streptococcus gallolyticus* bacteria colonizing colorectal tumors: inflammation-driven potential of carcinogenesis via IL-1, COX-2, and IL-8. Mol Cancer. 2010;9(1):249.

240. Kumar R, Herold JL, Taylor J, Xu J, Xu Y. Variations among *Streptococcus gallolyticus* subsp. gallolyticus strains in connection with colorectal cancer. Sci Rep. 2018 Jan 24;8(1):1514.

241. Aymeric L, Donnadieu F, Mulet C, du Merle L, Nigro G, Saffarian A, et al. Colorectal cancer specific conditions promote *Streptococcus gallolyticus* gut colonization. Proceedings of the National Academy of Sciences. 2018 Jan 9;115(2).

242. Wang Y, Zhang Y, Qian Y, Xie Y, Jiang S, Kang Z, et al. Alterations in the oral and gut microbiome of colorectal cancer patients and association with host clinical factors. Int J Cancer. 2021 Aug 15;149(4):925–35.

243. Huang K, Gao X, Wu L, Yan B, Wang Z, Zhang X, et al. Salivary Microbiota for Gastric Cancer Prediction: An Exploratory Study. Front Cell Infect Microbiol. 2021 Mar 10;11.

244. Abdi H, Kordi-Tamandani DM, Lagzian M, Bakhshipour A. Microbiome Analysis in Patients with Colorectal Cancer by 16S Ribosomal RNA Sequencing in the Southeast of Iran. Jundishapur J Microbiol. 2022 May 25;15(4).

245. Salgia NJ, Bergerot PG, Maia MC, Dizman N, Hsu J, Gillece JD, et al. Stool Microbiome Profiling of Patients with Metastatic Renal Cell Carcinoma Receiving Anti–PD-1 Immune Checkpoint Inhibitors. Eur Urol. 2020 Oct;78(4):498–502.

246. Zeber-Lubecka N, Kulecka M, Lindner B, Krynicki R, Paziewska A, Nowakowski A, et al. Increased diversity of a cervical microbiome associates with cervical cancer. Front Oncol. 2022 Sep 28;12.

247. Yang Y, Cai Q, Shu X, Steinwandel MD, Blot WJ, Zheng W, et al. Prospective study of oral microbiome and colorectal cancer risk in low-income and African American populations. Int J Cancer. 2019 May 15;144(10):2381–9.

248. Ringel Y, Maharshak N, Ringel-Kulka T, Wolber EA, Sartor RB, Carroll IM. High throughput sequencing reveals distinct microbial populations within the mucosal and luminal niches in healthy individuals. Gut Microbes. 2015 May 4;6(3):173–81.

249. Rezasoltani S, Ghanbari R, Looha MA, Mojarad EN, Yadegar A, Stewart D, et al. Expression of Main Toll-Like Receptors in Patients with Different Types of Colorectal Polyps and Their Relationship with Gut Microbiota. Int J Mol Sci. 2020 Nov 26;21(23):8968.

List of papers published during the PhD (1-11-2019 / 31-1-2023)

1) **Jasemi, S**., Paulus, K., Noli, M., Simula, E. R., Ruberto, S., & Sechi, L. A. (2022). Antibodies against HSV-1 and Curli Show the Highest Correlation in Parkinson's Disease Patients in Comparison to Healthy Controls. International journal of molecular sciences, 23(23), 14816. https://doi.org/10.3390/ijms232314816

2) **Jasemi, S**., Erre, G. L., Cadoni, M. L., Bo, M., & Sechi, L. A. (2021). Humoral Response to Microbial Biomarkers in Rheumatoid Arthritis Patients. Journal of clinical medicine, 10(21), 5153. https://doi.org/10.3390/jcm10215153

3) **Jasemi, S**., Emaneini, M., Ahmadinejad, Z., Fazeli, M. S., Sechi, L. A., Sadeghpour Heravi, F., & Feizabadi, M. M. (2021). Antibiotic resistance pattern of *Bacteroides fragilis* isolated from clinical and colorectal specimens. Annals of clinical microbiology and antimicrobials, 20(1), 27. https://doi.org/10.1186/s12941-021-00435-w

4) **Jasemi, S**., Emaneini, M., Fazeli, M. S., Ahmadinejad, Z., Nomanpour, B., Sadeghpour Heravi, F., Sechi, L. A., & Feizabadi, M. M. (2020). Toxigenic and non-toxigenic patterns I, II and III and biofilm-forming ability in *Bacteroides fragilis* strains isolated from patients diagnosed with colorectal cancer. Gut pathogens, 12, 28. https://doi.org/10.1186/s13099-020-00366-5

5) Rezasoltani, S., Aghdaei, H. A., **Jasemi, S**., Gazouli, M., Dovrolis, N., Sadeghi, A., Schlüter, H., Zali, M. R., Sechi, L. A., & Feizabadi, M. M. (2022). Oral Microbiota as Novel Biomarkers for Colorectal Cancer Screening. Cancers, 15(1), 192. https://doi.org/10.3390/cancers15010192

6) Bo, M., **Jasemi, S**., Uras, G., Erre, G. L., Passiu, G., & Sechi, L. A. (2020). Role of Infections in the Pathogenesis of Rheumatoid Arthritis: Focus on *Mycobacteria*. Microorganisms, 8(10), 1459. https://doi.org/10.3390/microorganisms8101459

7) Zamani, S., Taslimi, R., Sarabi, A., **Jasemi, S**., Sechi, L. A., & Feizabadi, M. M. (2020). Enterotoxigenic *Bacteroides fragilis*: A Possible Etiological Candidate for Bacterially-Induced Colorectal Precancerous and Cancerous Lesions. Frontiers in cellular and infection microbiology, 9, 449. https://doi.org/10.3389/fcimb.2019.00449

8) Simula, E. R., Manca, M. A., **Jasemi, S**., Uzzau, S., Rubino, S., Manchia, P., Bitti, A., Palermo, M., & Sechi, L. A. (2020). HCoV-NL63 and SARS-CoV-2 Share Recognized Epitopes by the Humoral Response in Sera of People Collected Pre- and during CoV-2 Pandemic. Microorganisms, 8(12), 1993. https://doi.org/10.3390/microorganisms8121993

9) Noli, M., Meloni, G., Ruberto, S., **Jasemi, S**., Simula, E. R., Cossu, D., Bo, M., Palermo, M., & Sechi, L. A. (2022). HERV-K Envelope Protein Induces Long-Lasting Production of Autoantibodies in T1DM Patients at Onset in Comparison to ZNT8 Autoantibodies. Pathogens (Basel, Switzerland), 11(10), 1188. https://doi.org/10.3390/pathogens11101188

10) Simula, E. R., Manca, M. A., Noli, M., **Jasemi, S**., Ruberto, S., Uzzau, S., Rubino, S., Manca, P., & Sechi, L. A. (2022). Increased Presence of Antibodies against Type I Interferons and Human Endogenous Retrovirus W in Intensive Care Unit COVID-19 Patients. Microbiology spectrum, 10(4), e0128022. https://doi.org/10.1128/spectrum.01280-22

11) Ashraf, H., Cossu, D., Ruberto, S., Noli, M., **Jasemi, S**., Simula, E. R., & Sechi, L. A. (2023). Latent Potential of Multifunctional Selenium Nanoparticles in Neurological Diseases and Altered Gut Microbiota. Materials (Basel, Switzerland), 16(2), 699. https://doi.org/10.3390/ma16020699